SSSU 95
ISSN 0140 3818

UNIVERSITY OF SOUTHAMPTON

DEPARTMENT OF SHIP SCIENCE

FACULTY OF ENGINEERING AND APPLIED SCIENCE

Report on Contract SSDH300023
Trimaran Seakeeping Code Validation - Phase 1

Prediction of Heave, Pitch and Roll Motions for Three Trimaran Models

P. Temarel and D. Hudson

Ship Science Report 95
March 1996

Report on Contract SSDH300023

TRIMARAN SEAKEEPING CODE VALIDATION - Phase 1

Prediction of Heave, Pitch and Roll Motions for Three Trimaran Models

by

P.Temarel and D.A.Hudson

Department of Ship Science

University of Southampton

CONTENTS

1. Introduction

The motions of a trimaran travelling in regular waves encountered at arbitrary heading at two different forward speeds, corresponding to Froude numbers Fn=0.24 (18 knots) and 0.40 (30 knots), are predicted using three-dimensional potential flow analysis. The analytical calculations are performed for three models namely, model A (narrow beam with larger outriggers), model D (wide beam with smaller outriggers and bilge keels) and model F (wide beam with smaller rectangular outriggers). These predictions are compared with available measurements obtained from model experiments for models A and D carried out at DRA Haslar. Experimental data were not, as yet, available for the model referred to as F at the time of completion of this report. Experiments, we believe, were also carried out for model B (wide beam with smaller outriggers; no bilge keels) and models C and E (wide beam with smaller outriggers and bilge keels; different GM and roll gyradius compared to model D). Analytical predictions were not performed for models B, C and E ; hence, they are not discussed in this report.

The three-dimensional potential flow analysis makes use of the Green's function approach and idealises the wetted surface of the vessel using quadrilateral panels (triangular panels are also defined using four nodes) which contain at their centre a pulsating source of unknown strength, determined from the application of boundary conditions [1,2]. This type of analysis has been applied successfully to the investigation of seakeeping characteristics of multi-hulls such as SWATHs [3] and catamarans [4]. The application to catamarans revealed an overestimation of the resonance effect due to the interaction between the hulls, for heave and pitch RAOs in head waves, particularly with increasing forward speed. In this respect two- (strip theory) and three-dimensional potential flow analyses are very similar. Better prediction of the interaction effects between the hulls was achieved using a version of translating/pulsating source distribution on the wetted hull surface [2,4]. This, however, lead to overestimation of the RAOs at the speed dependent resonance [4]. The prediction of motion RAOs at high speeds and, especially, for multi-hulls is under development with the objective being to account for nonlinearities arising from the boundary conditions (i.e. various types of translating/pulsating source distribution), in particular at high forward speeds, and viscous effects. The latter is very important in predicting the roll amplitude at resonance.

The three-dimensional analysis used to predict the motion RAOs for the trimaran adopts a pulsating source distribution on the wetted surface. This is because significant interaction effects between the outriggers and the hull were not anticipated, particularly within the frequency range tested. Use of a translating/pulsating source distribution is computationally time consuming. The current version was used sparingly and did not, in general, reveal any substantial differences for the lower Froude number. At the higher Froude number the predictions suffered, in general, from similar problems to those encountered for the catamarans [4]. It should be noted, however, that the analysis using translating/pulsating source distributions is still under development. No attempt was made to adjust the (potential flow) damping for roll motion and that arising from the bilge keels. A nonlinear analysis will be more suitable for modelling such effects.

2. Numerical Modelling

All three models have the same main hull and different outrigger shapes and athwartships configurations. The length and position of the outriggers along the hull is the same for all three models. Model A has a narrow beam configuration with a larger outrigger whilst models D and F have a wide beam configuration with smaller outriggers. The outriggers for models A and D have contoured cross sections, whilst those for model F are rectangular. In addition, model D has bilge keels fitted on the inside of the outriggers. The models have different displacements, metacentric heights (GM) and roll and pitch radii of gyration. The properties used for the wetted surface idealisation and the data for the subsequent calculations were supplied by DRA Haslar. For model F the values of LCG, GM and roll and pitch radii of

gyration given for model D were used. The wetted surfaces for models A and D were idealised using the actual running water line , whilst for model F the design load water line was used with the outriggers extending to a draught corresponding to the $1\times B$ case, as requested - B being the maximum outrigger breadth at the design waterline..
The wetted surface of the main hull was idealised using 240 panels, whilst 60, 80 and 60 panels were used to model each outrigger wetted surface for models A, D and F respectively. This will put all models, having either large or small outriggers, on the same basis making them suitable for parametric studies should the need arise. The differences between the number of panels in models A and D arise from the allowance for the running water line. This results in a narrow strip of high aspect ratio panels adjacent to the water line for model D which may affect the accuracy of the predictions. In addition for model D the outrigger panel idealisation is modified to fit the bilge keel panels resulting in 96 panels for each outrigger. The wetted surface panel idealisations for model A (360 panels in total), model D (432 panels in total) and model F (360 panels in total) are shown in Figs.1(a, b and c) respectively. It was felt that the adopted idealisation of the wetted surface provided an adequate description of the main hull and outrigger underwater geometries without using an excessive number of panels on the wetted surface. A more refined idealisation was tried using more panels in the longitudinal direction, for main hull as well as outriggers, as shown in Fig.1(d) for model A (720 panels in total). The displacements obtained from the above underwater idealisations are shown in Table 1.

Table 1 Model scale displacements obtained from the wetted surface idealisations

Model	A	Refined A	D	F
Displacement (kg)	340.99	341.31	350.95	279.57

3. Comparison of Analytical Predictions and Measurements for Motions (RAOs)

The analytically predicted and, where available, measured motion RAOs for models A, D and F are shown in Figs.2 (Heave), 3 (Pitch) and 4 (Roll) for Fn=0.24 and Figs.5 (Heave), 6 (Pitch) and 7 (Roll) for Fn=0.4. Seven heading values were used, namely 0, 30, 60, 90, 120, 150 and 180 degrees. Heave and pitch RAOs for the same speed and heading are shown on the same page for convenience. Heave RAO is defined as heave amplitude per wave amplitude whilst pitch and roll RAOs are motion amplitudes per wave slope. The RAOs are plotted against a non-dimensional wave frequency $\delta = \omega\sqrt{L/g}$, where ω is the wave frequency, g acceleration due to gravity and $L = 6$m in model scale. Analytical predictions were calculated at the wave frequencies used for the model experiments as supplied by DRA Haslar and the points were joined together by straight lines.
The predicted RAOs for all three models are also presented in tabular form in Appendix A. The RAO plots for model F alone (both Froude numbers) are also given in Appendix B to allow for incorporation of measurements obtained at a later date.

3.1 Model A - Fn=0.24

3.1.1 Heave RAOs

Predictions are a little larger than the measured ones for headings of 0, 30 and 60 deg. For beam waves (90 deg heading) predictions are a little larger than the measured ones up to $\delta = 2.27$, where the measured RAOs peak, and continue to increase and then fall below the measured values. For 120 deg heading the predictions are above and below the measured ones with the trough at $\delta = 2.27$ being lower than the corresponding measured value. Predictions and measurements agree for 150 deg heading except at the highest wave frequency tested where the prediction is a little larger than the measured value. For head waves (180 deg heading) the predictions are smaller than the measured values, in particular at low wave frequencies. Nevertheless, the measurement at $\delta = 1.8$ may be suspect and a measurement at a

lower wave frequency would have clarified the trend.

3.1.2 Pitch RAOs

Predictions are a little larger than measurements for 0 deg heading and agree with the measurements for 30 deg heading except at the largest wave frequency tested where the prediction is slightly above the measurement. Predictions are a little smaller than the measured values for 60 deg heading. Good agreement between predictions and measurements is attained for beam waves (90 deg heading) except at the largest wave frequency tested where the predictions are above the measured values. For 120 deg heading predictions match the measured values at the lowest three and highest wave frequencies tested; however, the predicted values display a peak at $\delta = 2.27$ which is not observed in the measurements. Good agreement is observed between predictions and measurements for 150 deg heading, although the predictions are a little above the measured values in the vicinity of $\delta = 2$. For head waves the agreement is very good at the two highest wave frequencies tested. Nevertheless, in the lower frequencies the measured values oscillate above and below the predicted results. The measurements in this range follow the heave RAOs.

3.1.3 Roll RAOs

For 30 deg heading predictions are smaller than the measured values and they do not display the peak observed at $\delta = 2.5$ in the measurements. For 60 deg heading the predictions are smaller than the measurements up to $\delta = 2$ but then continue to increase well above the measured values. It is difficult to ascertain the reason for this apparent peak (roll RAOs reduce when calculations are carried out at higher wave frequencies). For beam waves there is agreement between predictions and measurements at the lowest and two highest wave frequencies tested. The predicted values around the resonance are well above the measurements; nevertheless, the position of the resonance is correct. Reasonably good agreement is obtained between predictions and measurements for the 120 deg heading except when approaching the resonance region which is at a lower frequency than those tested. One also notes, for the 120 deg heading, that the predicted results display a small peak around $\delta = 2.5$. The resonance region is at even lower wave frequencies for 150 deg heading and there is reasonably good agreement between predictions and measurements in the lower wave frequencies tested; however, the peak observed at $\delta = 2.5$ for 120 deg heading is now more evident and, as expected, at a lower frequency corresponding to $\delta = 2.27$.

3.2 Refined Model A (720 panels) - Fn=0.24

The predicted heave and pitch RAOs for headings of 0, 30 and 180 degrees show hardly any difference when using two different wetted surface idealisations (360 and 720 panels). In the case of 60 and 150 deg headings there are some small differences between the two idealisations. The differences, however, are larger for the 90 and 120 deg headings resulting, for either heading, in smooth RAO variations with wave frequency. For these two headings the agreement between predictions using this refined model and measurements is better. However, the resonance observed in the measured heave RAO in beam waves is not apparent in the predictions obtained from the refined model.

The roll RAOs predicted using the refined idealisation are smaller than those obtained with the 360 panel model for headings 30 and 60 deg. Nevertheless the apparent peak observed for the 60 deg heading is still there. For 120 and 150 deg headings the predictions of the refined idealisation are, in general, in better agreement with the measured roll RAOs at the wave frequencies outside the resonance region. For these headings the second peak observed in the roll RAO predictions when using the cruder idealisation is not present in the predictions obtained from the refined idealisation, as can be seen from Figs.4(d, e). On the other hand the refined model predicts the roll resonance at a slightly higher frequency, as can be seen from the roll RAOs in beam waves shown in Fig.4(c).

3.3 Model A - Fn=0.4

Only a limited number of measured RAOs were supplied; thus, a comprehensive discussion is not possible.

Of the two measured heave RAO values in following waves (0 deg heading) one is smaller than the predicted value whilst the other matches. For the 60 deg heading measured heave and pitch RAOs oscillate about the predicted RAOs. For this heading the agreement is good enough for pitch RAOs but it is difficult to discern the trend of measured heave RAOs at high wave frequencies. The predicted heave RAOs for head waves (180 deg heading) are above the measured values which give the impression of an almost constant heave RAO due to few measurements. There are too few measurements for the pitch RAOs in beam waves (90 deg heading) to establish a trend; nevertheless the measured value at $\delta = 1.8$ matches the prediction. For the head waves (180 deg heading) predicted pitch RAOs are a little larger than the measured values to begin with, then the predictions are a little smaller than the measurements and above the measured values at the highest wave frequency tested; nevertheless, the trends are similar.

For the 60 deg heading measured roll RAOs are larger than the predicted values. It is difficult to ascertain the trend of the measured roll RAO at low wave frequencies and the apparent indication of a resonance. For the roll RAOs in beam waves (90 deg heading) the situation is similar to the lower Fn=0.24 with good agreement between predictions and measurements at the high wave frequencies and larger predictions in the resonance region, with the resonance occurring at the same wave frequency, as can be seen from Fig.7(c).

3.4 Model D - Fn=0.24

3.4.1 Heave RAOs

Measured values are larger than the predictions for 30, 60, 150 and 180 deg headings , although the trends are similar. For beam waves (90 deg heading) the measured RAOs are below the predicted values to begin with, then they become a little larger and also tend to a peak. The predicted values for beam waves remain more or less constant throughout the wave frequency range tested. For 120 deg heading the measured values are larger than the predictions with similar trends except the trough observed in the measurements at $\delta = 2.27$.

3.4.2 Pitch RAOs

For 30 deg heading the measured values are a little larger then the predictions at low wave frequencies and smaller at the highest wave frequency tested leaving a region in between where the agreement is good. Measured values are larger than the predictions for 60, 120 and 150 deg headings with similar trends, except for the latter two where the measured values display a small trough at $\delta = 2.27$ not observed in the predictions. For beam waves (90 deg heading) there are only two measured values at the lowest two wave frequencies tested which are larger then the predictions with the difference decreasing as the wave frequency increases. For head waves (180 deg heading) the measured values are above the predictions but the differences decrease with increasing wave frequency.

3.4.3 Roll RAOs

For 30 deg heading the predictions are smaller than the measurements except at the highest wave frequency tested where they match. For 60 deg heading the measured values are larger than the predictions, although the trends are similar. For 90 deg heading the predictions are smaller than the measured values at low wave frequencies ($\delta < 2.27$). For this heading one should note that the predicted roll resonance occurs near the highest wave frequency tested. This becomes more apparent for headings 120 and 150 deg when the predicted roll resonance can be observed clearly. This results in a predicted (full-scale) roll natural period of approximately 9s, whilst the measurements indicate a value of 10s. This may be due to hydrodynamic effects. A reasonable match is attained between predictions and measurements

outside the roll resonance region, in particular for 120 deg heading. However, for 150 deg heading at high wave frequencies ($\delta > 2.27$) the predictions are lower than the measured RAOs.

3.5 Model D - Fn=0.4

There are few measured RAOs to make a thorough comparison.
Measured heave, pitch and roll RAOs for 60 deg heading are larger than the predicted values but display similar trends. In beam waves the measured heave RAO for $\delta = 1.8$ is larger and for $\delta = 2.03$ a little smaller than the predictions. Nevertheless, the trend of the measured heave RAOs in beam waves is unclear. The pitch RAO in beam waves measured at $\delta = 2.03$ is a little larger than the corresponding prediction. The two measured roll RAOs in beam waves are larger than the predicted values.

4. Comparison of Motion Characteristics for Models A, D and F

The effects of outrigger geometry can be assessed by comparing models A and B, although this comparison will also include the effects of athwartships spacing. These effects can also be assessed by comparing models D and F, inclusive of bilge keel influences. The effects of bilge keels on the motion RAOs can be assessed by comparing the results for models B and C or D and F, or even models B and D. Any comparison between models A and D will combine the effects of outrigger geometry and athwartships spacing as well as the bilge keels.

4.1 Experimental measurements

The measured heave and pitch RAOs for Fn=0.24 and, where available, Fn=0.4 show differences, in general large, between models A and D. In general, the measured heave and pitch RAOs for model D are larger than the corresponding ones for model A, a notable exception being heave RAOs in head waves at Fn=0.24. In some cases measured heave RAOs for model D (e.g. Fn=0.24 and headings 60, 120 and 150 deg; Fn=0.4 and heading 60 deg) appear to tend to magnitudes larger than 1 at low wave frequencies. This appears to contravene conventional trends of heave RAOs at low wave frequencies, which usually approach unity. On the other hand, one would expect smaller heave (whilst still maintaining the trend of approaching to unity as the frequency tends to zero) and pitch RAOs in model D, by comparison to model B, due to the damping effects caused by the bilge keels. It is difficult to justify the differences observed between measured heave and pitch RAOs in models A and D even when the effects of differing outrigger geometries and spacing are allowed for. In this respect, comparison of measured results between models B and D will be useful.
The measured roll RAOs in headings less than 90 degrees reflect the effect of damping due to the presence of the bilge keels with smaller RAO values measured for model D compared to model A. For headings of equal to and more than 90 degrees, the roll RAO at resonance of model A is much larger than model D, though not necessarily so at the higher Froude number due to few measurements. Furthermore, the roll RAO for model D is smoother and displays a wider peak region compared to model A. Model A has a roll natural period of the order of 13s whilst model D 10s.

4.2 Analytical Predictions

The predictions for heave and pitch RAOs, in general, show small differences between models A, D and F, except for 90 and 120 deg headings, for either Froude number. Some of the differences in these headings appear to be a function of the panel density, as was shown for model A. Nevertheless, the larger differences between the models still occur in these headings. The differences between the models also appear to increase with increasing speed.
It should be noted that it is expected that the heave and pitch RAO predictions for model A at Fn=0.4 and headings 90 and 120 degrees will change in a similar manner to those at Fn=0.24 with a refined wetted surface idealisation. The effects of similar refinements on models D and F are not known, but may be negligible as the RAOs are already rather smooth.

The predicted roll RAOs in headings less than 90 degrees reflect the trend of the experiments with lower RAOs for model D (and model F) compared to model A. The roll resonance predicted for model A is in agreement with the measured value of 13s full-scale natural roll period. The natural roll period predicted for model D (approximately 9s) appears to be smaller than the full-scale value of 10s obtained from the measurements. This may be due to hydrodynamic effects. The natural roll period for model F is approximately 9s (full-scale). The roll magnitudes at resonance are large, as can be seen from Figs.4(c,d,e) and 7(c,d,e), for all models due to not accounting for non-linear effects such as viscous damping. However, it can be seen that the magnitudes of roll RAOs in the roll resonance region tend to be smaller for model D compared to models F and A. Overall it appears that the predicted roll RAOs for model F are closer to those of model D than model A. It is worthwhile noting that the peaks observed in the predicted roll RAOs for model A in the high wave frequencies are not associated with roll resonance and they disappear when a more refined idealisation is used. Furthermore, the apparent peak for the predicted roll RAO at 60 deg heading and Fn=0.24 cannot be explained with certainty, although it may be attributed to interactions between the hull and outriggers.

4.3 Forward Speed Effects

The predicted heave and pitch RAOs, for models A, D and F show small variations for the two Froude numbers used and headings less than or equal to 90 deg. The limited measurements available for model A show slightly larger variations with speed. The differences with forward speed are more notable in the heave and pitch RAOs for all models for headings larger than 90 deg. The limited number of measurements available for Fn=0.4 at these headings cannot be used to assess the trend in the heave and pitch RAOs with speed. There is also some doubt as to the accuracy of the measurements in head waves (180 deg heading).

The effects of forward speed can be seen in the predicted roll RAOs for all headings used. It is difficult to identify any clear trends. However, for headings of equal to and more than 90 deg the shifts of roll resonance with forward speed can be observed in the predictions as well as the measurements.

These effects can be clearly seen in the figures for model F in Appendix B.

5. Conclusions

- The heave and pitch RAO predictions compare, in general, well with the measured values for model A over a range of headings and speeds - within the limited measurements for the higher Froude number.

- Within the context of heave and pitch RAOs, the use of a more refined wetted surface idealisation for model A results in even better overall agreement at some headings.

- The agreement between predicted and measured heave and pitch RAOs is not, in general, as good for model D with the predictions being smaller than the measurements. Nevertheless, some of the measured heave RAOs at low wave frequencies do not inspire confidence.

- Predicted and measured roll RAOs for stern waves (heading less than 90 deg) are, in general, of the same order of magnitude. However, for beam and bow (heading greater than 90 degrees) waves the roll RAOs at resonance appear to be over predicted by the potential flow analysis. The correct roll resonance is predicted for model A. It is suspected that the predicted higher roll resonance for model D (i.e. roll natural period approximately 9s) may be due to hydrodynamic effects such as roll added mass moment of inertia and the effects of bilge keels. It should be noted, however, that more calculations in the vicinity of the roll resonance are required to pinpoint the resonance frequency with accuracy.

- The predictions show, in general, small differences between the heave and pitch RAOs for models A, D and F; although there are some exceptions.

- The predictions show differences between the roll RAOs for model A and models D and F mainly, but not exclusively, due to the different roll resonance frequencies. The roll RAOs of models D and F are, in general, similar and lower than those for model A. Furthermore model D has smaller roll RAOs than model F.

- The predictions reveal that forward speed effects are more apparent in heave and pitch RAOs for headings greater than 90 deg. For roll RAOs the shift with forward speed in roll resonance can be observed; however, it is difficult to identify any other trends.

References

1- Inglis, R.B.I and Price, W.G., A three-dimensional ship motion theory: calculation of wave loading and responses with forward speed, Trans RINA, 1982, 124, 183-192.

2- Inglis, R.B.I and Price, W.G., The influence of speed dependent boundary conditions in three-dimensional ship motion problems, Int. Shipbuilding Prog., 1981, 18, 22-29.

3- Bishop, R.E.D., Price, W.G. and Wu, Y., A general linear hydroelasticity theory of floating structures moving in a seaway, Phil. Trans. Roy. Soc., 1986, A316, 375-426.

4- Hudson, D.A., Price, W.G. and Temarel, P., Seakeeping performance of high speed displacement craft, Proc. Int. Conf. FAST'95, Lubeck, 1995, 877-892.

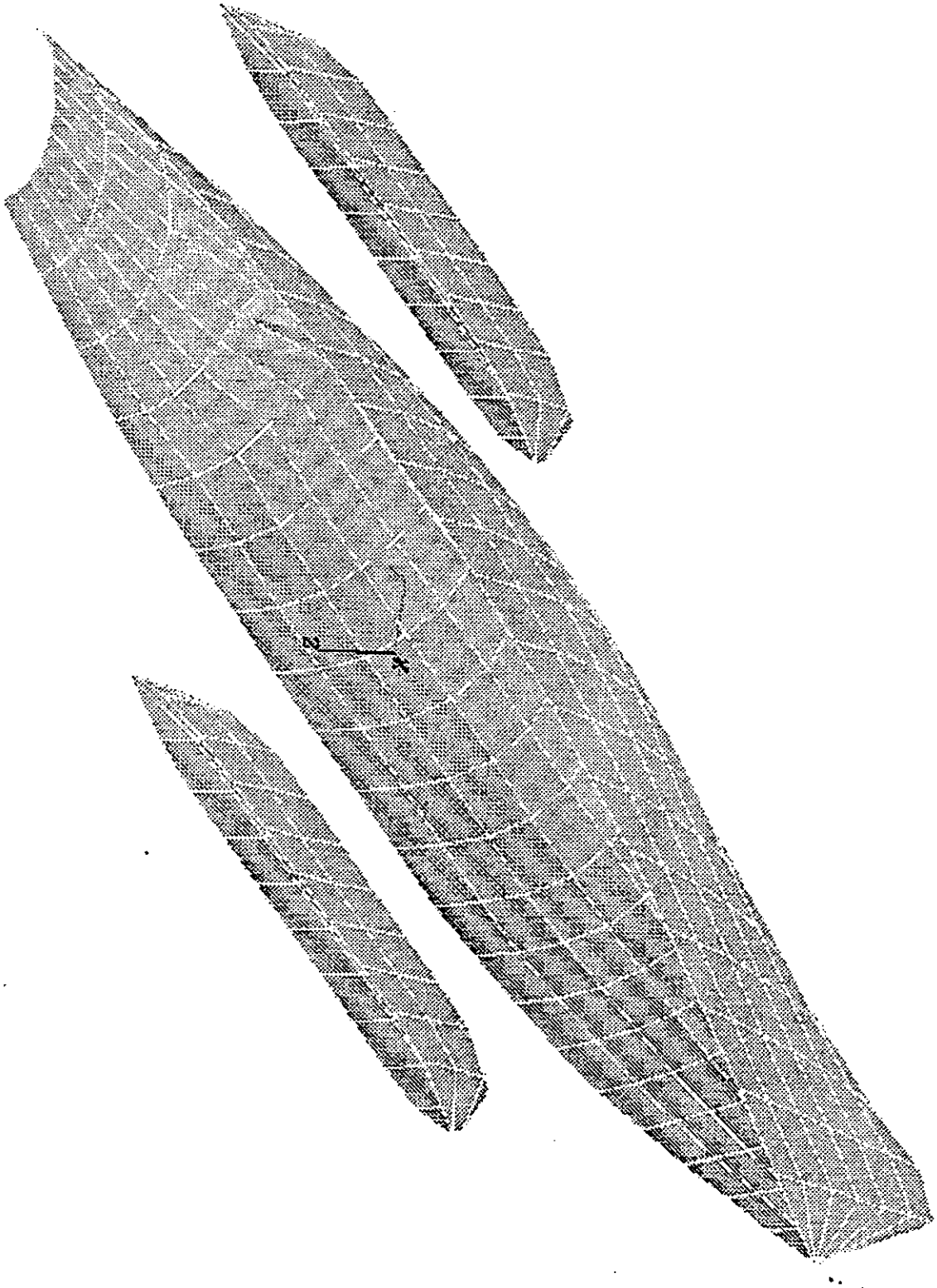

Fig.1(a) Wetted surface panel idealisation for model A (360) panels.

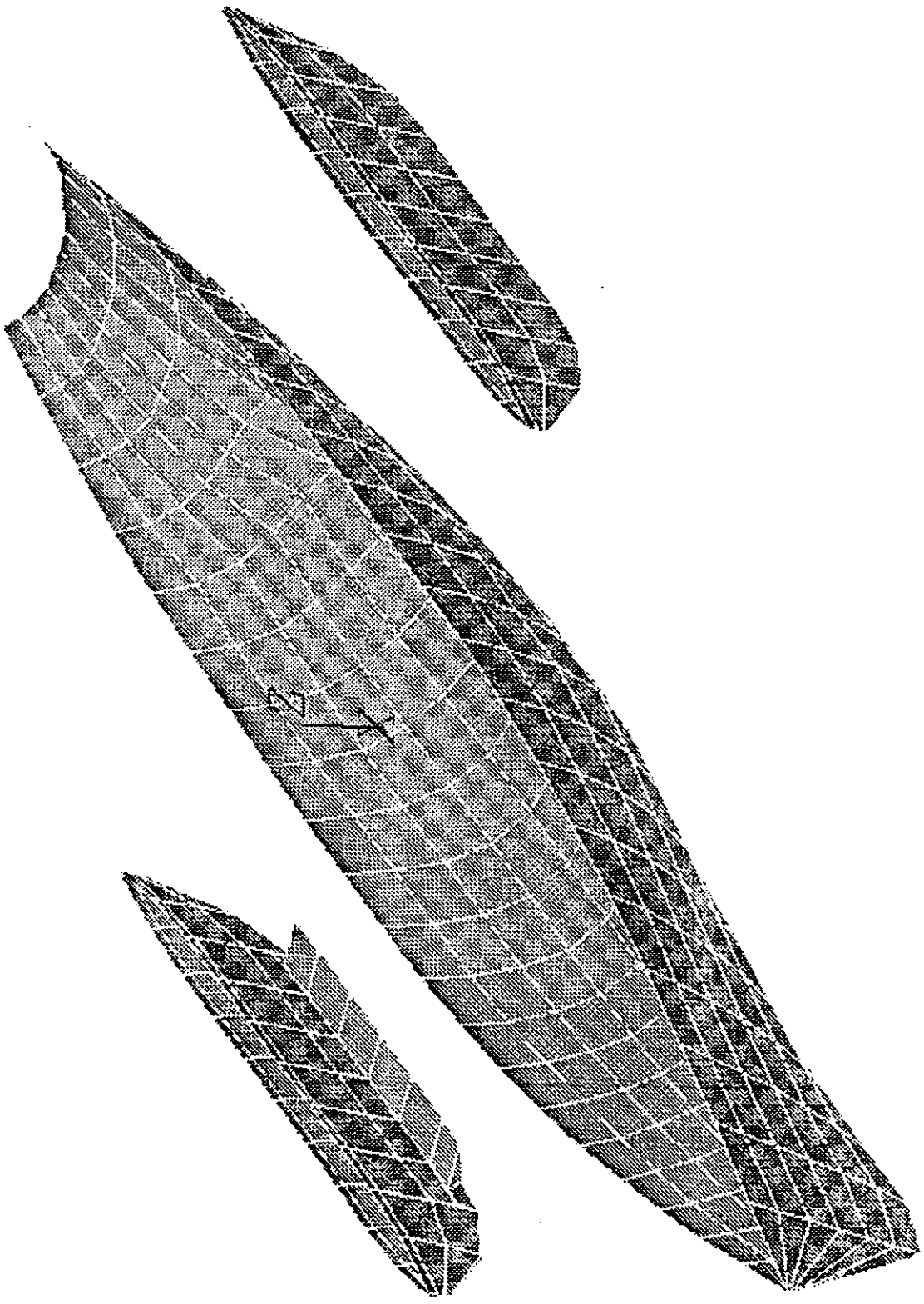

Fig.1(b) Wetted surface panel idealisation for model D (432) panels.

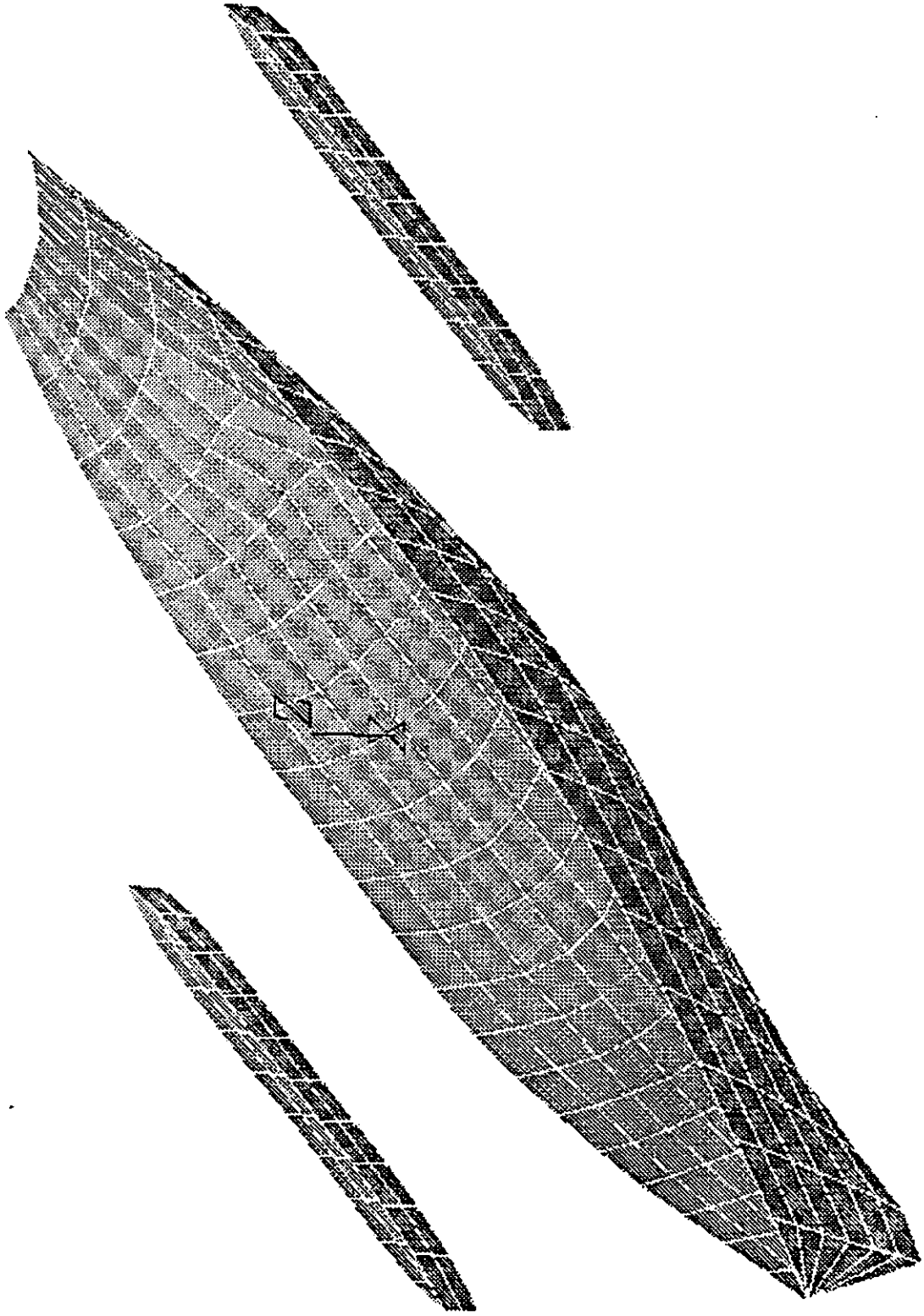

Fig.1(c) Wetted surface panel idealisation for model F (360) panels.

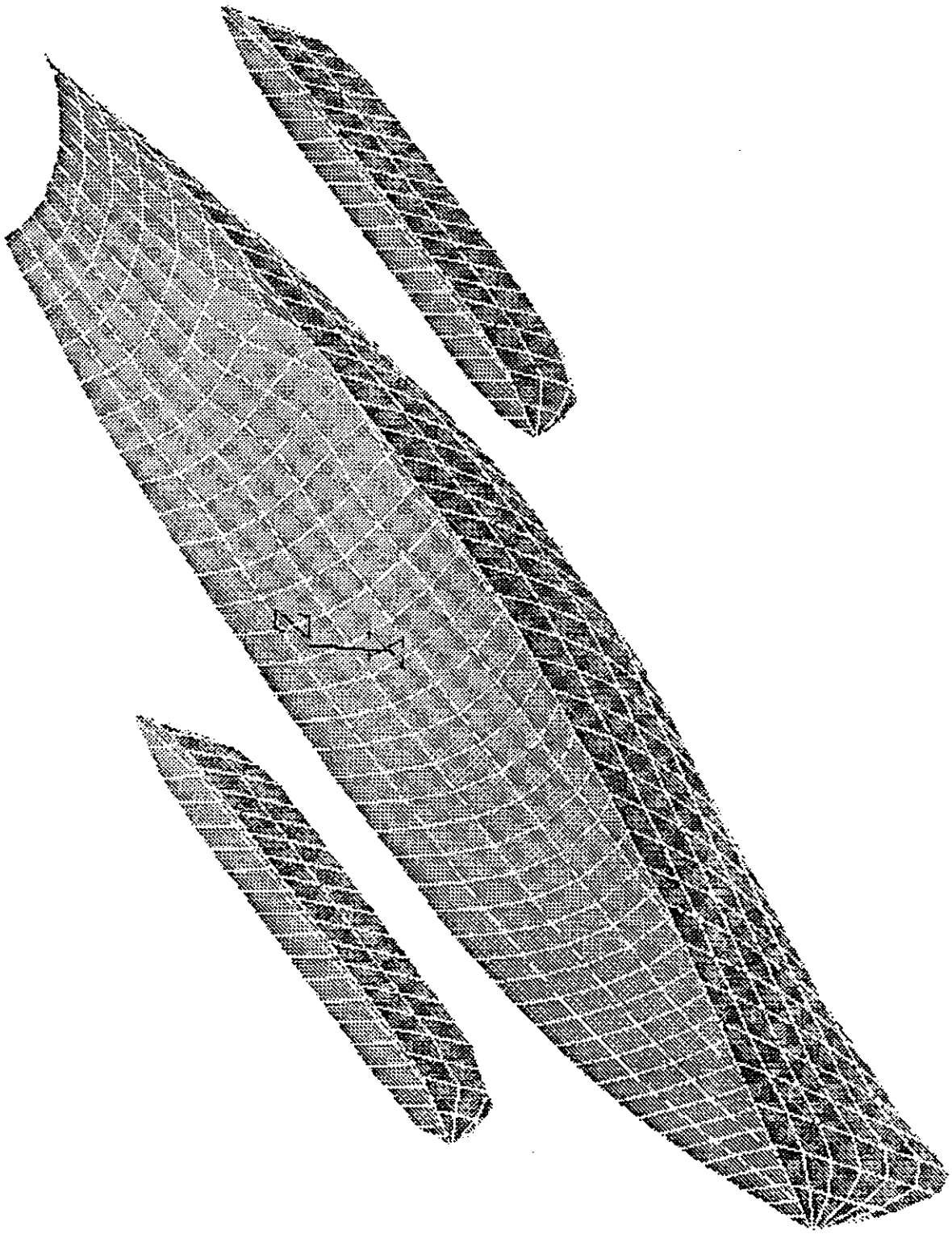

Fig.1(d) Refined wetted surface panel idealisation for model A (720) panels.

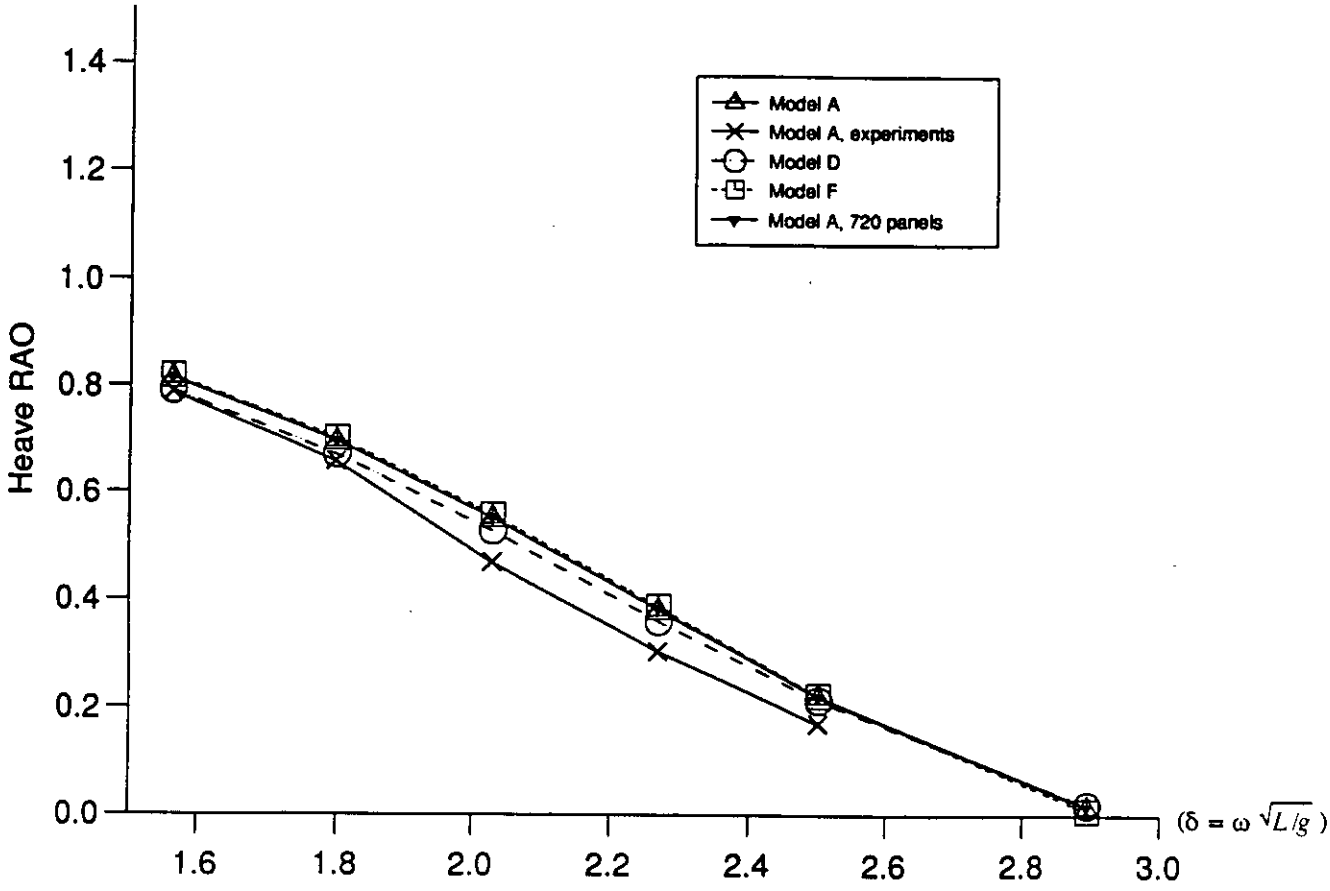

Fig.2(a) Heave RAOs for Trimaran models A, D and F; Fn=0.24, heading 0 deg.

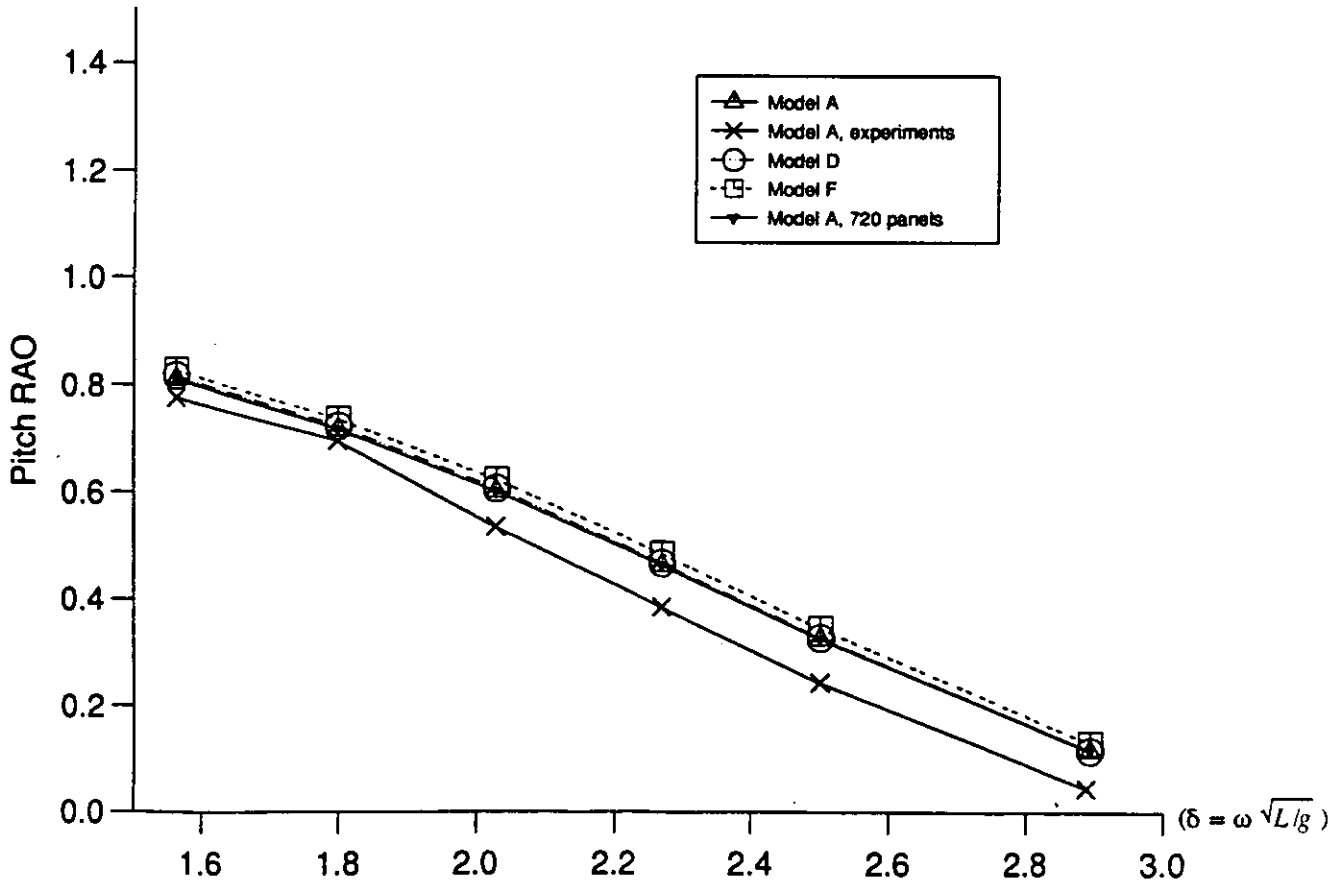

Fig.3(a) Pitch RAOs for Trimaran models A, D and F; Fn=0.24, heading 0 deg.

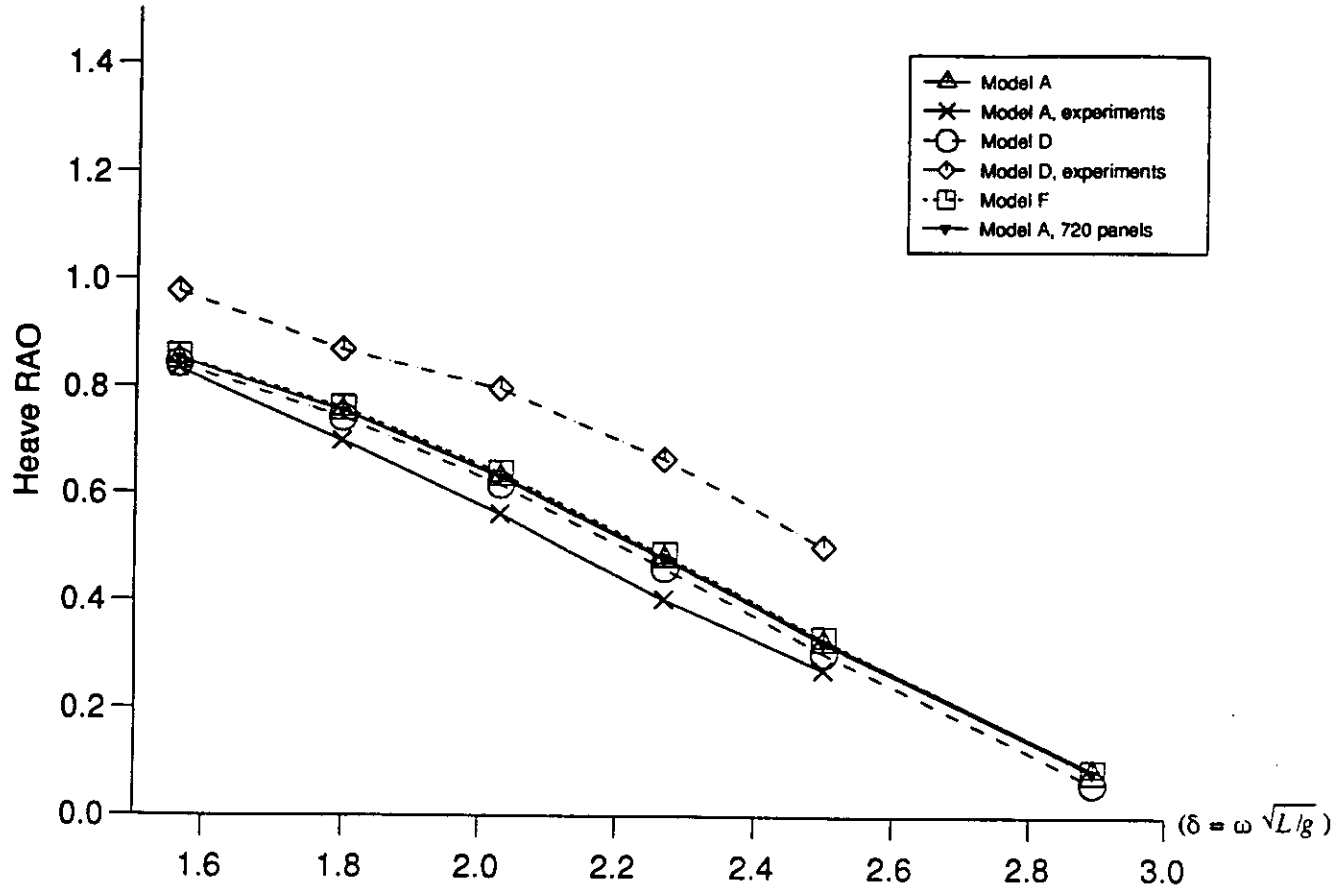

Fig.2(b) Heave RAOs for Trimaran models A, D and F; Fn=0.24, heading 30 deg.

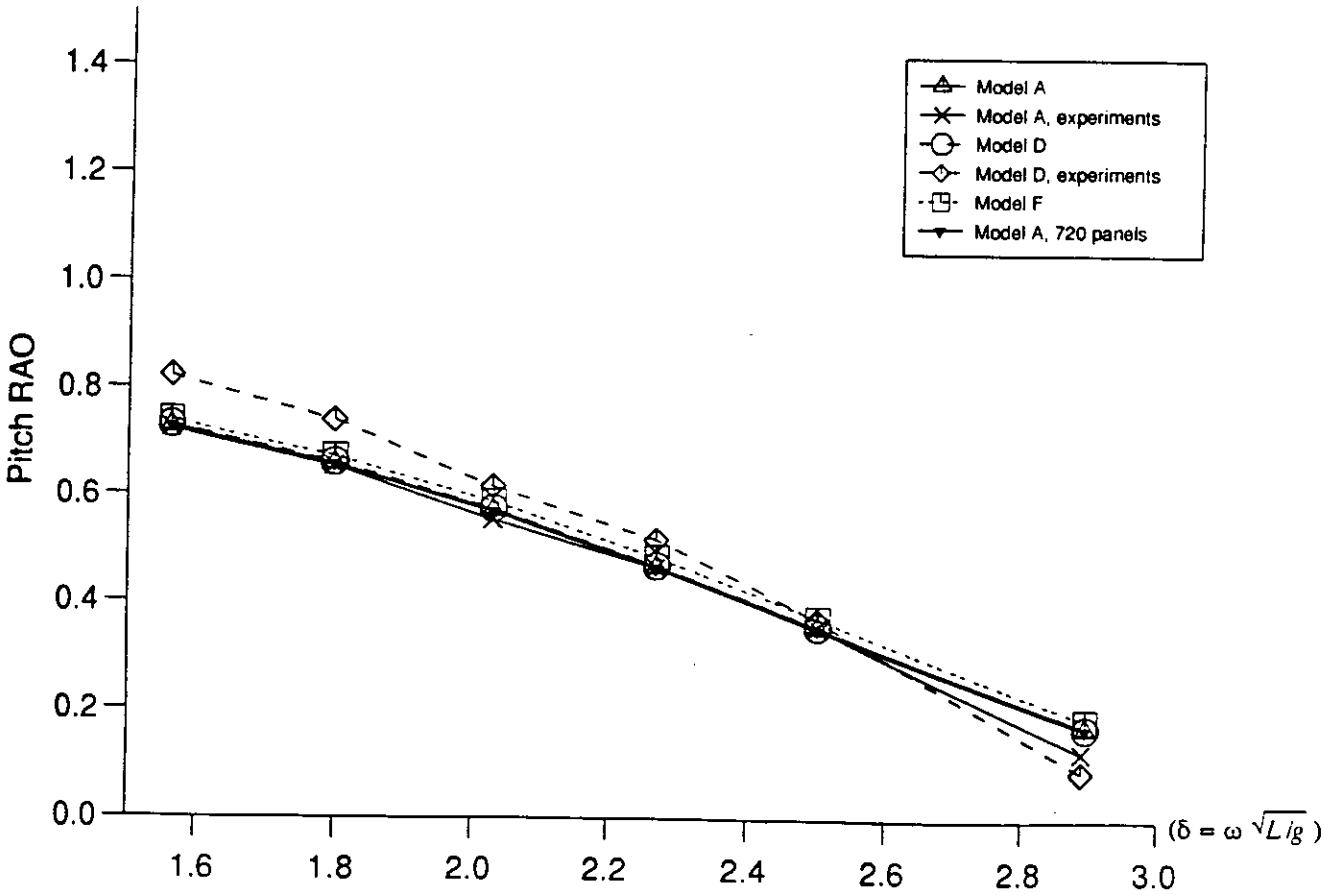

Fig.3(b) Pitch RAOs for Trimaran models A, D and F; Fn=0.24, heading 30 deg.

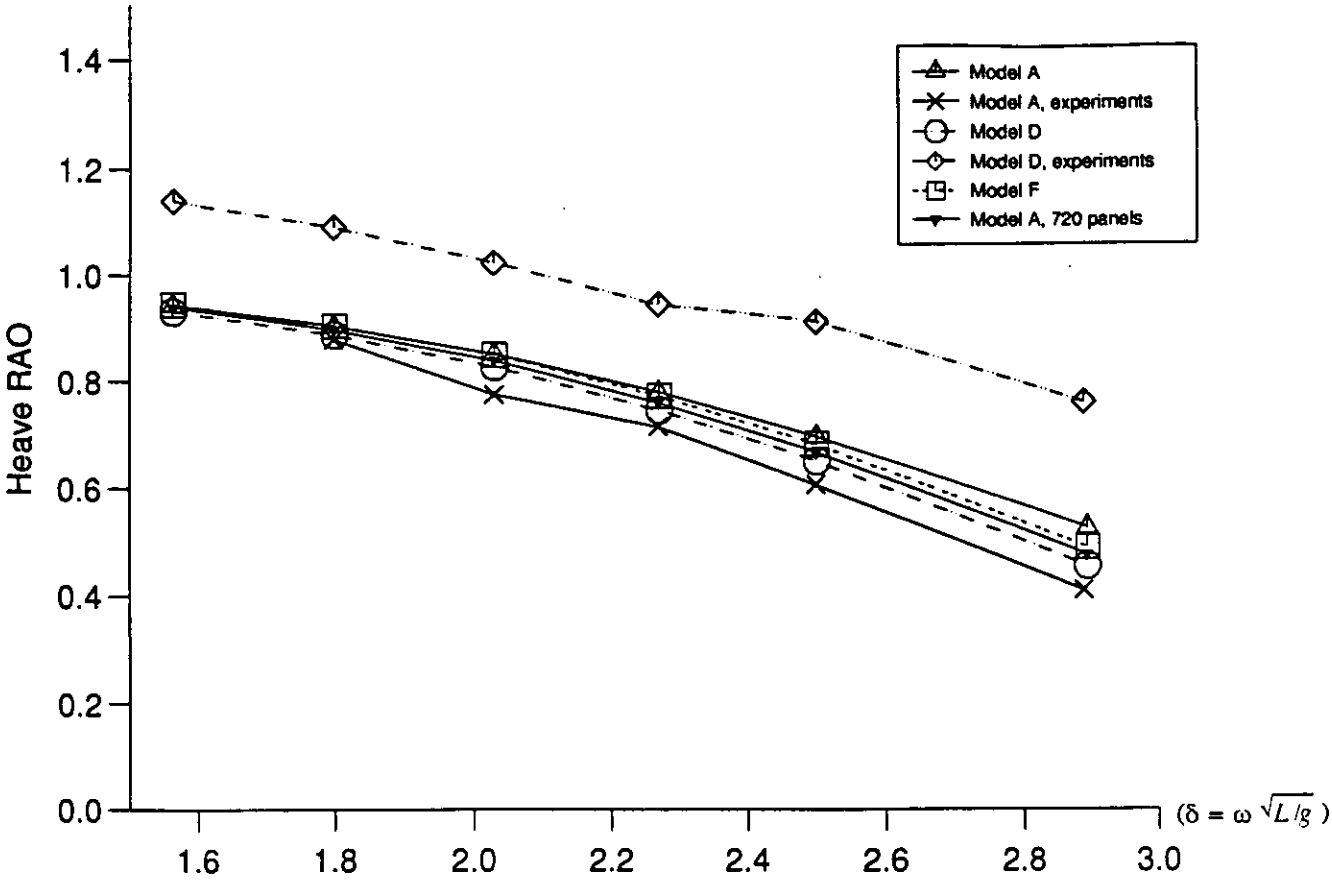

Fig.2(c) Heave RAOs for Trimaran models A, D and F; Fn=0.24, heading 60 deg.

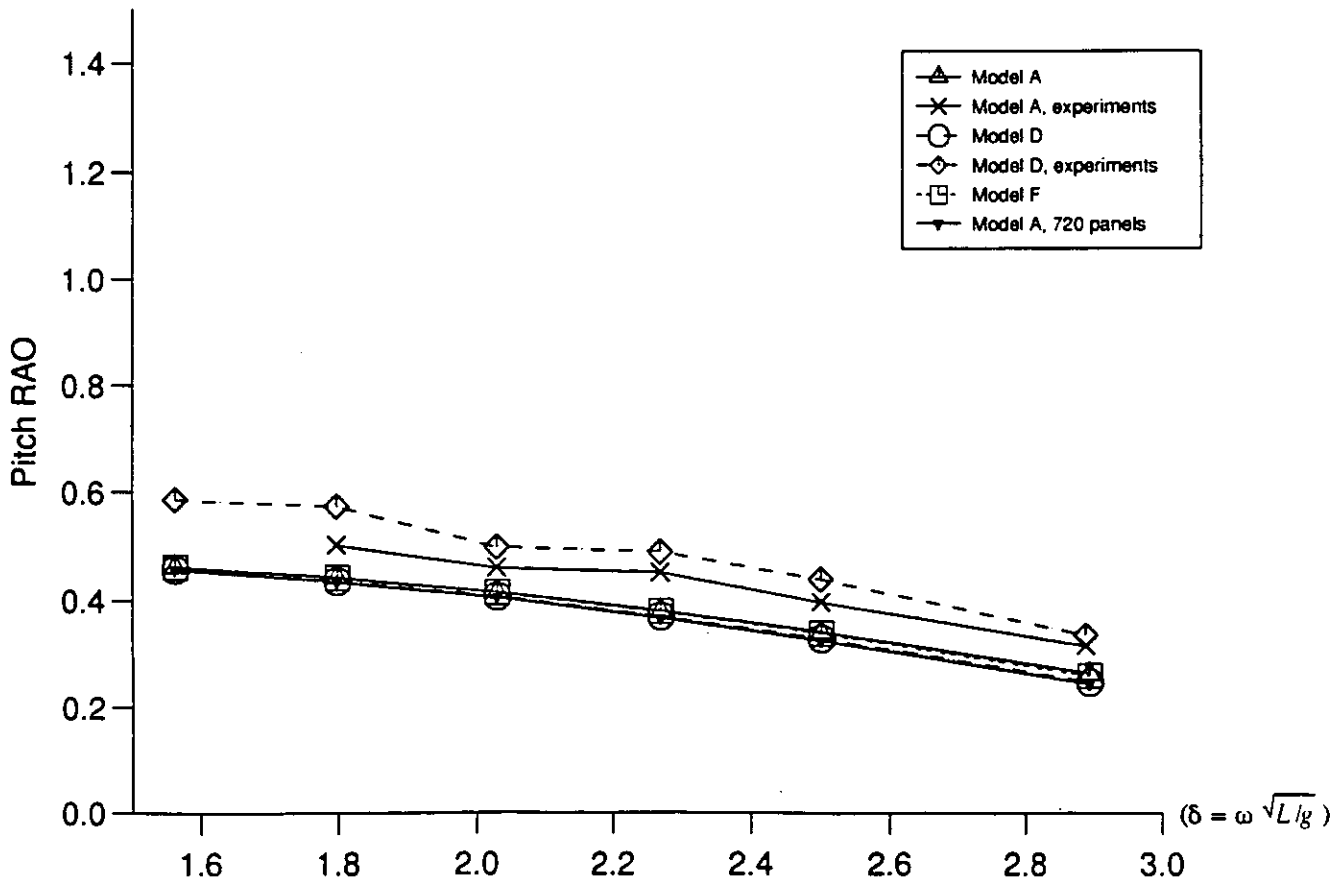

Fig.3(c) Pitch RAOs for Trimaran models A, D and F; Fn=0.24, heading 60 deg.

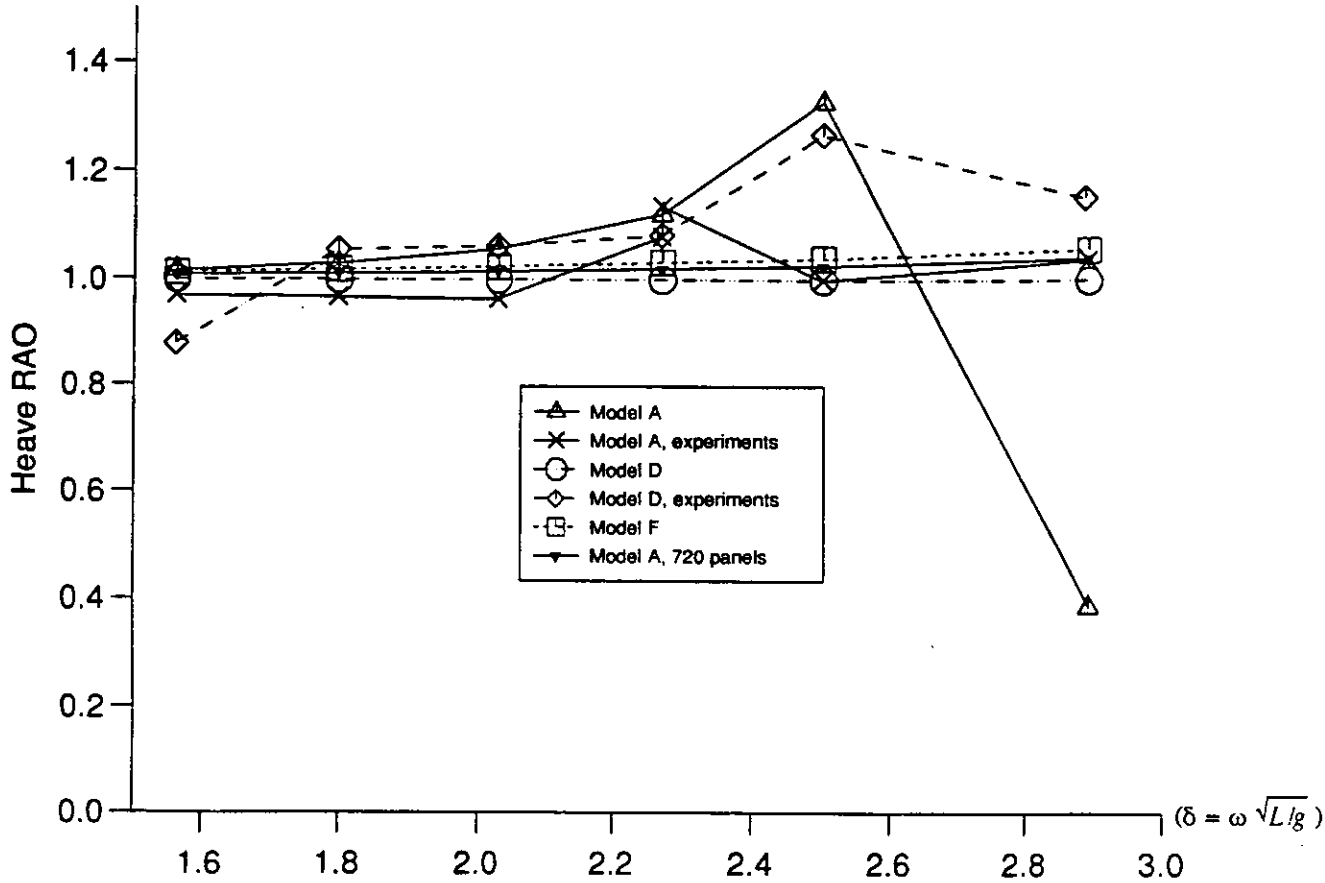

Fig.2(d) Heave RAOs for Trimaran models A, D and F; Fn=0.24, heading 90 deg.

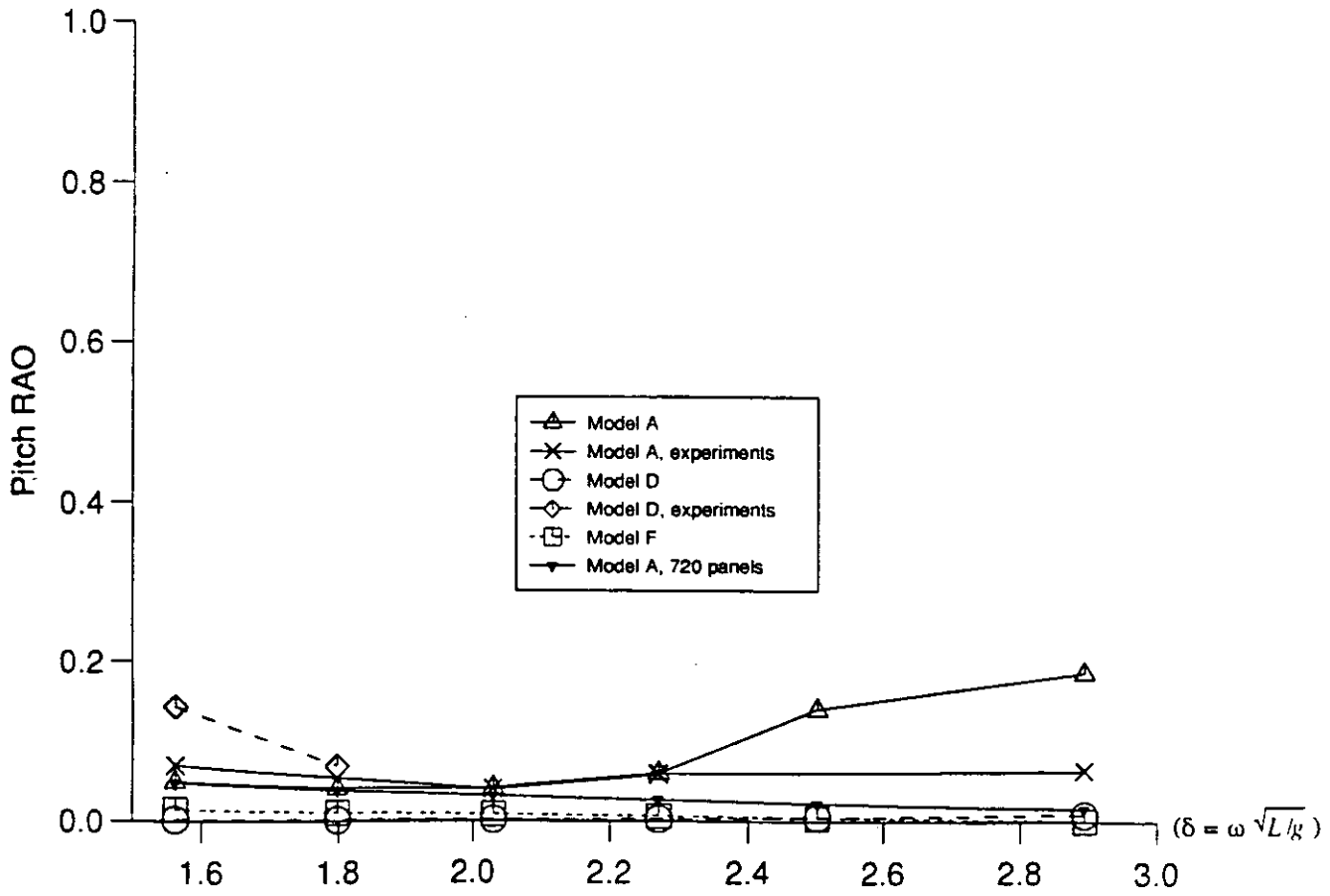

Fig.3(d) Pitch RAOs for Trimaran models A, D and F; Fn=0.24, heading 90 deg.

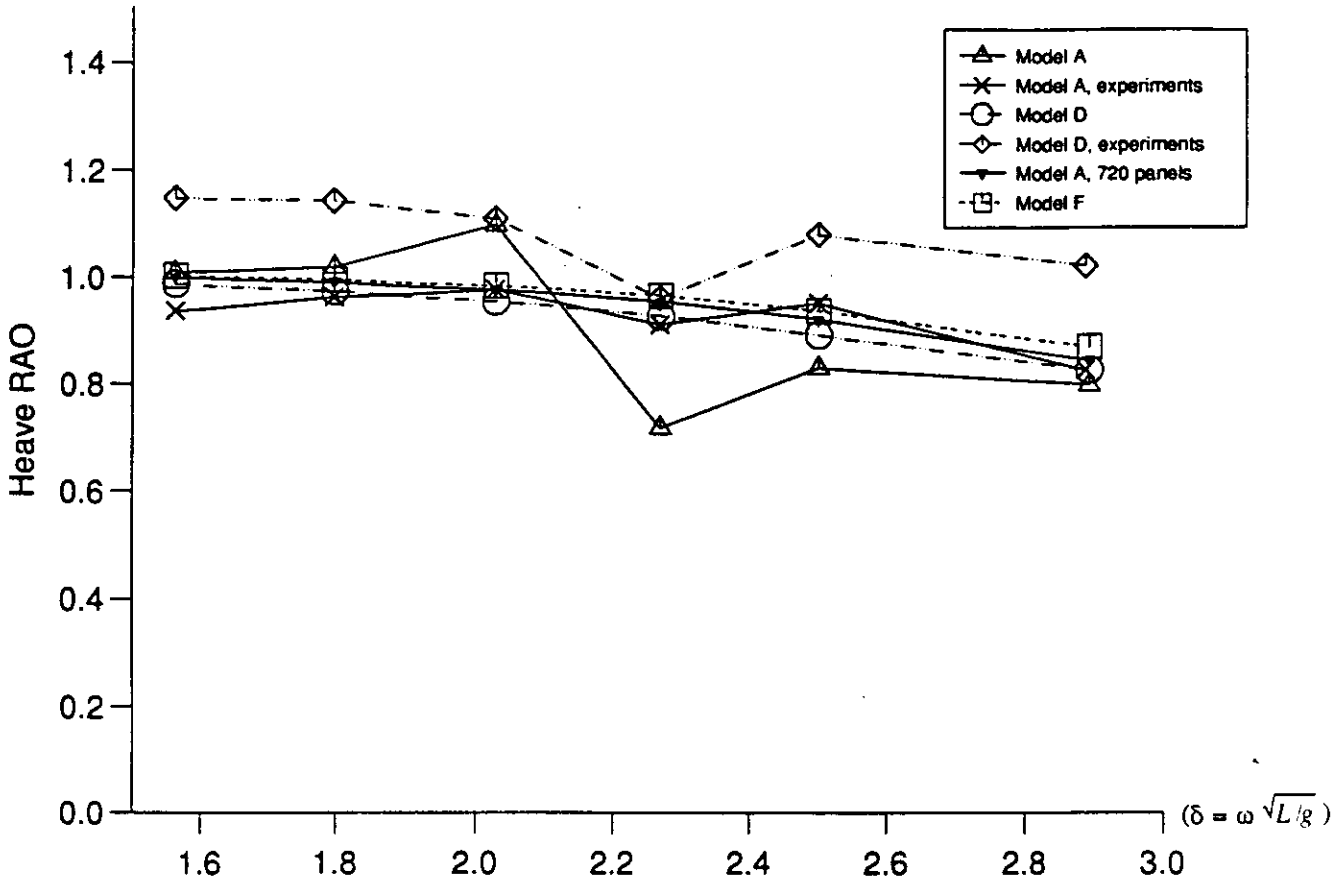

Fig.2(e) Heave RAOs for Trimaran models A, D and F; Fn=0.24, heading 120 deg.

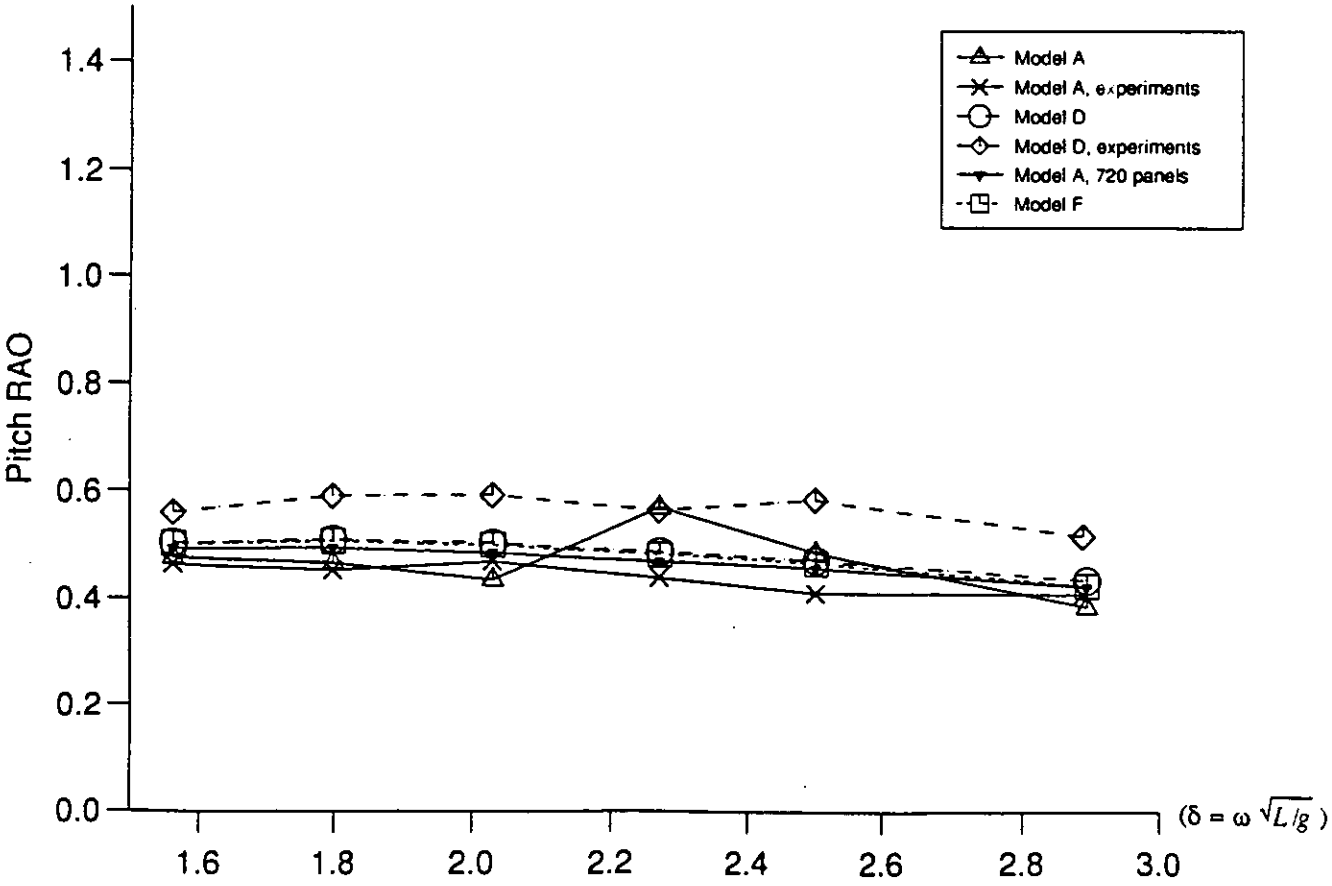

Fig.3(e) Pitch RAOs for Trimaran models A, D and F; Fn=0.24, heading 120 deg.

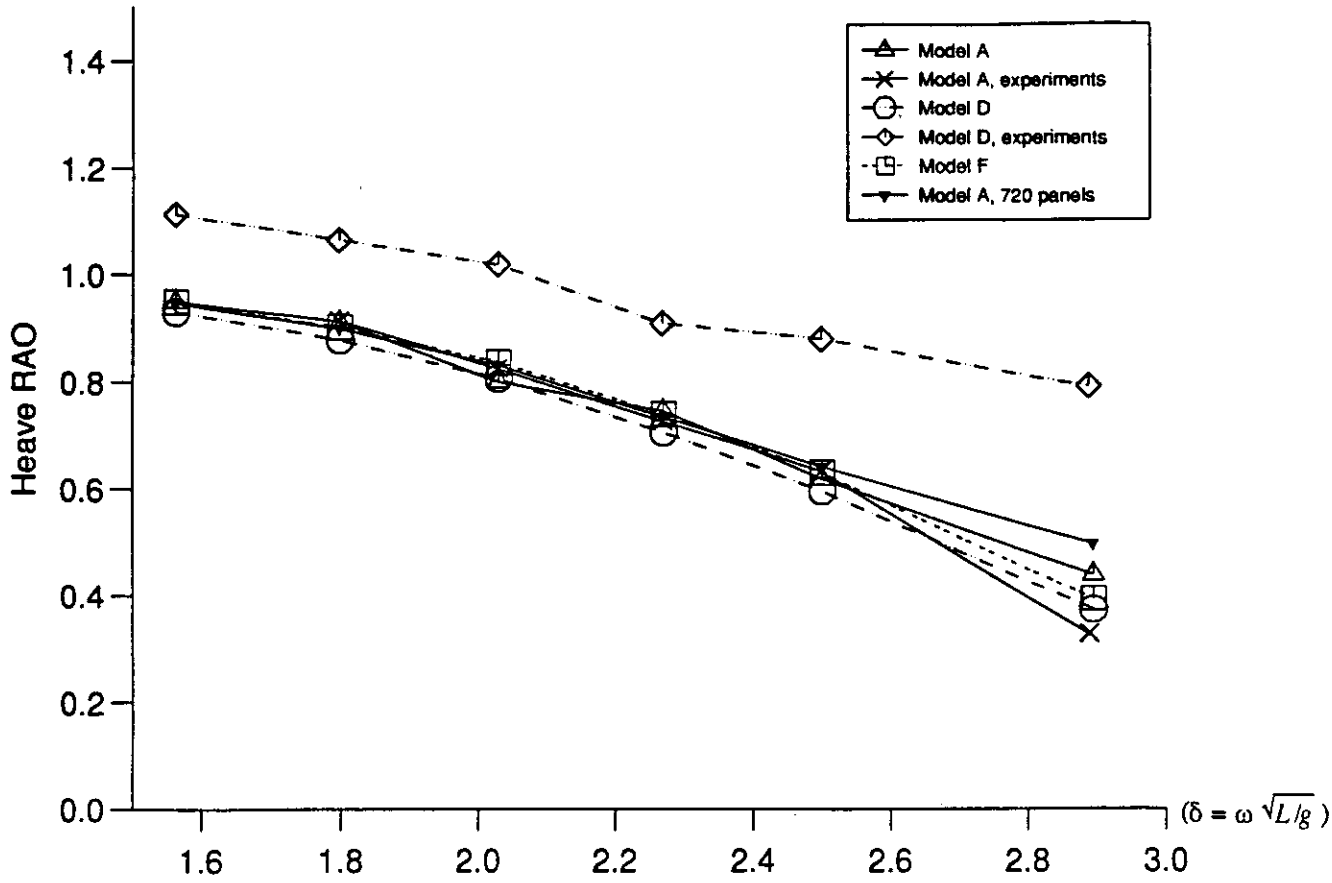

Fig.2(f) Heave RAOs for Trimaran models A, D and F; Fn=0.24, heading 150 deg.

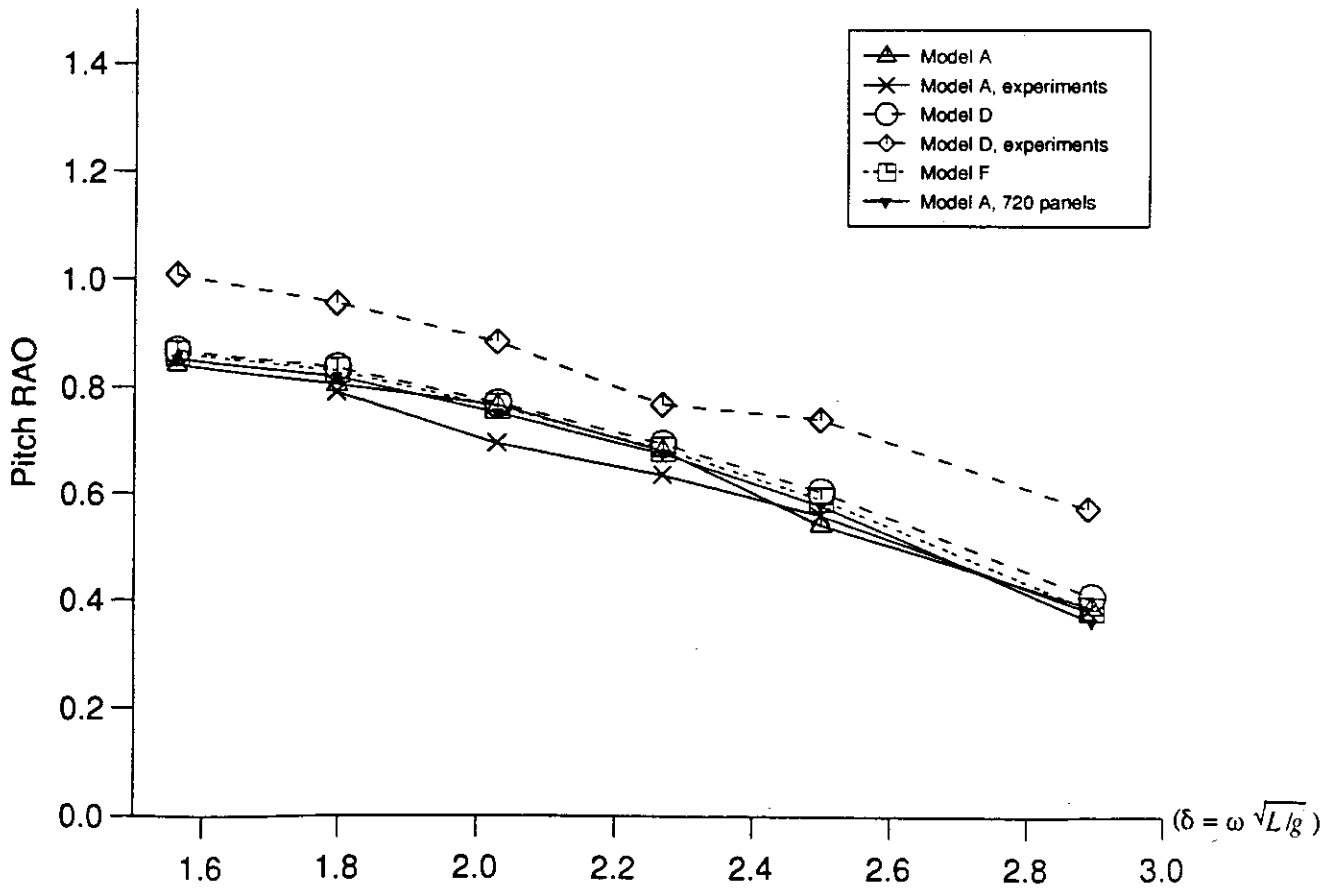

Fig.3(f) Pitch RAOs for Trimaran models A, D and F; Fn=0.24, heading 150 deg.

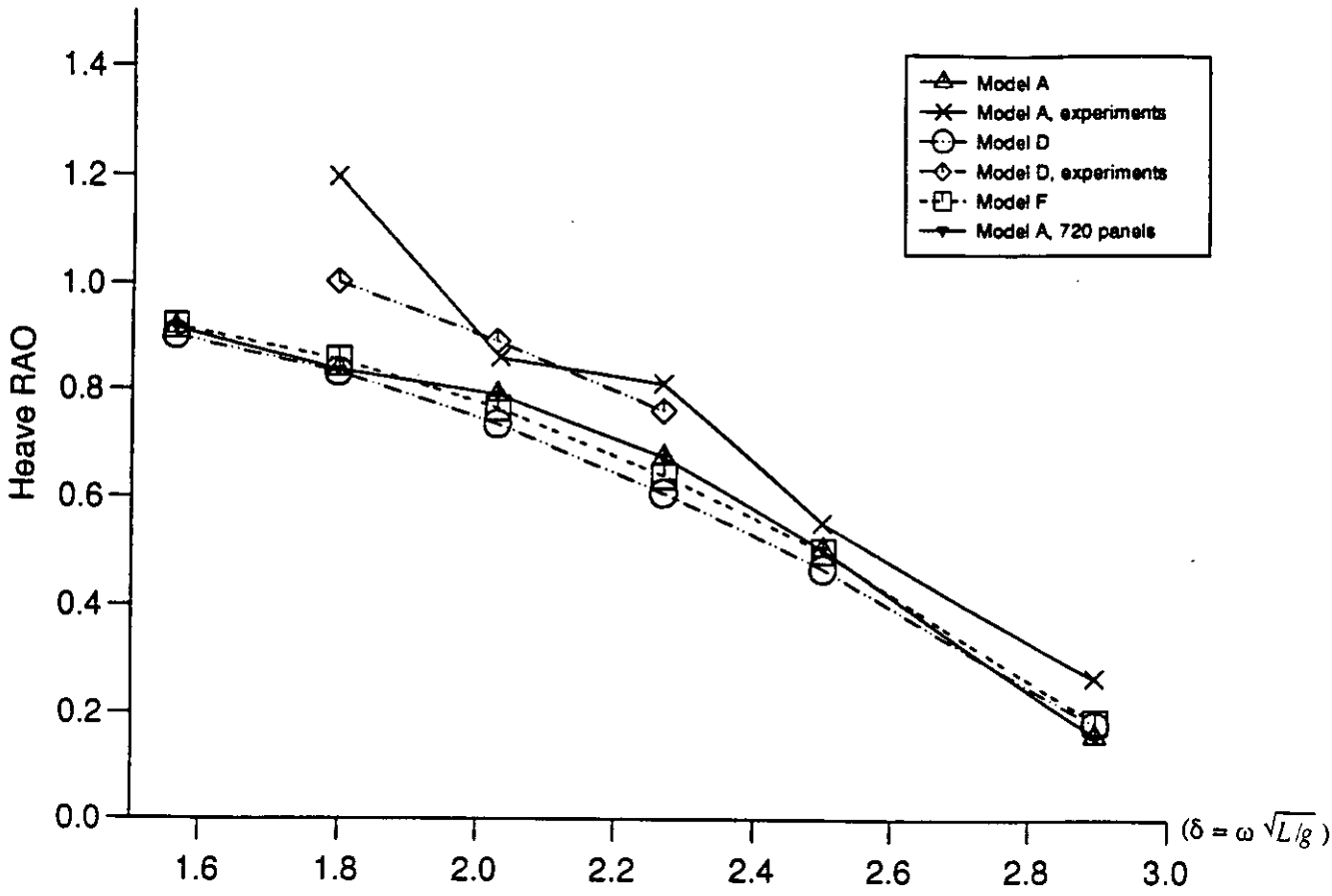

Fig.2(g) Heave RAOs for Trimaran models A, D and F; Fn=0.24, heading 180 deg.

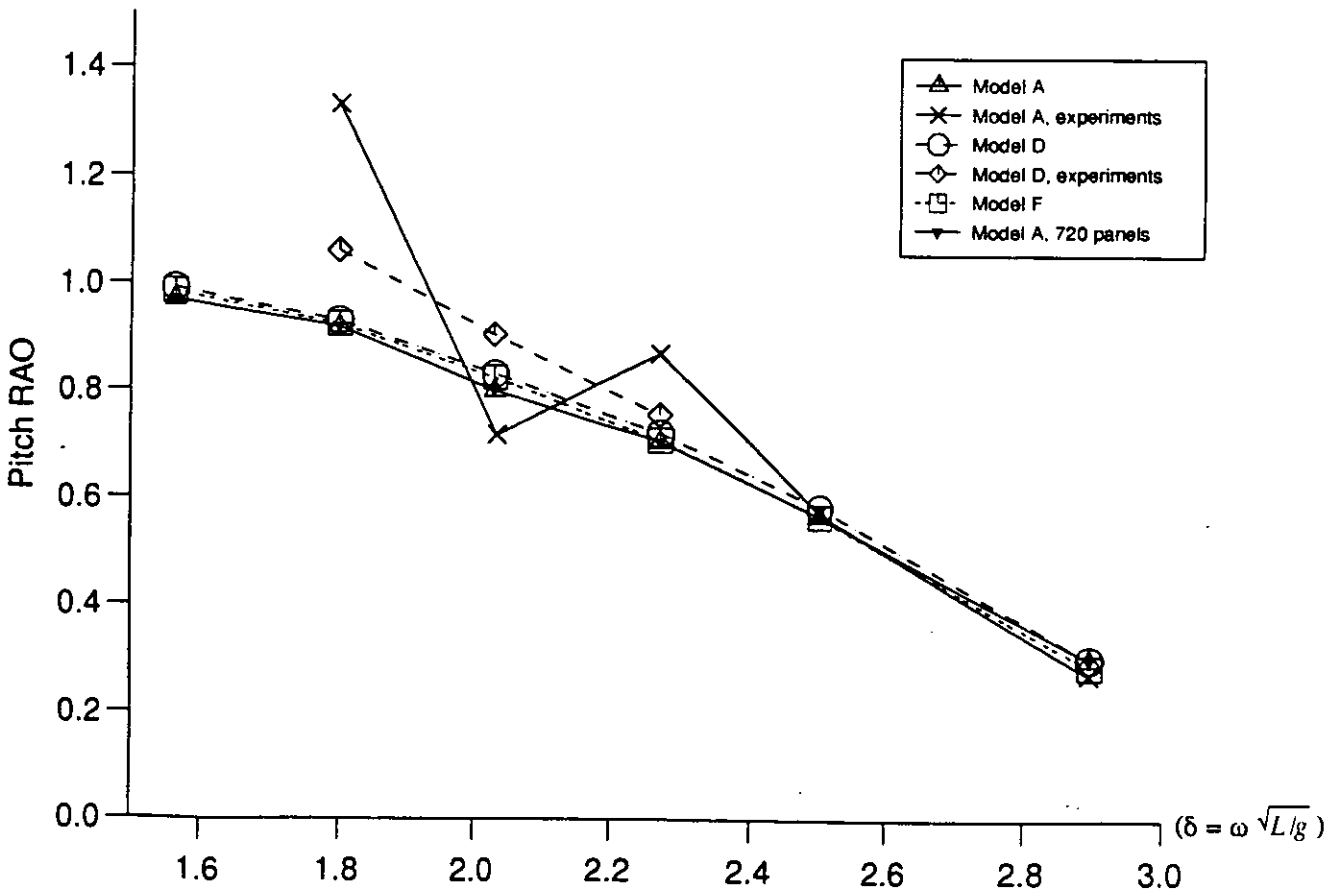

Fig.3(g) Pitch RAOs for Trimaran models A, D and F; Fn=0.24, heading 180 deg.

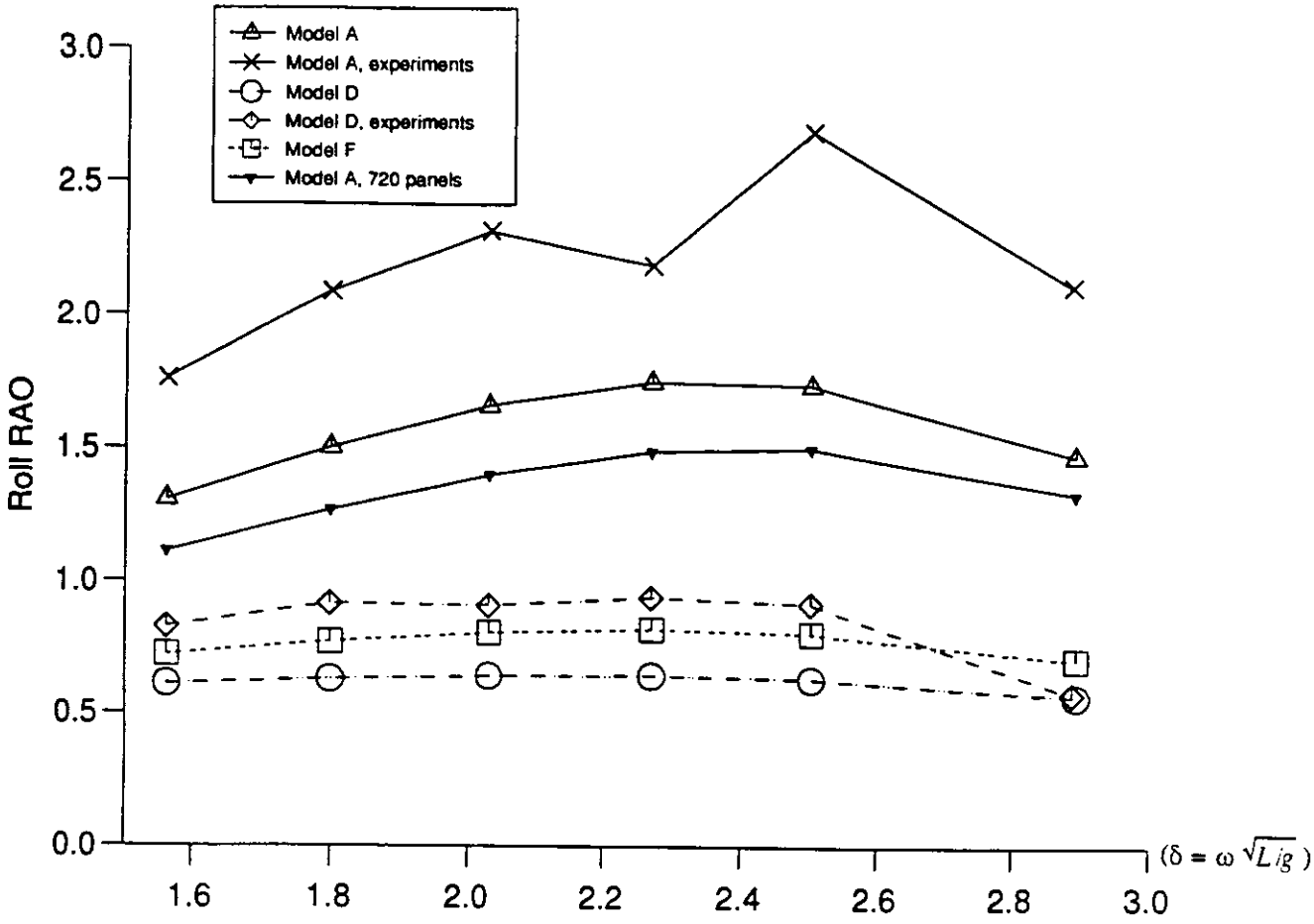

Fig.4(a) Roll RAOs for Trimaran models A, D and F; Fn=0.24, heading 30 deg.

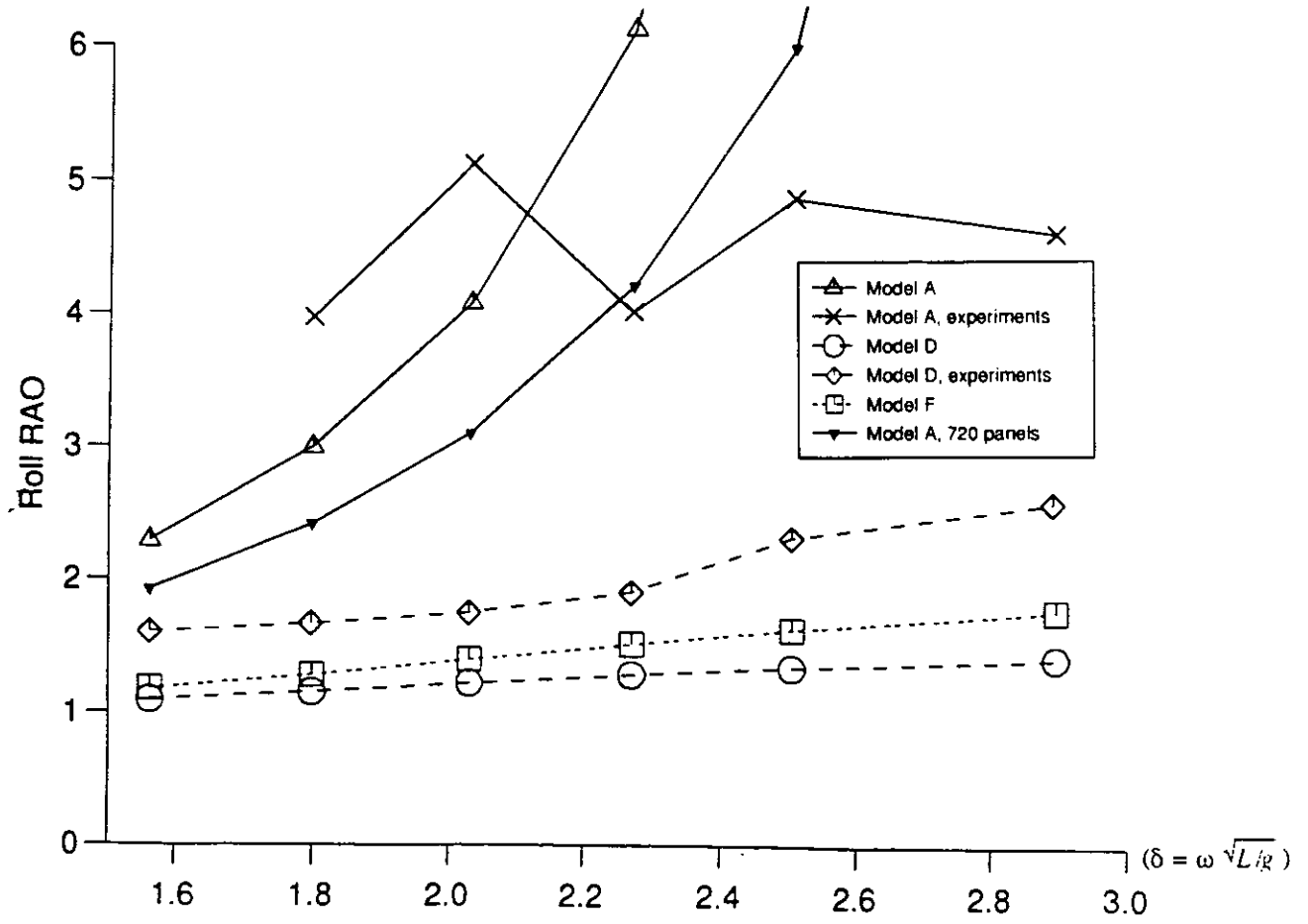

Fig.4(b) Roll RAOs for Trimaran models A, D and F; Fn=0.24, heading 60 deg.

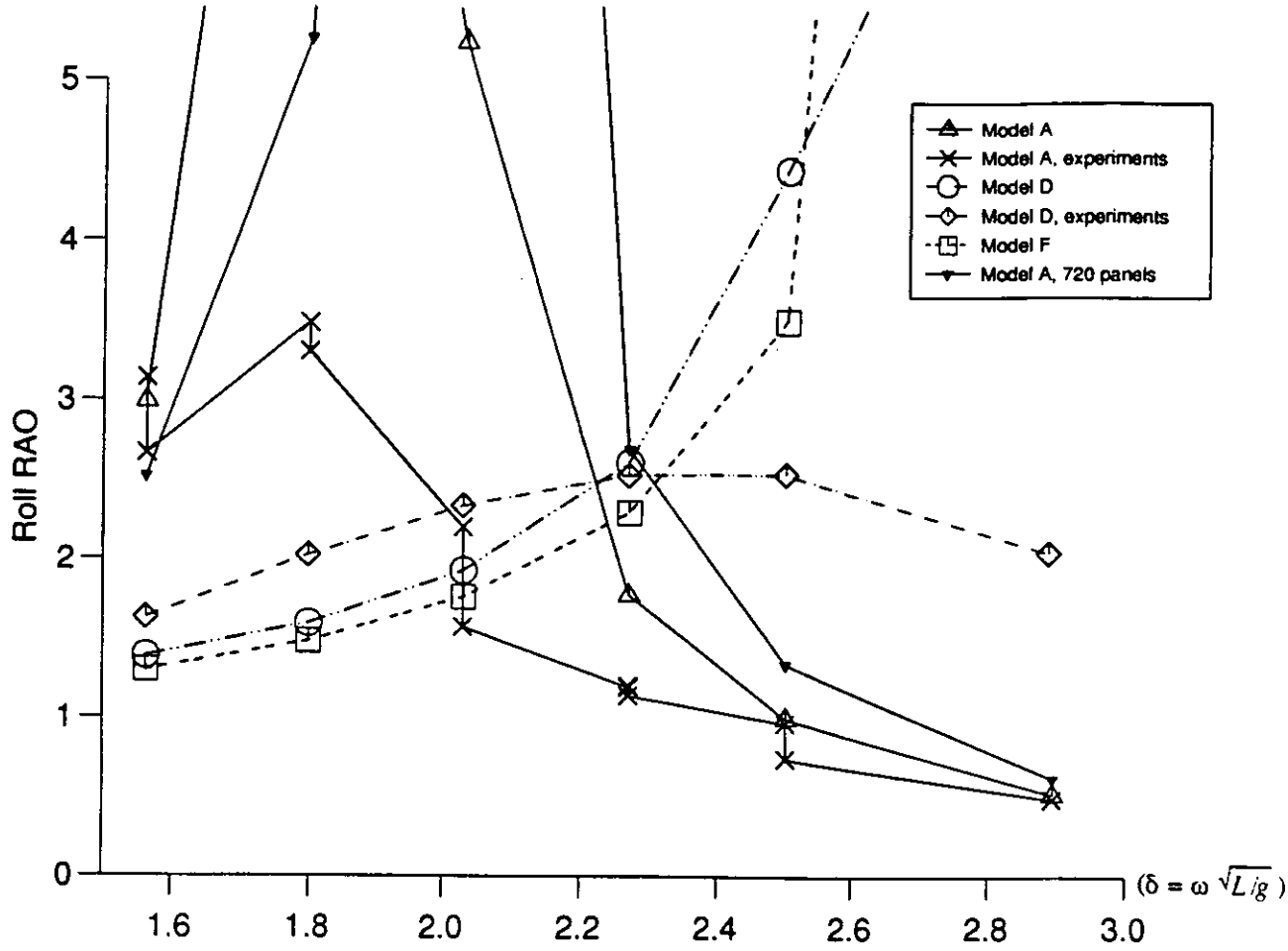

Fig.4(c) Roll RAOs for Trimaran models A, D and F; Fn=0.24, heading 90 deg.

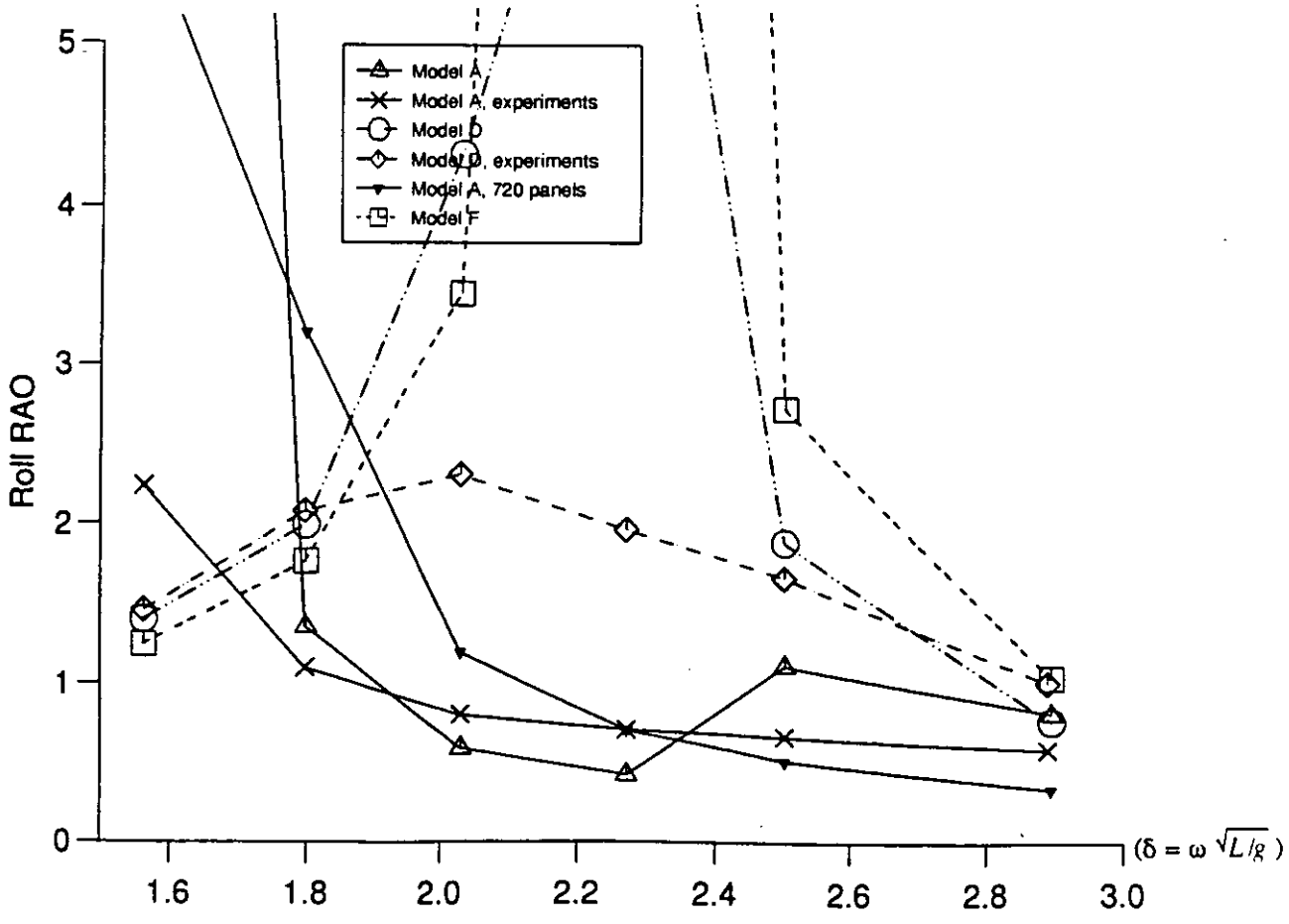

Fig.4(d) Roll RAOs for Trimaran models A, D and F; Fn=0.24, heading 120 deg.

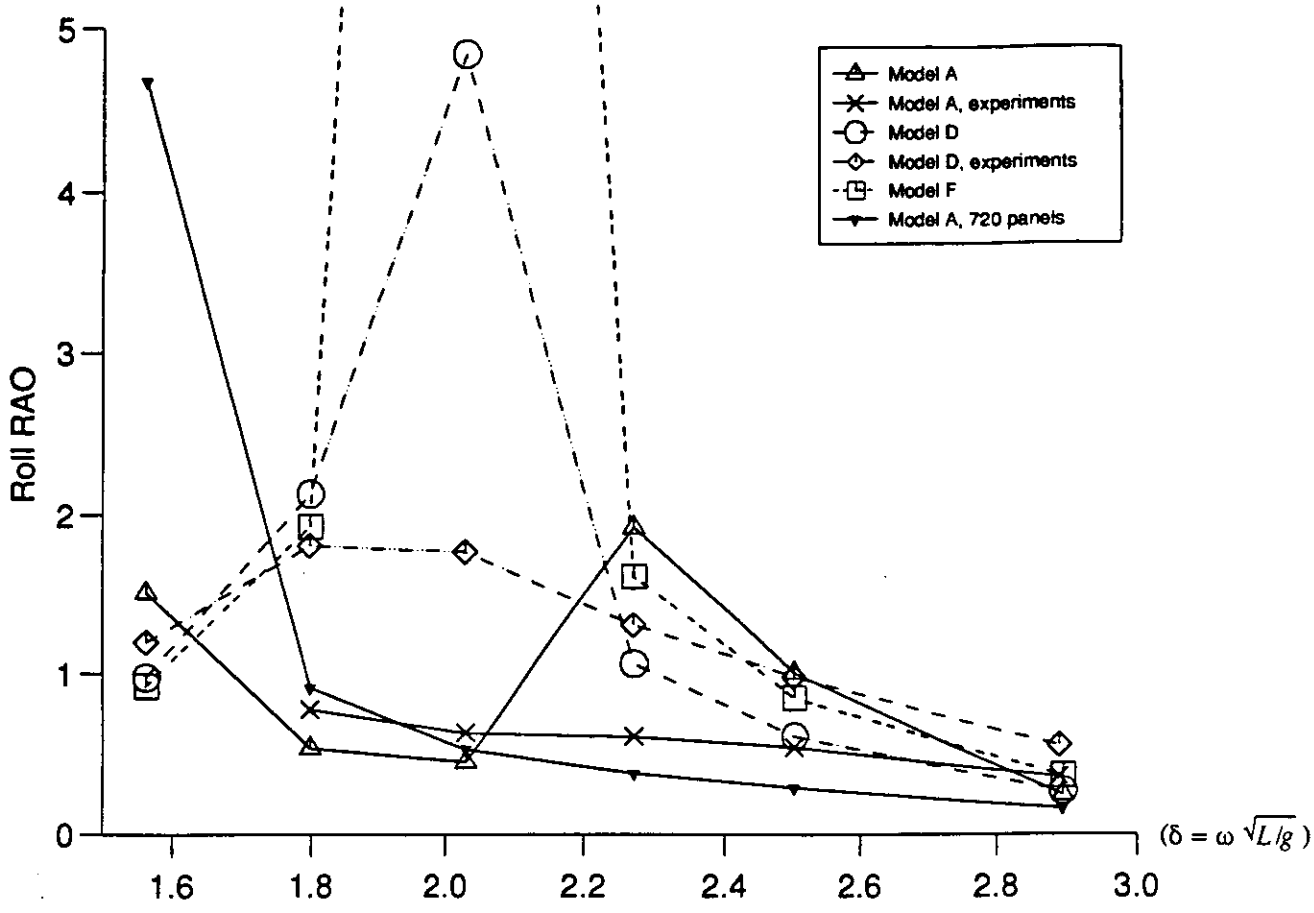

Fig.4(e) Roll RAOs for Trimaran models A, D and F; Fn=0.24, heading 150 deg.

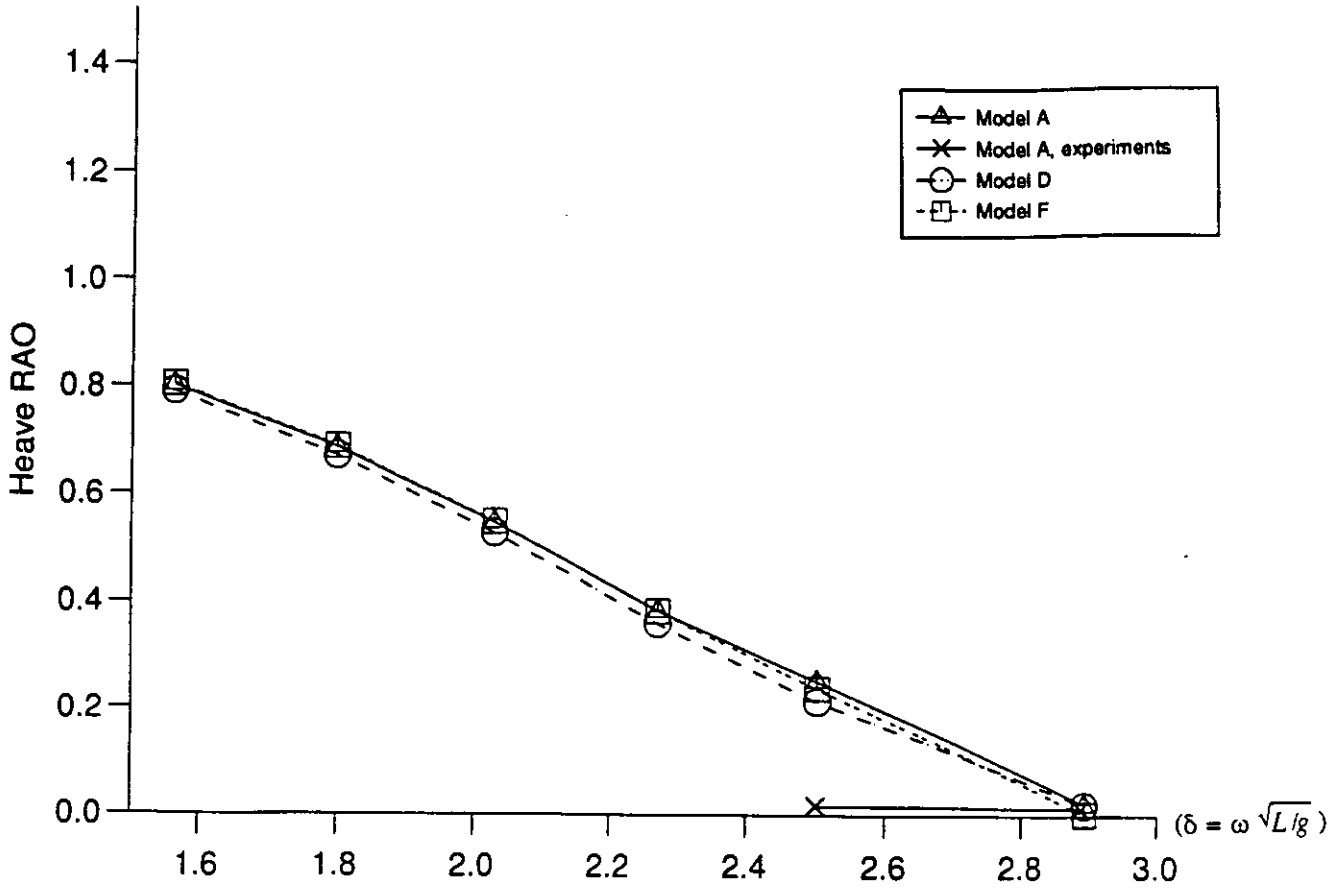

Fig.5(a) Heave RAOs for Trimaran models A, D and F; Fn=0.40, heading 0 deg.

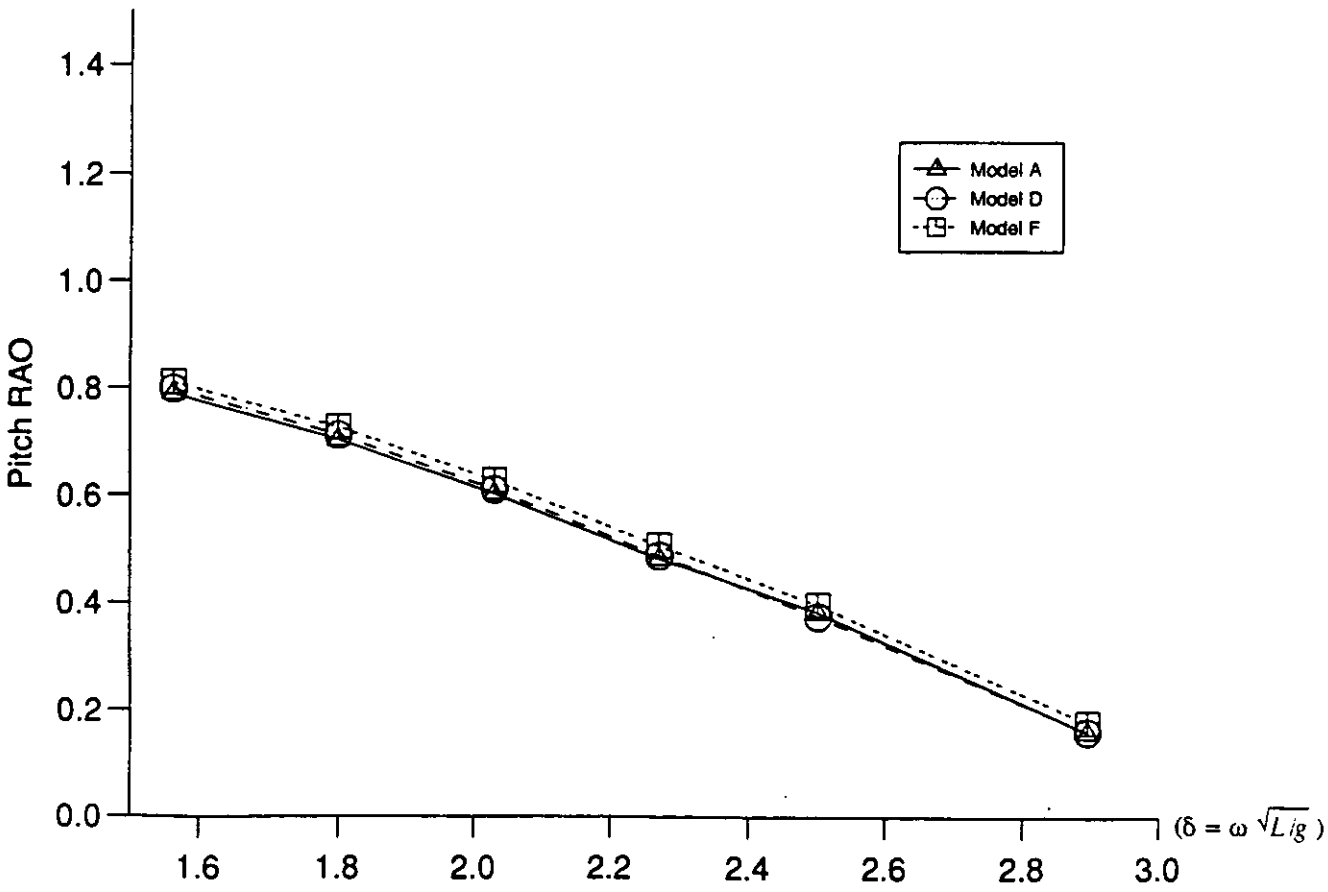

Fig.6(a) Pitch RAOs for Trimaran models A, D and F; Fn=0.40, heading 0 deg.

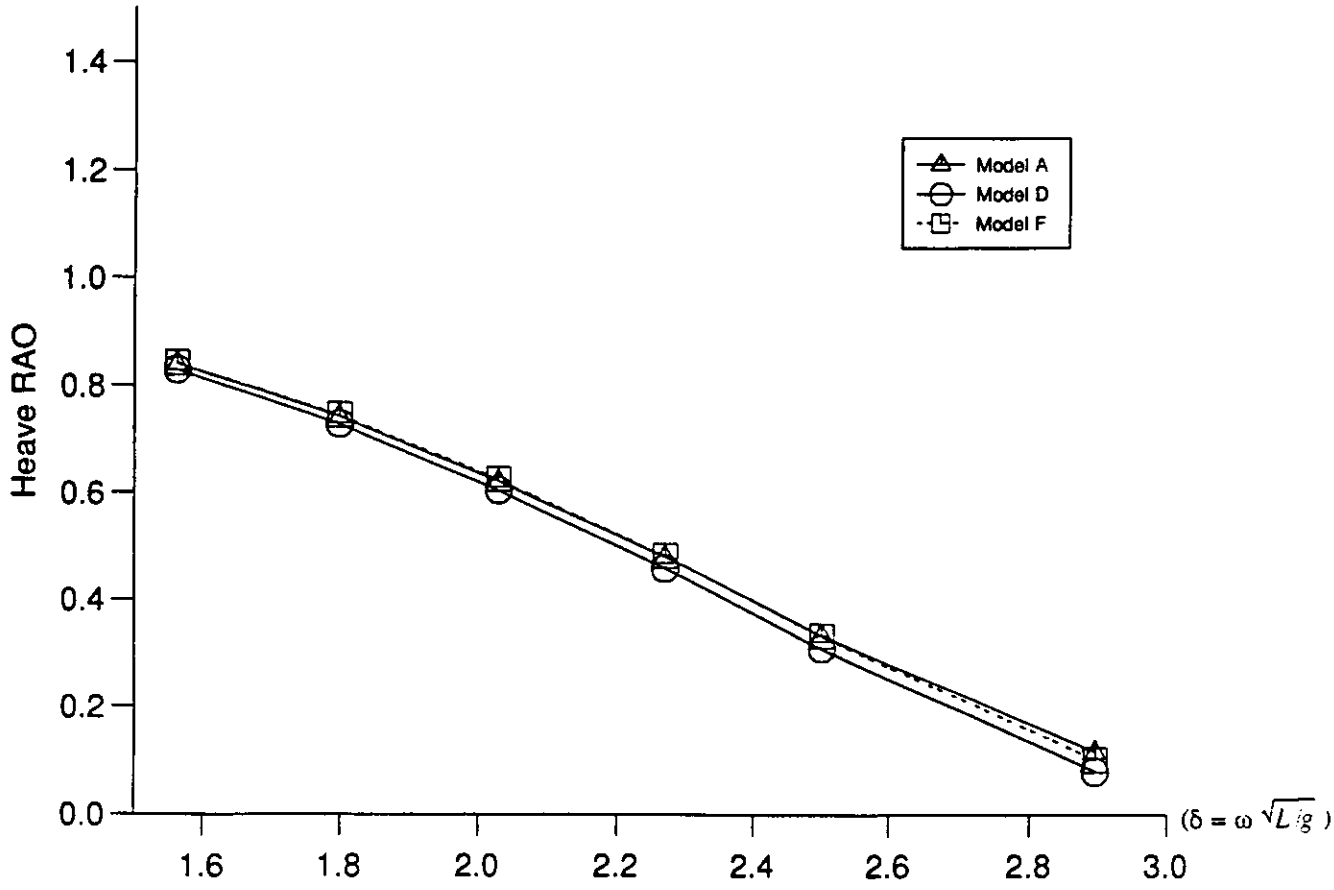

Fig.5(b) Heave RAOs for Trimaran models A, D and F; Fn=0.40, heading 30 deg.

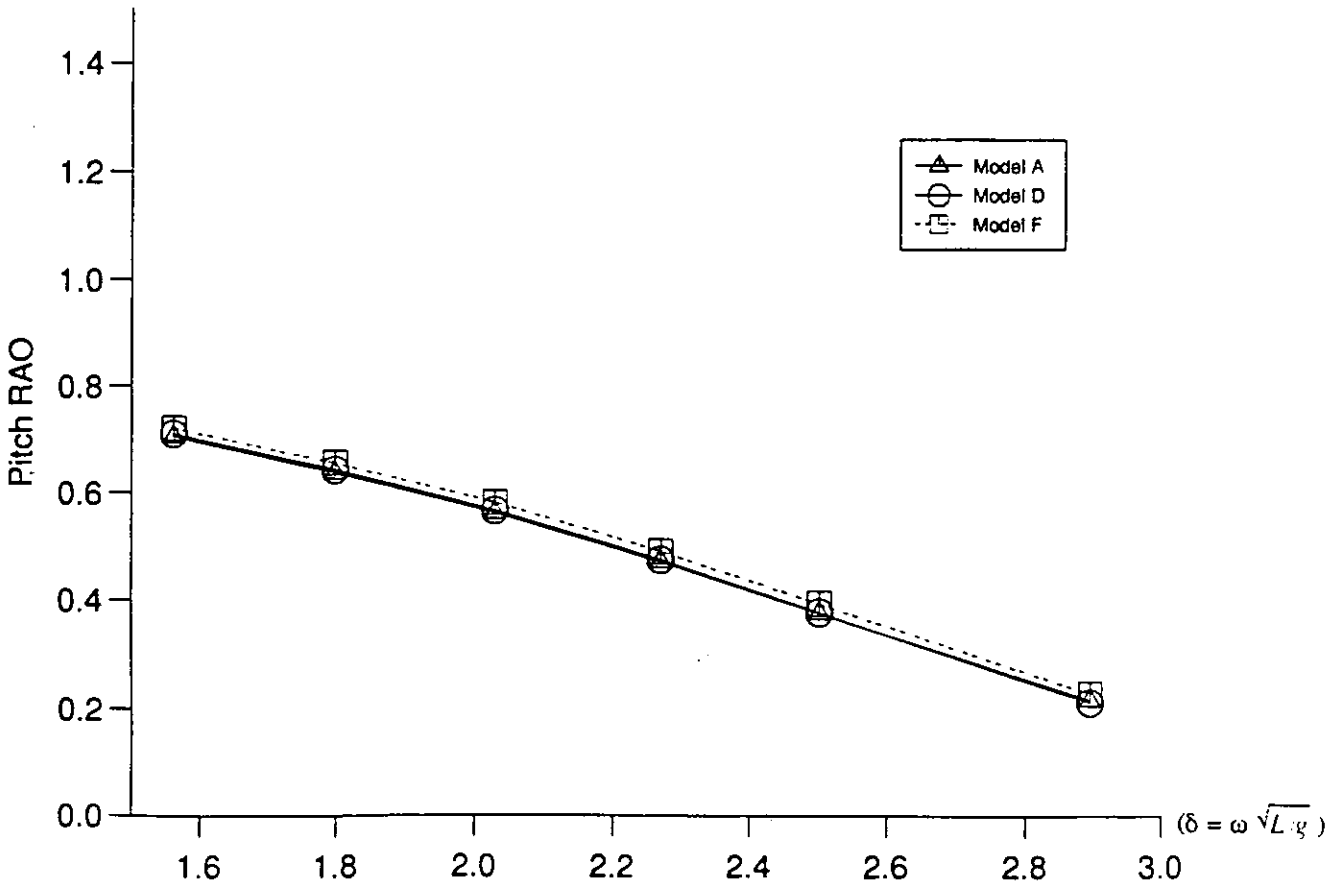

Fig.6(b) Pitch RAOs for Trimaran models A, D and F; Fn=0.40, heading 30 deg.

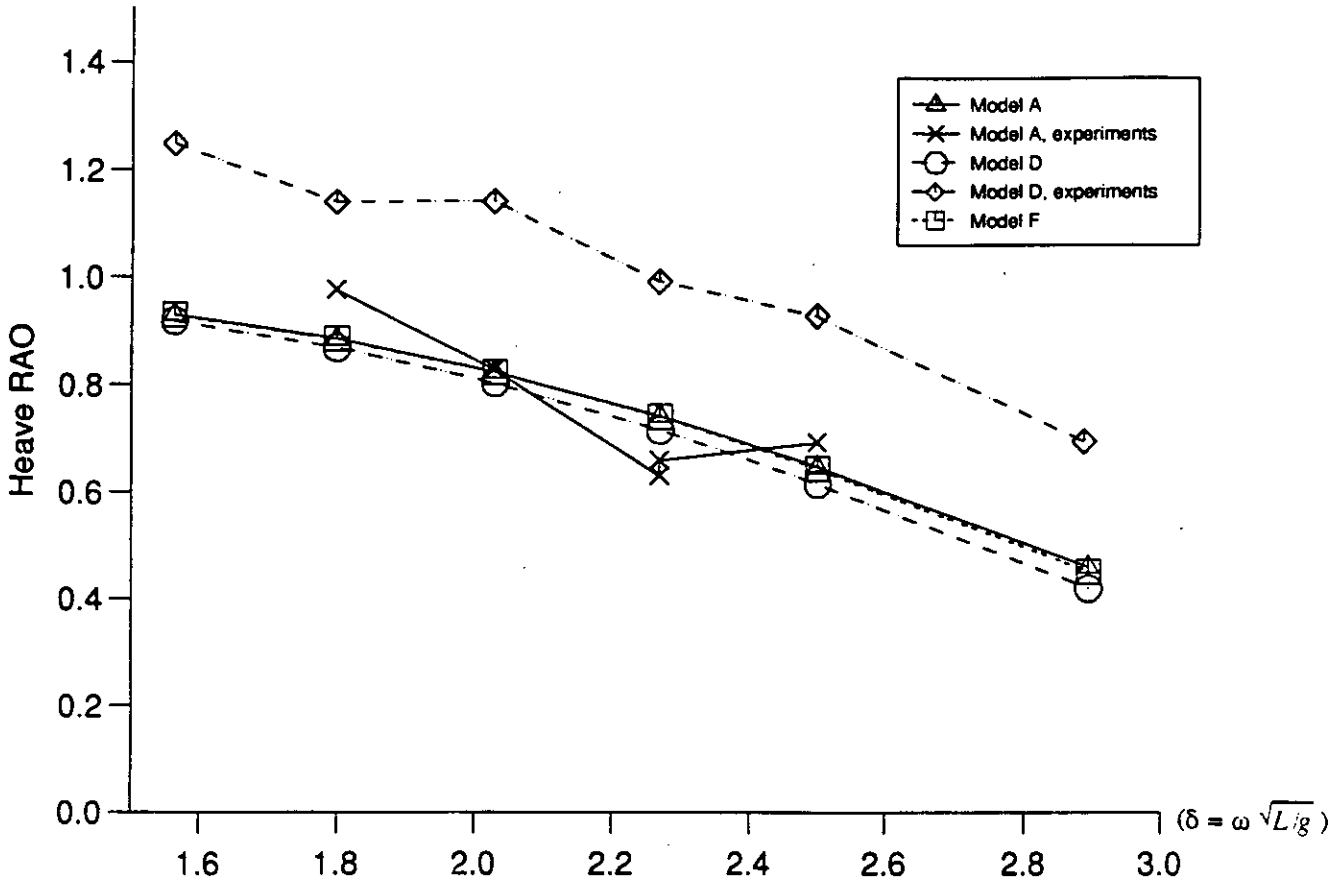

Fig.5(c) Heave RAOs for Trimaran models A, D and F; Fn=0.40, heading 60 deg.

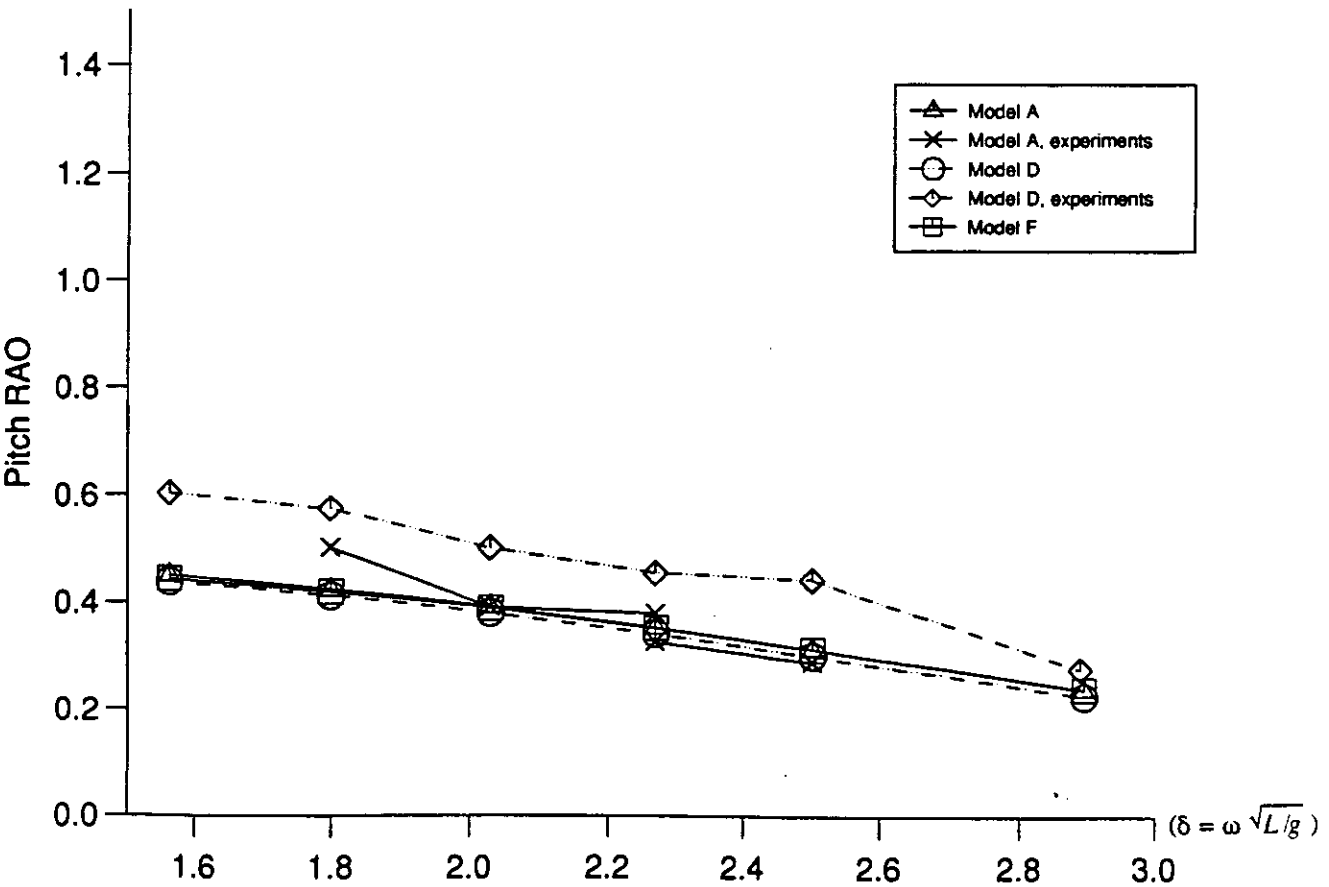

Fig.6(c) Pitch RAOs for Trimaran models A, D and F; Fn=0.40, heading 60 deg.

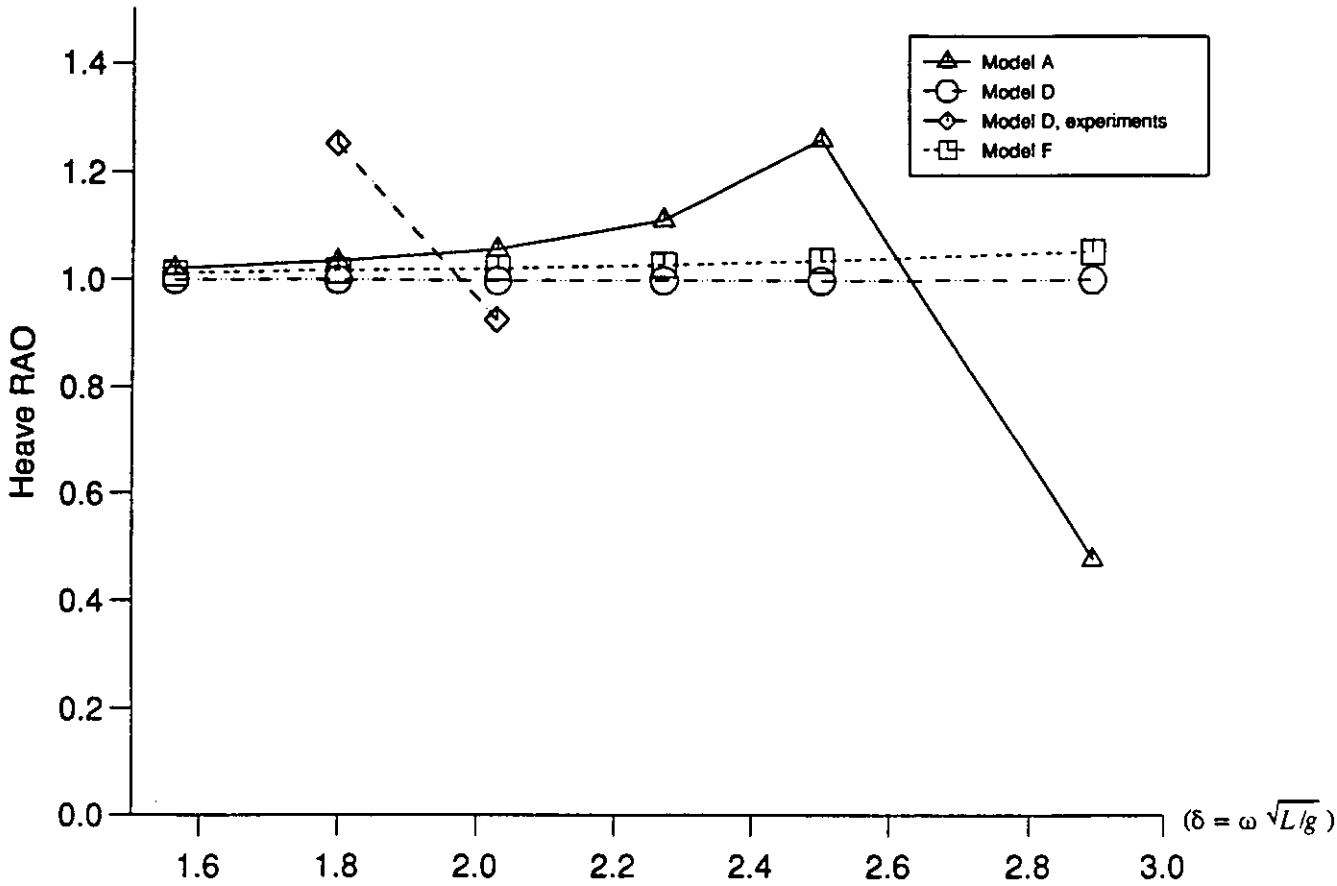

Fig.5(d) Heave RAOs for Trimaran models A, D and F; Fn=0.40, heading 90 deg.

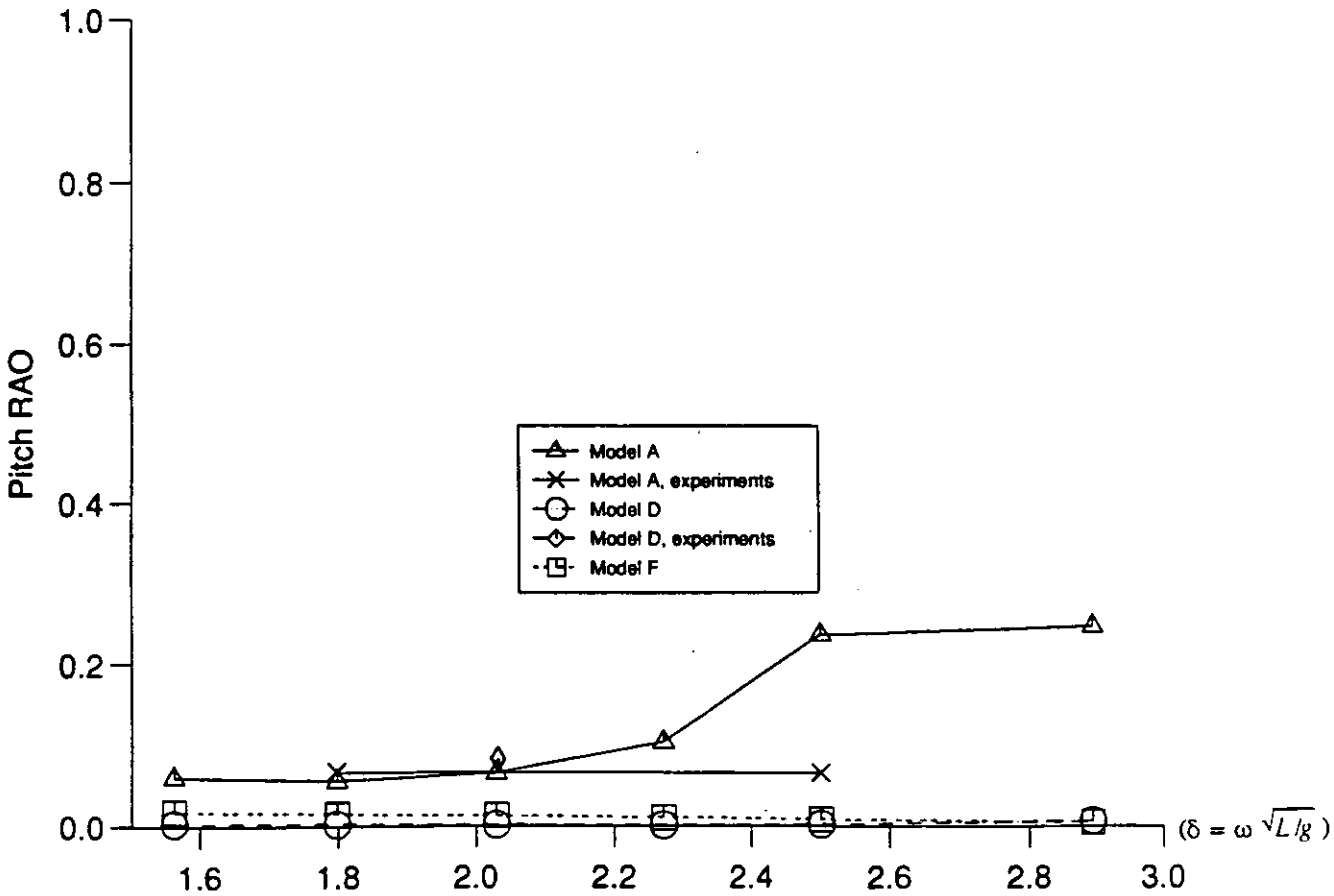

Fig.6(d) Pitch RAOs for Trimaran models A, D and F; Fn=0.40, heading 90 deg.

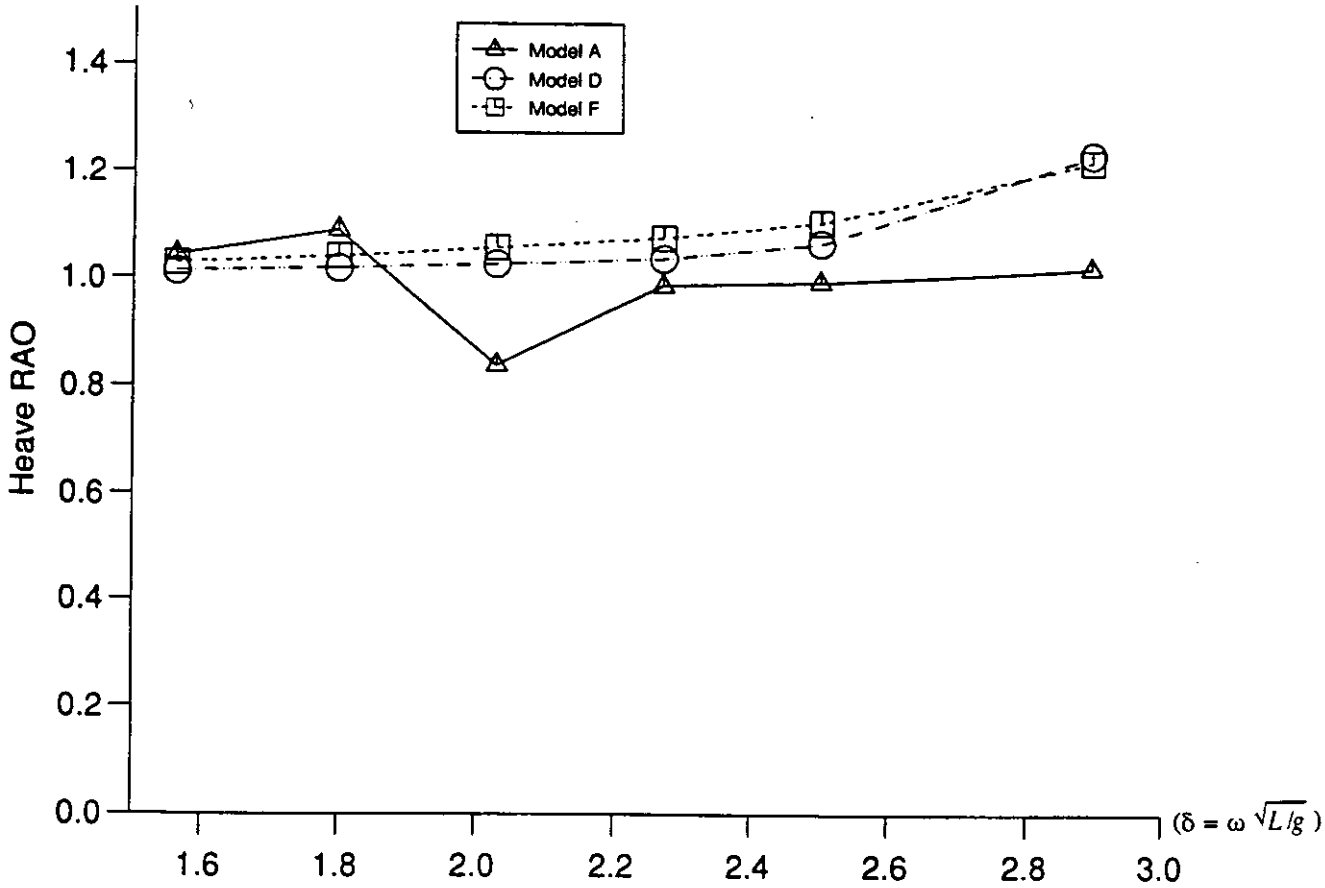

Fig.5(e) Heave RAOs for Trimaran models A, D and F; Fn=0.40, heading 120 deg.

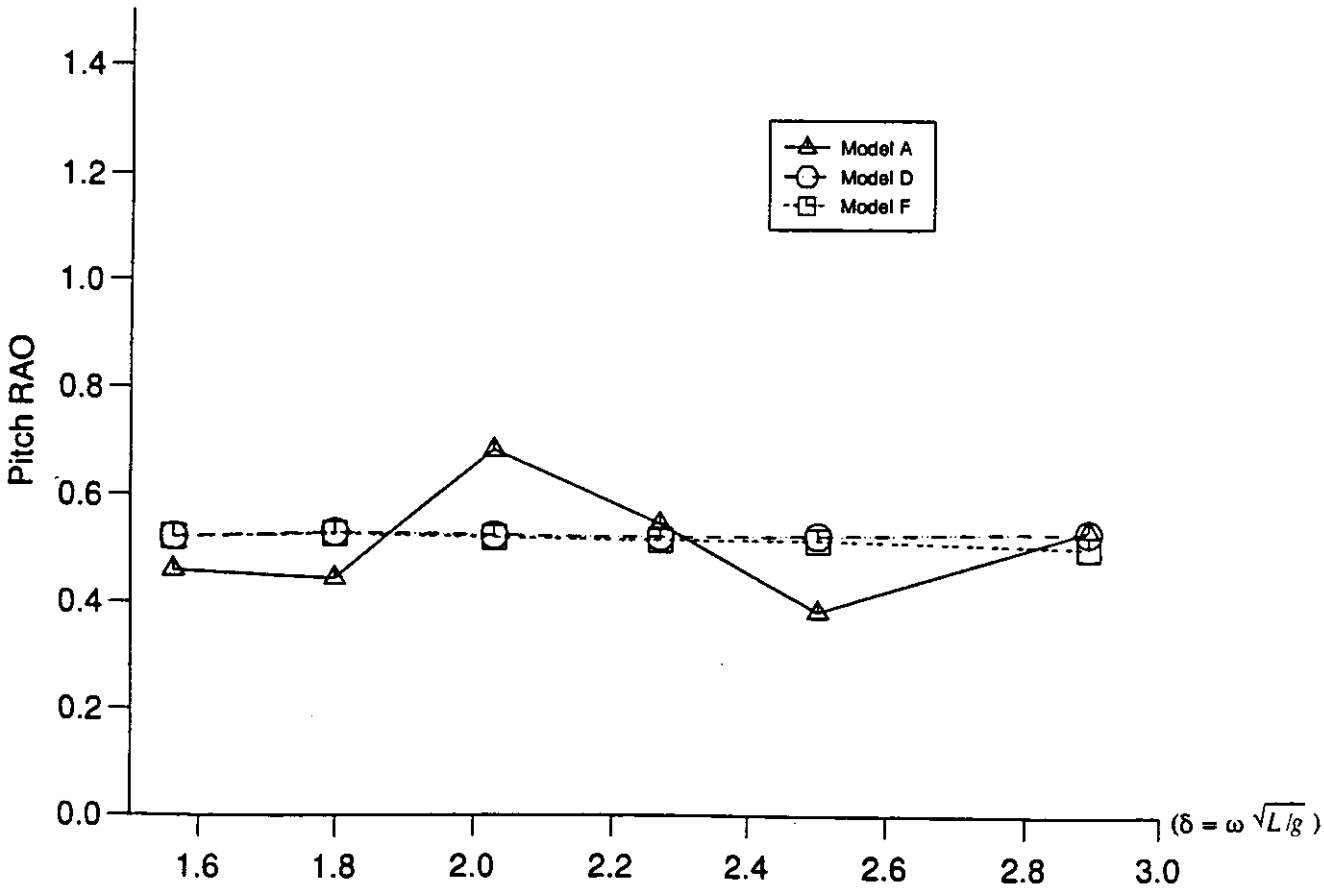

Fig.6(e) Pitch RAOs for Trimaran models A, D and F; Fn=0.40, heading 120 deg.

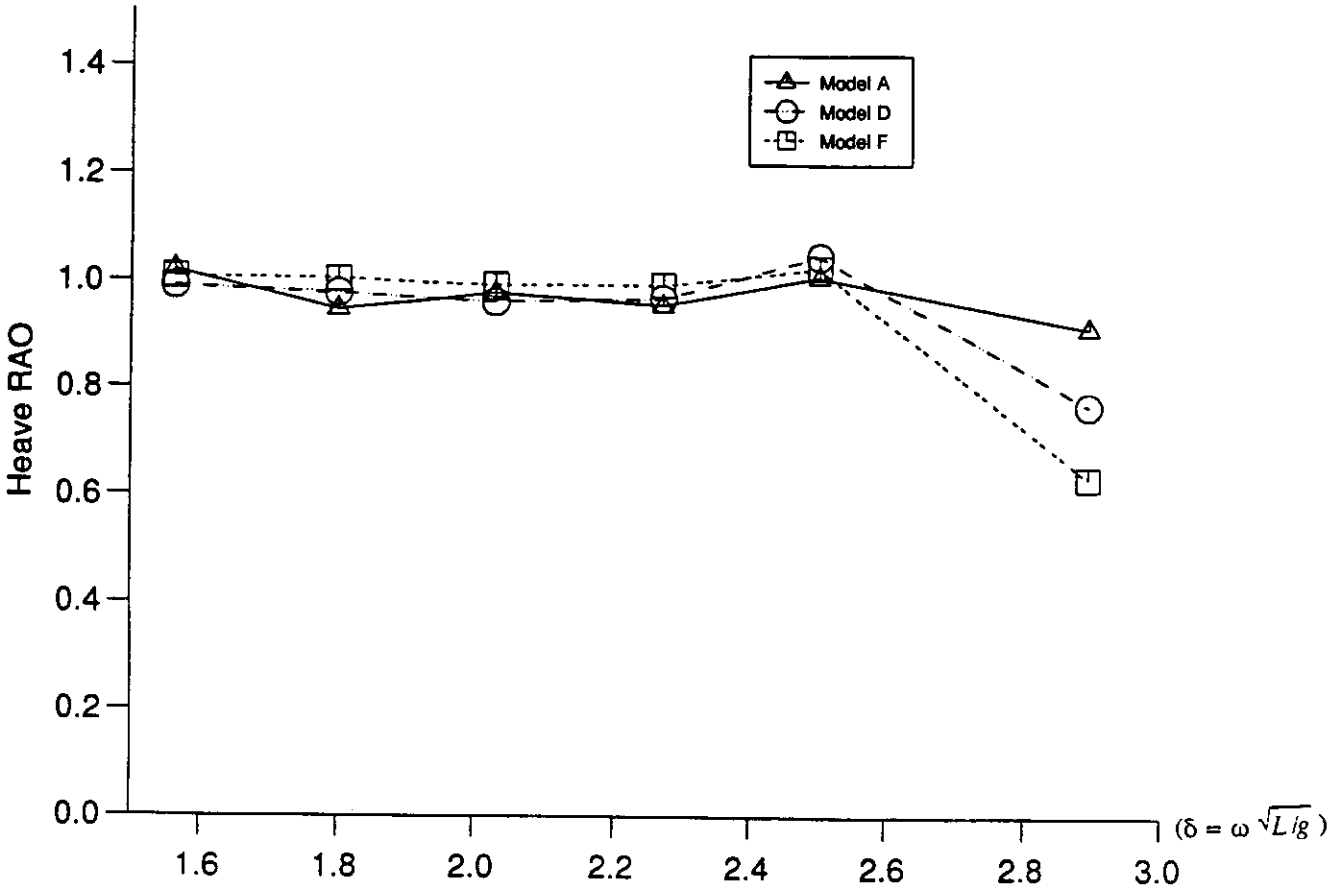

Fig.5(f) Heave RAOs for Trimaran models A, D and F; Fn=0.40, heading 150 deg.

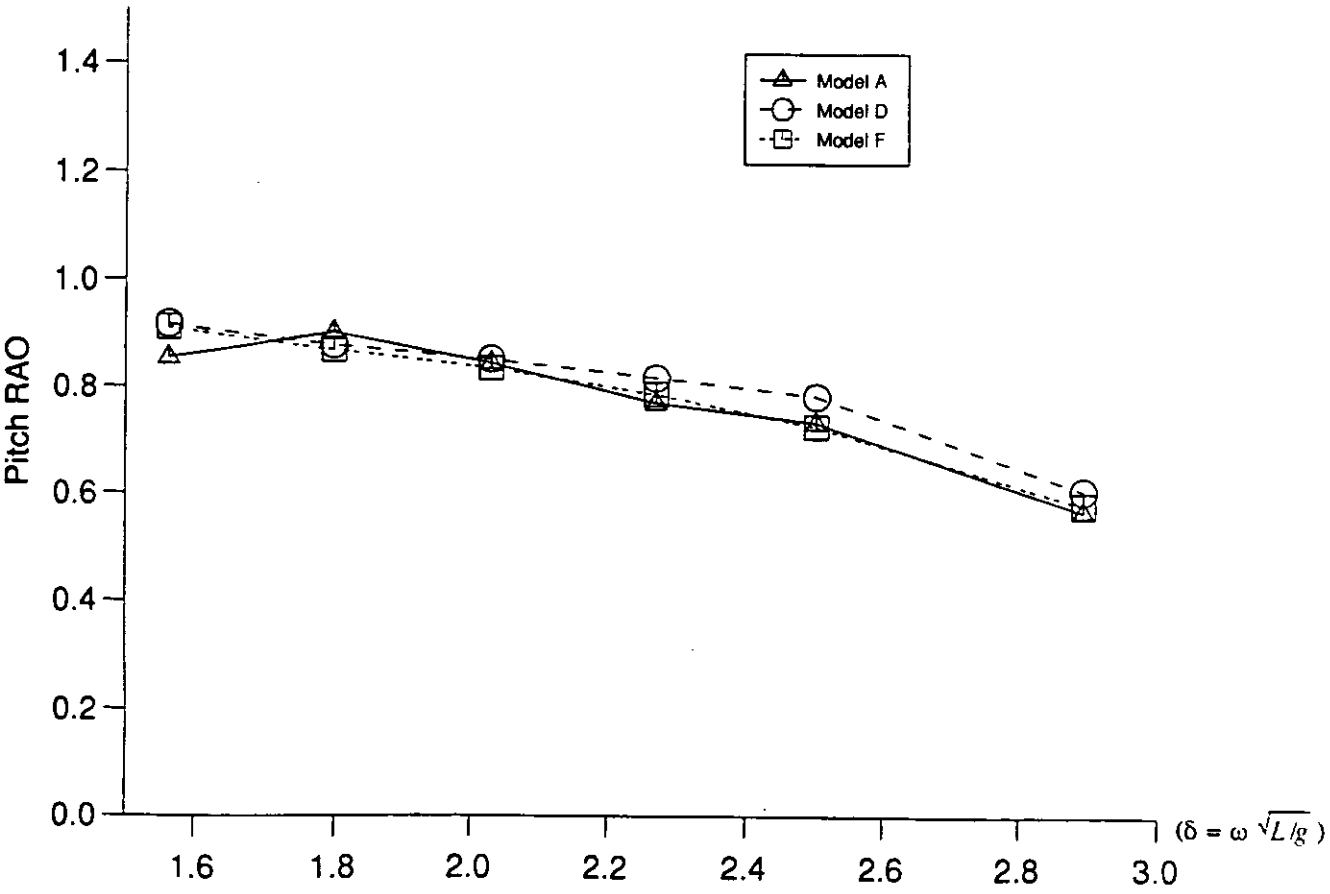

Fig.6(f) Pitch RAOs for Trimaran models A, D and F; Fn=0.40, heading 150 deg.

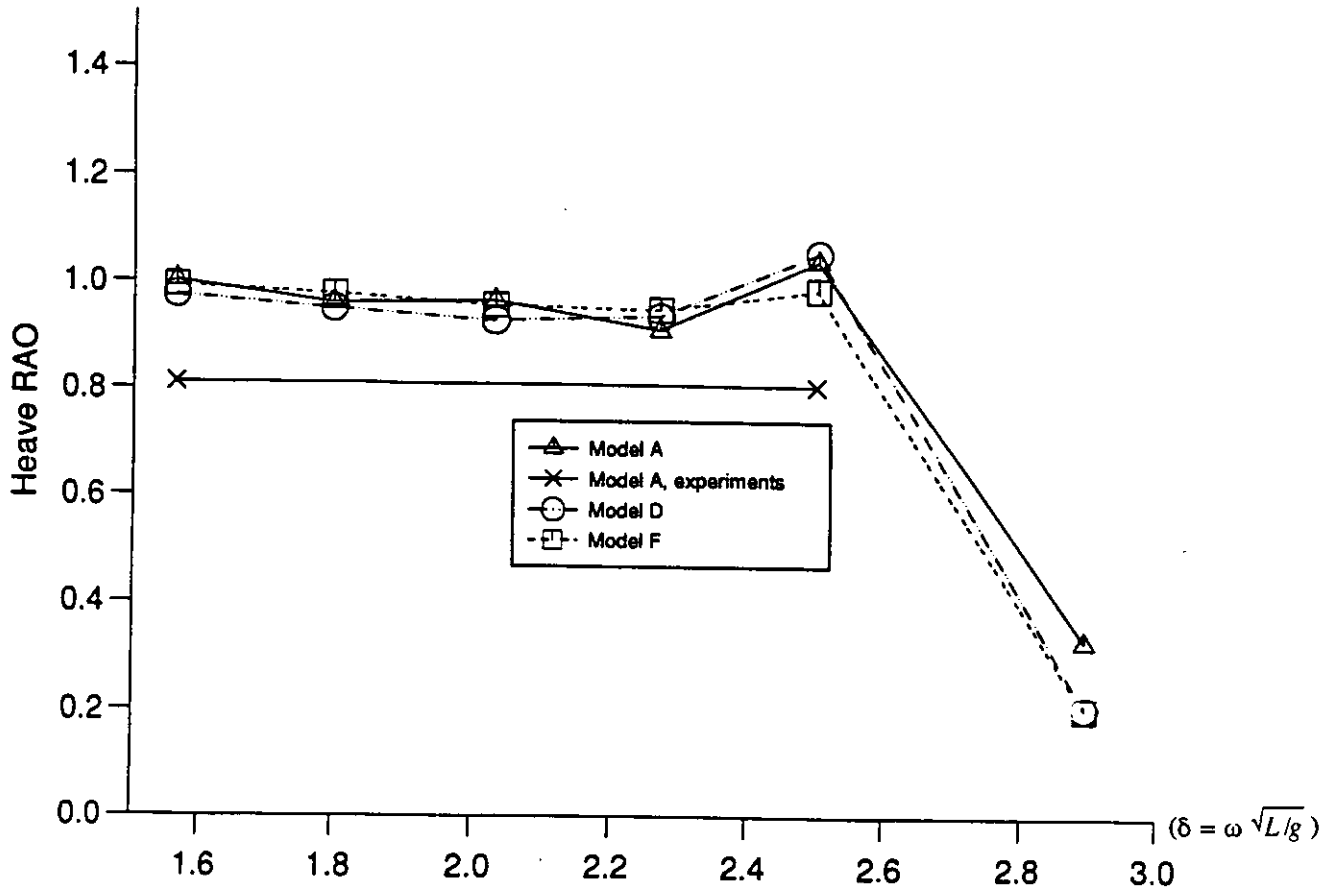

Fig.5(g) Heave RAOs for Trimaran models A, D and F; Fn=0.40, heading 180 deg.

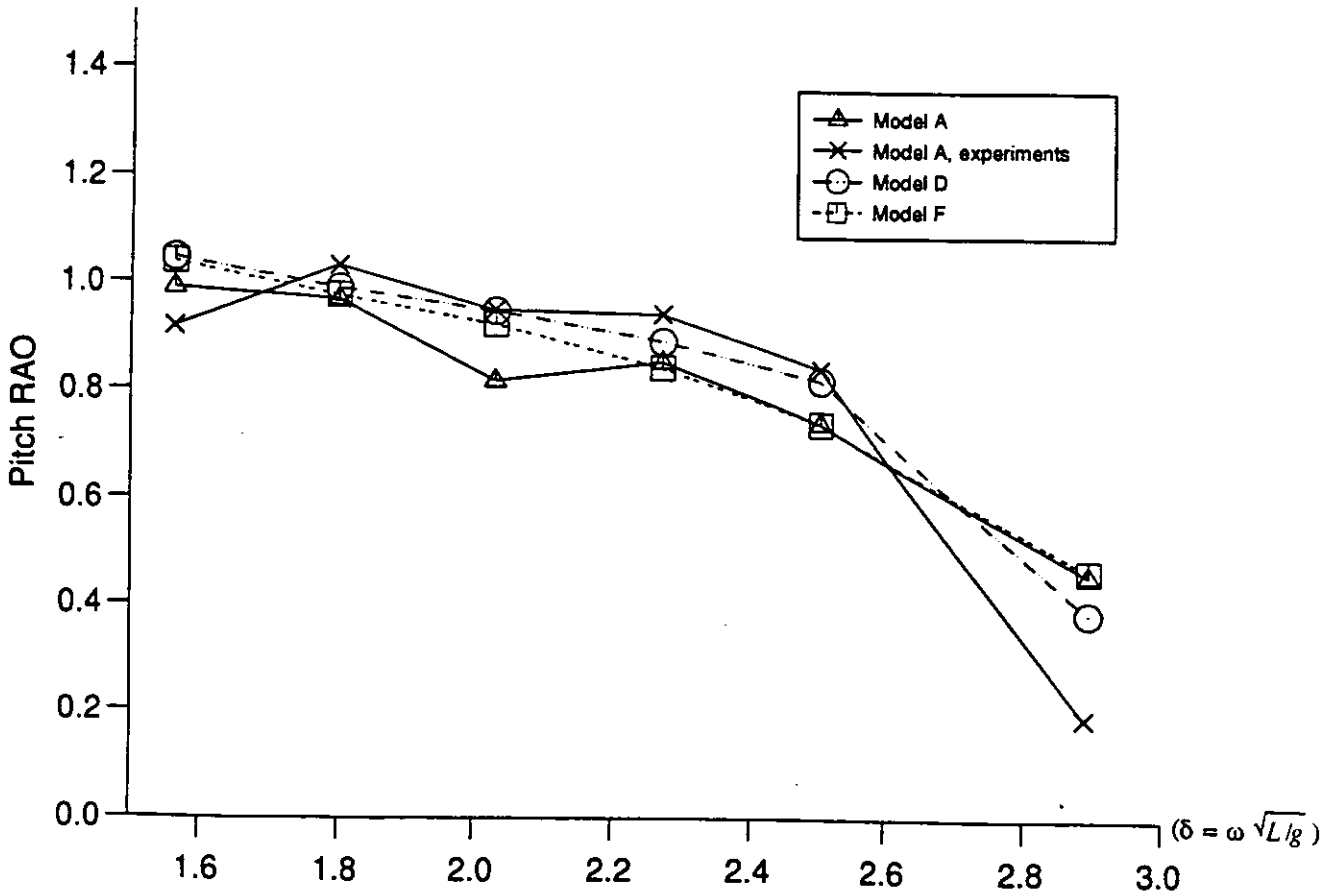

Fig.6(g) Pitch RAOs for Trimaran models A, D and F; Fn=0.40, heading 180 deg.

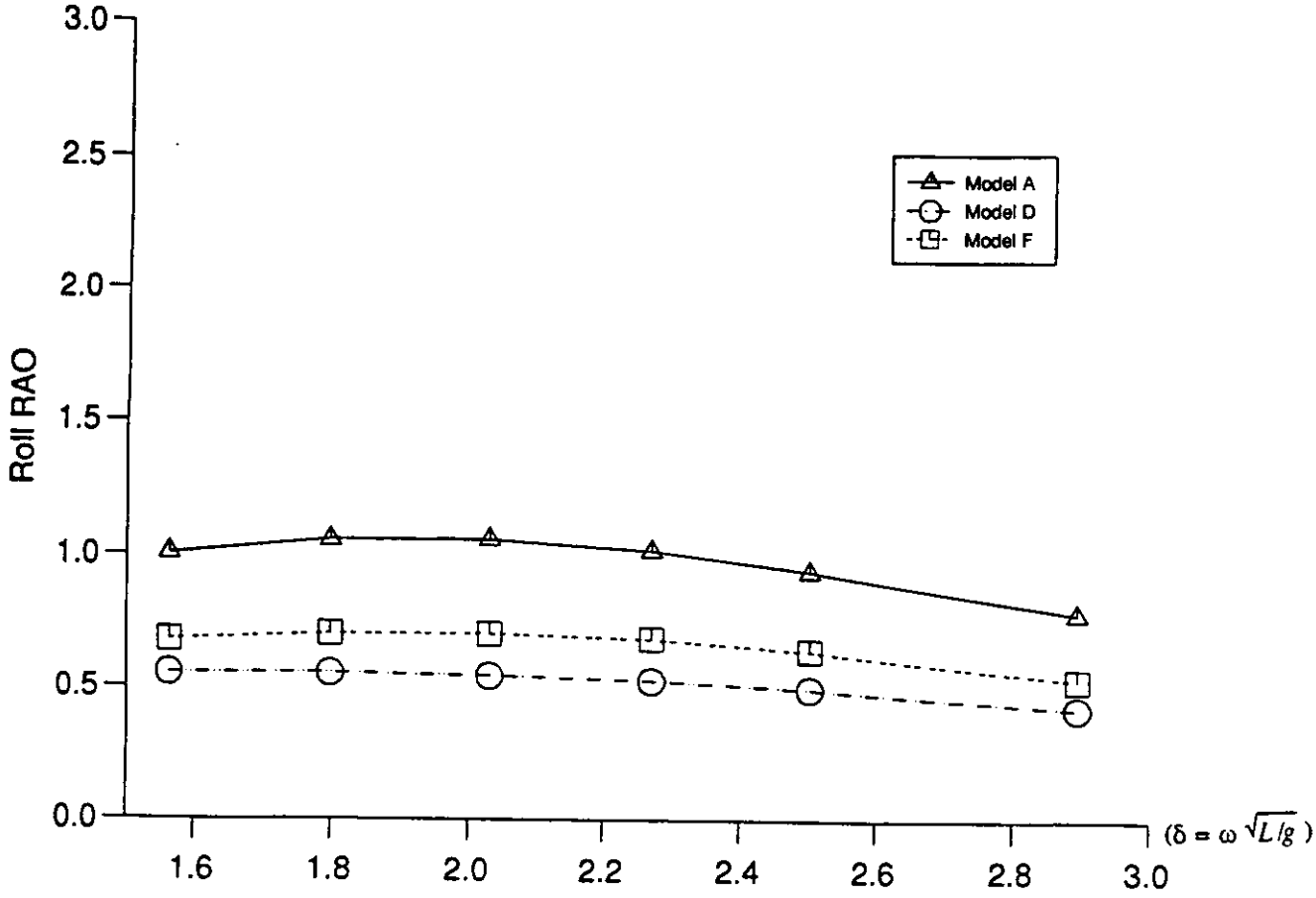

Fig.7(a) Roll RAOs for Trimaran models A, D and F; Fn=0.40, heading 30 deg.

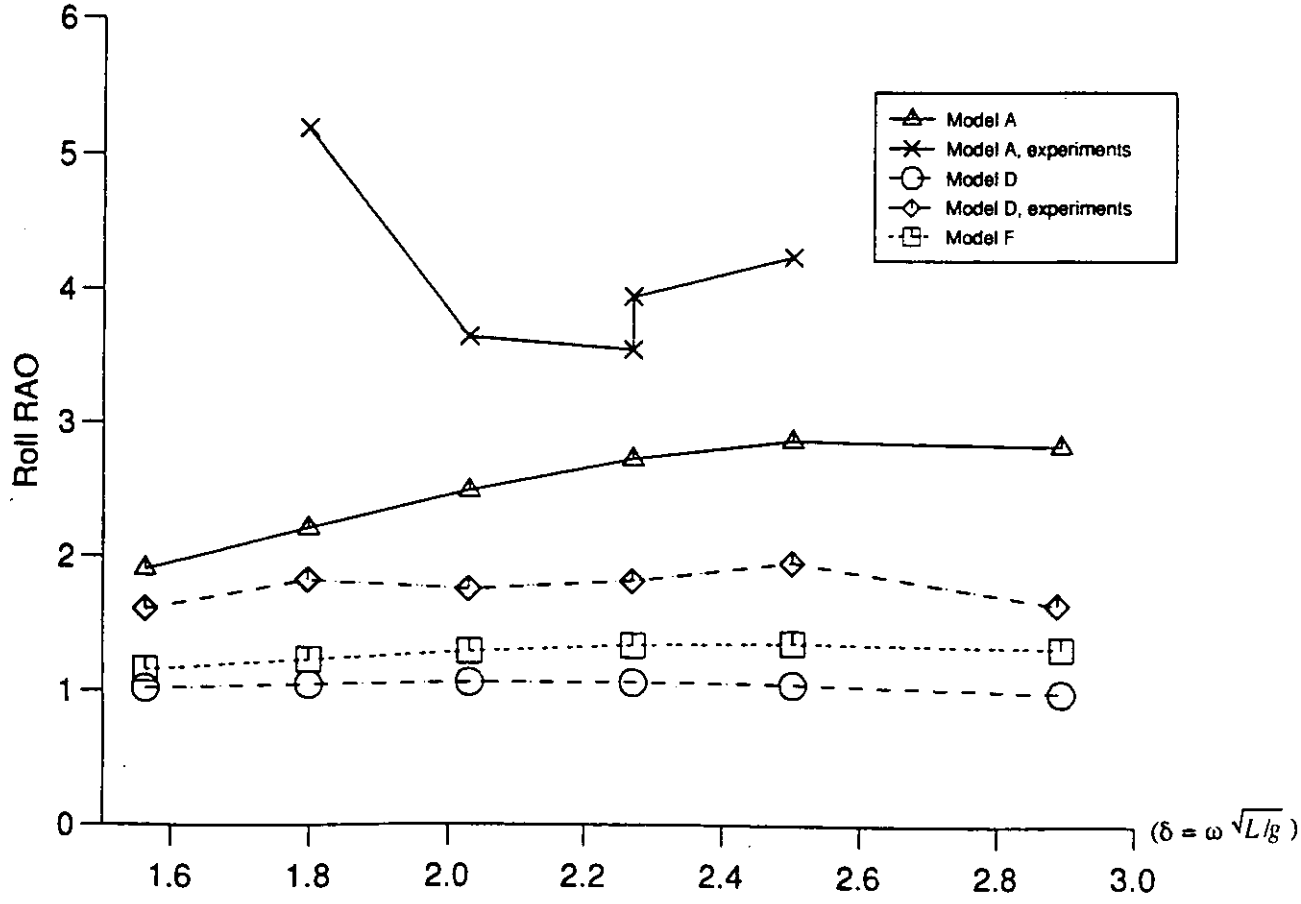

Fig.7(b) Roll RAOs for Trimaran models A, D and F; Fn=0.40, heading 60 deg.

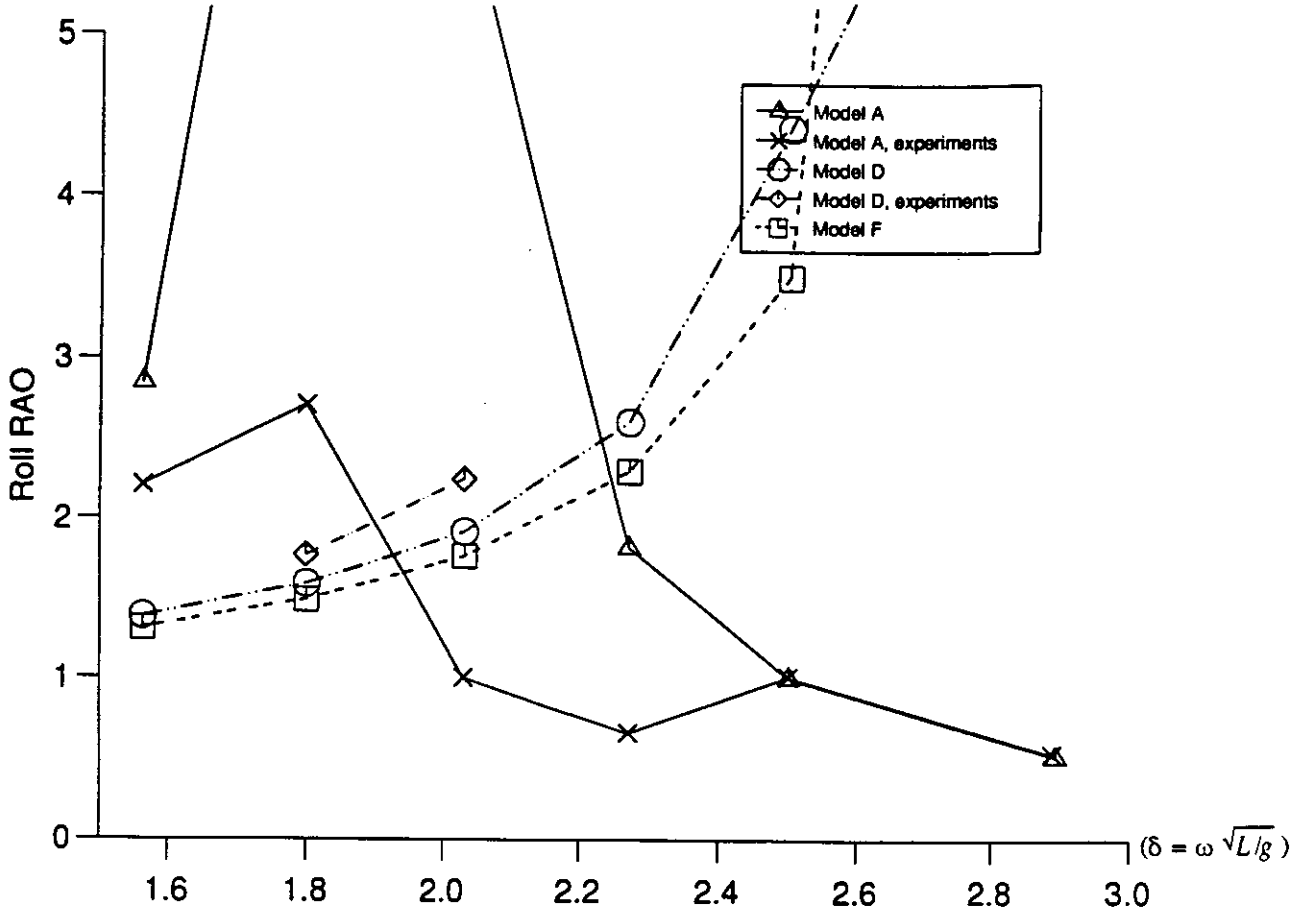

Fig.7(c) Roll RAOs for Trimaran models A, D and F; Fn=0.40, heading 90 deg.

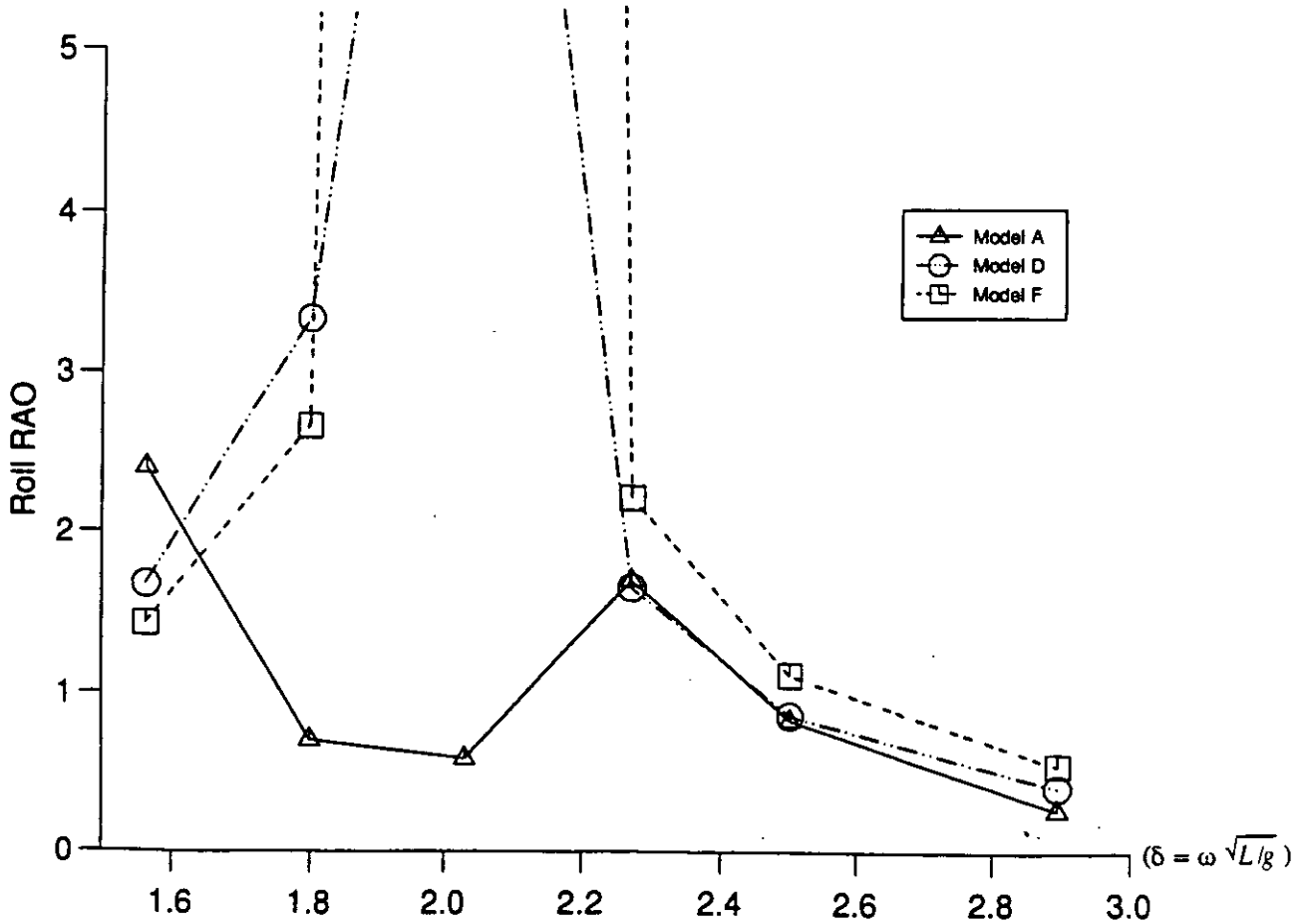

Fig.7(d) Roll RAOs for Trimaran models A, D and F; Fn=0.40, heading 120 deg.

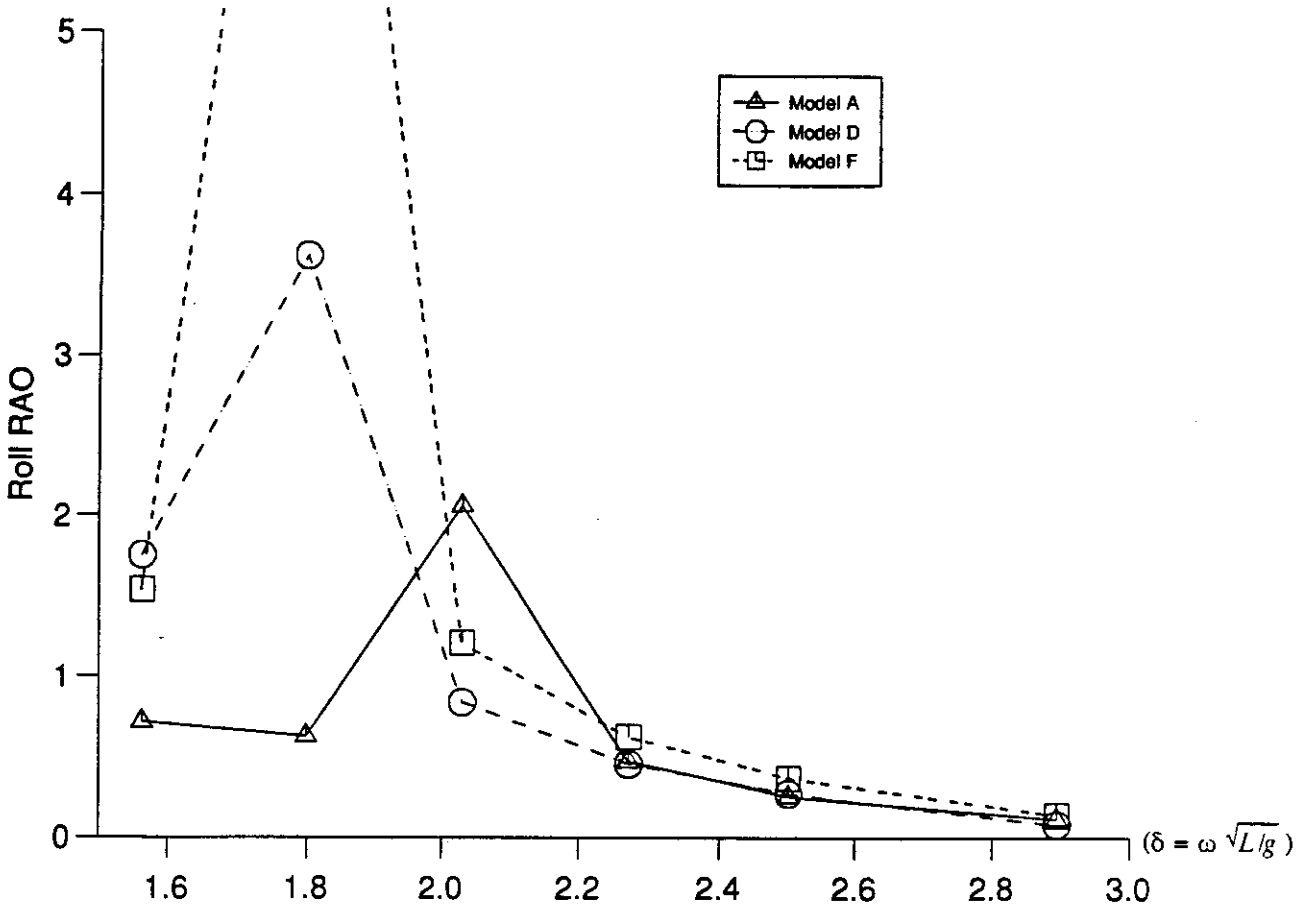

Fig.7(e) Roll RAOs for Trimaran models A, D and F; Fn=0.40, heading 150 deg.

Appendix A

Model A
Fn=0.240

HEAVE RAOs

	H E A D I N G S <deg>						
$w\sqrt{L/g}$	0	30	60	90	120	150	180
1.563	0.816	0.855	0.945	1.017	1.011	0.951	0.917
1.799	0.699	0.759	0.906	1.031	1.021	0.915	0.839
2.030	0.554	0.637	0.853	1.057	1.100	0.805	0.793
2.271	0.384	0.485	0.782	1.122	0.721	0.750	0.677
2.502	0.221	0.329	0.698	1.329	0.833	0.623	0.507
2.895	0.015	0.088	0.529	0.388	0.801	0.441	0.159

PITCH RAOs

	H E A D I N G S <deg>						
$w\sqrt{L/g}$	0	30	60	90	120	150	180
1.563	0.812	0.730	0.463	0.049	0.478	0.843	0.971
1.799	0.716	0.659	0.442	0.041	0.466	0.807	0.920
2.030	0.601	0.573	0.416	0.041	0.435	0.768	0.799
2.271	0.463	0.467	0.381	0.060	0.569	0.684	0.706
2.502	0.326	0.357	0.342	0.140	0.486	0.543	0.568
2.895	0.117	0.173	0.265	0.187	0.387	0.390	0.304

ROLL RAOs

	H E A D I N G S <deg>						
$w\sqrt{L/g}$	0	30	60	90	120	150	180
1.563		1.310	2.289	2.994	19.581	1.514	
1.799		1.506	2.996	10.387	1.351	0.539	
2.030		1.663	4.092	5.238	0.589	0.453	
2.271		1.755	6.146	1.777	0.425	1.932	
2.502		1.743	10.546	0.998	1.111	1.012	
2.895		1.477	502.703	0.519	0.821	0.247	

Model A
Fn=0.400

HEAVE RAOs

	H E A D I N G S <deg>						
$w\sqrt{L/g}$	0	30	60	90	120	150	180
1.563	0.803	0.841	0.932	1.022	1.044	1.020	1.004
1.799	0.688	0.744	0.886	1.035	1.090	0.948	0.963
2.030	0.549	0.626	0.825	1.059	0.840	0.980	0.968
2.271	0.386	0.482	0.744	1.113	0.988	0.957	0.914
2.502	0.254	0.335	0.649	1.261	0.994	1.011	1.045
2.895	0.021	0.116	0.461	0.479	1.018	0.915	0.331

PITCH RAOs

	H E A D I N G S <deg>						
$w\sqrt{L/g}$	0	30	60	90	120	150	180
1.563	0.790	0.706	0.451	0.061	0.461	0.855	0.990
1.799	0.703	0.639	0.424	0.057	0.444	0.903	0.969
2.030	0.603	0.562	0.393	0.066	0.684	0.847	0.816
2.271	0.484	0.472	0.355	0.104	0.548	0.772	0.852
2.502	0.383	0.378	0.314	0.236	0.383	0.735	0.740
2.895	0.160	0.219	0.240	0.247	0.538	0.569	0.459

ROLL RAOs

	H E A D I N G S <deg>						
$w\sqrt{L/g}$	0	30	60	90	120	150	180
1.563		1.006	1.909	2.850	2.402	0.718	
1.799		1.058	2.212	8.762	0.703	0.627	
2.030		1.065	2.495	5.757	0.586	2.071	
2.271		1.025	2.738	1.825	1.697	0.473	
2.502		0.948	2.878	1.008	0.833	0.258	
2.895		0.786	2.843	0.519	0.267	0.117	

Model A - Refined
Fn=0.240

HEAVE RAOs

$w\sqrt{L/g}$	HEADINGS <deg> 0	30	60	90	120	150	180
1.563	0.816	0.854	0.941	1.009	1.002	0.948	0.917
1.799	0.699	0.758	0.899	1.012	0.992	0.902	0.839
2.030	0.555	0.635	0.841	1.016	0.979	0.835	0.793
2.271	0.385	0.482	0.762	1.021	0.957	0.739	0.677
2.502	0.222	0.325	0.669	1.027	0.924	0.646	0.507
2.895	0.016	0.084	0.478	1.043	0.846	0.500	0.159

PITCH RAOs

$w\sqrt{L/g}$	HEADINGS <deg> 0	30	60	90	120	150	180
1.563	0.813	0.729	0.458	0.048	0.493	0.855	0.971
1.799	0.717	0.657	0.434	0.038	0.494	0.821	0.920
2.030	0.601	0.570	0.405	0.032	0.485	0.754	0.799
2.271	0.463	0.463	0.368	0.027	0.470	0.678	0.706
2.502	0.326	0.353	0.326	0.022	0.457	0.580	0.568
2.895	0.117	0.170	0.245	0.016	0.425	0.364	0.304

ROLL RAOs

$w\sqrt{L/g}$	HEADINGS <deg> 0	30	60	90	120	150	180
1.563		1.115	1.928	2.520	5.717	4.686	
1.799		1.273	2.414	5.261	3.202	0.918	
2.030		1.407	3.108	17.966	1.190	0.532	
2.271		1.497	4.228	2.697	0.709	0.379	
2.502		1.510	6.019	1.341	0.512	0.289	
2.895		1.336	14.329	0.620	0.341	0.162	

Model D
Fn=0.240

HEAVE RAOs

$w\sqrt{L/g}$	HEADINGS <deg> 0	30	60	90	120	150	180
1.563	0.792	0.844	0.933	1.000	0.989	0.932	0.903
1.799	0.673	0.745	0.889	1.001	0.976	0.881	0.835
2.030	0.530	0.620	0.830	1.001	0.957	0.810	0.738
2.271	0.362	0.465	0.749	1.001	0.930	0.710	0.610
2.502	0.215	0.305	0.653	1.001	0.895	0.600	0.471
2.895	0.019	0.063	0.457	1.002	0.829	0.375	0.181

PITCH RAOs

$w\sqrt{L/g}$	HEADINGS <deg> 0	30	60	90	120	150	180
1.563	0.818	0.733	0.457	0.002	0.505	0.870	0.993
1.799	0.722	0.663	0.436	0.002	0.509	0.839	0.932
2.030	0.606	0.576	0.408	0.002	0.503	0.772	0.831
2.271	0.467	0.469	0.371	0.003	0.487	0.697	0.721
2.502	0.328	0.358	0.330	0.005	0.472	0.607	0.585
2.895	0.116	0.172	0.248	0.009	0.438	0.411	0.305

ROLL RAOs

$w\sqrt{L/g}$	HEADINGS <deg> 0	30	60	90	120	150	180
1.563		0.613	1.100	1.388	1.402	0.983	
1.799		0.632	1.162	1.595	1.990	2.136	
2.030		0.644	1.226	1.929	4.319	4.865	
2.271		0.647	1.292	2.614	7.658	1.067	
2.502		0.635	1.351	4.429	1.885	0.613	
2.895		0.567	1.427	7.836	0.773	0.270	

Model D
Fn=0.400

HEAVE RAOs

$w\sqrt{L/g}$	HEADINGS <deg> 0	30	60	90	120	150	180
1.563	0.792	0.830	0.919	1.001	1.014	0.991	0.977
1.799	0.673	0.730	0.869	1.001	1.020	0.979	0.952
2.030	0.530	0.608	0.804	1.001	1.027	0.963	0.931
2.271	0.362	0.460	0.717	1.000	1.038	0.970	0.939
2.502	0.215	0.309	0.618	1.001	1.066	1.050	1.060
2.895	0.019	0.080	0.420	1.003	1.229	0.769	0.207

PITCH RAOs

$w\sqrt{L/g}$	HEADINGS <deg> 0	30	60	90	120	150	180
1.563	0.799	0.711	0.439	0.004	0.524	0.918	1.047
1.799	0.712	0.644	0.413	0.003	0.531	0.880	0.989
2.030	0.610	0.567	0.382	0.002	0.525	0.855	0.948
2.271	0.489	0.475	0.343	0.002	0.523	0.820	0.891
2.502	0.376	0.379	0.303	0.003	0.524	0.786	0.820
2.895	0.161	0.215	0.227	0.007	0.533	0.609	0.387

ROLL RAOs

$w\sqrt{L/g}$	HEADINGS <deg> 0	30	60	90	120	150	180
1.563		0.556	1.026	1.384	1.675	1.752	
1.799		0.555	1.050	1.591	3.336	3.627	
2.030		0.546	1.065	1.924	10.280	0.842	
2.271		0.528	1.068	2.609	1.652	0.458	
2.502		0.498	1.055	4.425	0.862	0.275	
2.895		0.422	0.994	7.754	0.411	0.083	

Model F
Fn=0.240

HEAVE RAOs

	HEADINGS <deg>						
w√L/g	0	30	60	90	120	150	180
1.563	0.819	0.858	0.946	1.014	1.005	0.950	0.921
1.799	0.703	0.763	0.907	1.019	0.998	0.905	0.858
2.030	0.560	0.642	0.852	1.025	0.987	0.841	0.768
2.271	0.389	0.490	0.776	1.032	0.968	0.744	0.642
2.502	0.223	0.332	0.684	1.041	0.939	0.634	0.504
2.895	0.009	0.085	0.492	1.059	0.872	0.395	0.186

PITCH RAOs

	HEADINGS <deg>						
w√L/g	0	30	60	90	120	150	180
1.563	0.828	0.741	0.462	0.014	0.503	0.865	0.986
1.799	0.735	0.674	0.441	0.011	0.506	0.833	0.926
2.030	0.622	0.589	0.415	0.009	0.500	0.766	0.824
2.271	0.485	0.485	0.380	0.007	0.483	0.686	0.708
2.502	0.346	0.374	0.340	0.004	0.466	0.592	0.567
2.895	0.131	0.187	0.260	0.001	0.427	0.387	0.290

ROLL RAOs

	HEADINGS <deg>						
w√L/g	0	30	60	90	120	150	180
1.563		0.724	1.186	1.299	1.246	0.926	
1.799		0.773	1.290	1.481	1.763	1.933	
2.030		0.808	1.402	1.763	3.449	18.473	
2.271		0.823	1.523	2.297	25.696	1.618	
2.502		0.808	1.635	3.492	2.727	0.854	
2.895		0.706	1.784	23.363	1.046	0.368	

Model F
Fn=0.400

HEAVE RAOs

	HEADINGS <deg>						
w√L/g	0	30	60	90	120	150	180
1.563	0.805	0.842	0.931	1.013	1.029	1.008	0.995
1.799	0.690	0.747	0.885	1.018	1.042	1.005	0.979
2.030	0.550	0.628	0.824	1.023	1.058	0.994	0.959
2.271	0.385	0.483	0.742	1.030	1.076	0.994	0.952
2.502	0.239	0.333	0.646	1.038	1.105	1.028	0.990
2.895	0.003	0.101	0.452	1.055	1.216	0.633	0.204

PITCH RAOs

	HEADINGS <deg>						
w√L/g	0	30	60	90	120	150	180
1.563	0.812	0.721	0.444	0.019	0.522	0.912	1.039
1.799	0.727	0.657	0.420	0.015	0.528	0.871	0.976
2.030	0.627	0.582	0.390	0.013	0.520	0.838	0.923
2.271	0.507	0.491	0.354	0.011	0.517	0.789	0.842
2.502	0.398	0.395	0.314	0.009	0.516	0.728	0.740
2.895	0.178	0.231	0.240	0.005	0.504	0.582	0.466

ROLL RAOs

	HEADINGS <deg>						
w√L/g	0	30	60	90	120	150	180
1.563		0.682	1.164	1.312	1.432	1.536	
1.799		0.703	1.235	1.490	2.657	9.025	
2.030		0.706	1.296	1.769	55.898	1.210	
2.271		0.687	1.343	2.301	2.214	0.623	
2.502		0.644	1.363	3.500	1.112	0.371	
2.895		0.532	1.327	22.012	0.552	0.141	

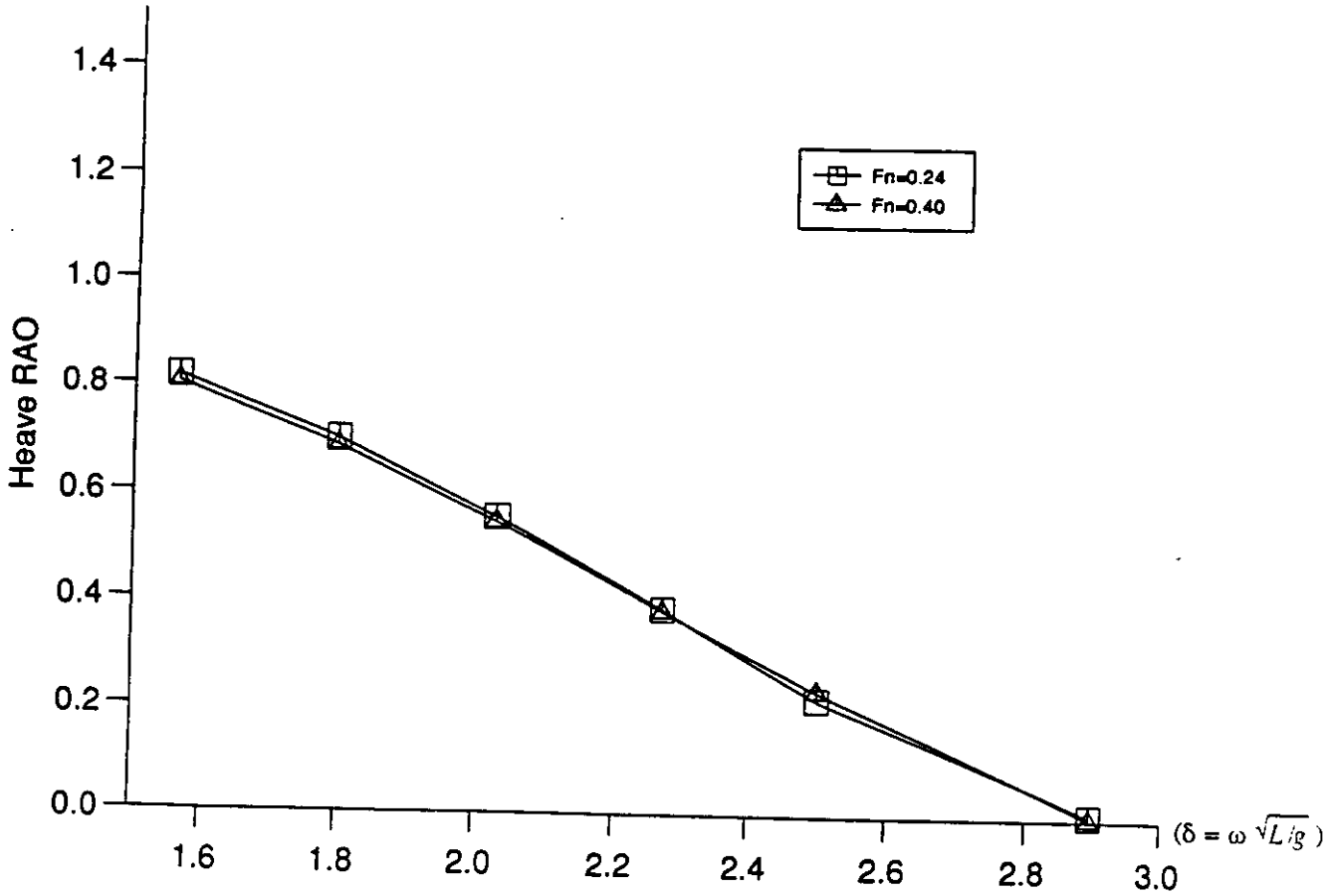

Fig.B1(a) Heave RAOs for Trimaran model F ; Fn=0.24 and 0.40, heading 0 deg.

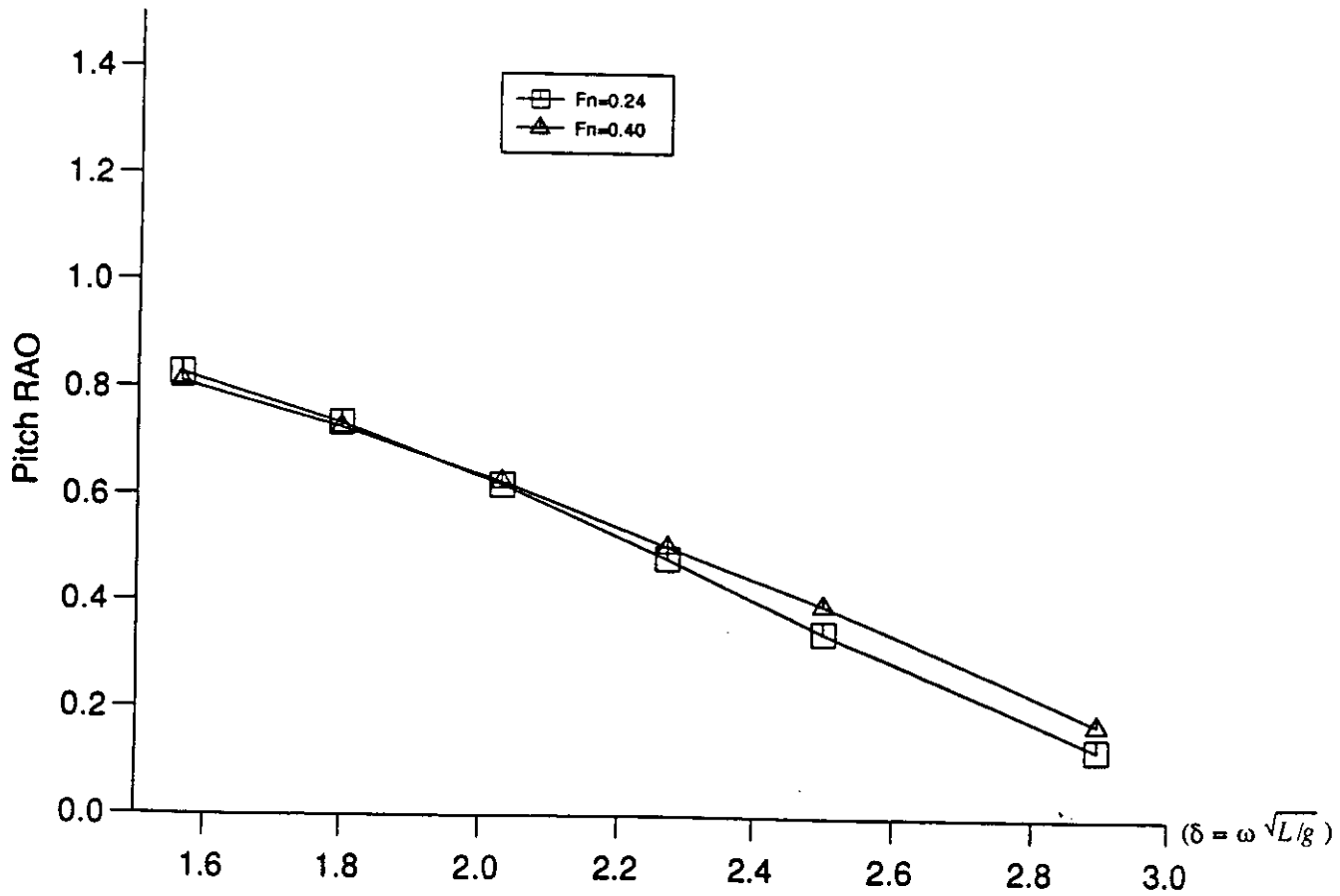

Fig.B2(a) Pitch RAOs for Trimaran model F ; Fn=0.24 and 0.40, heading 0 deg.

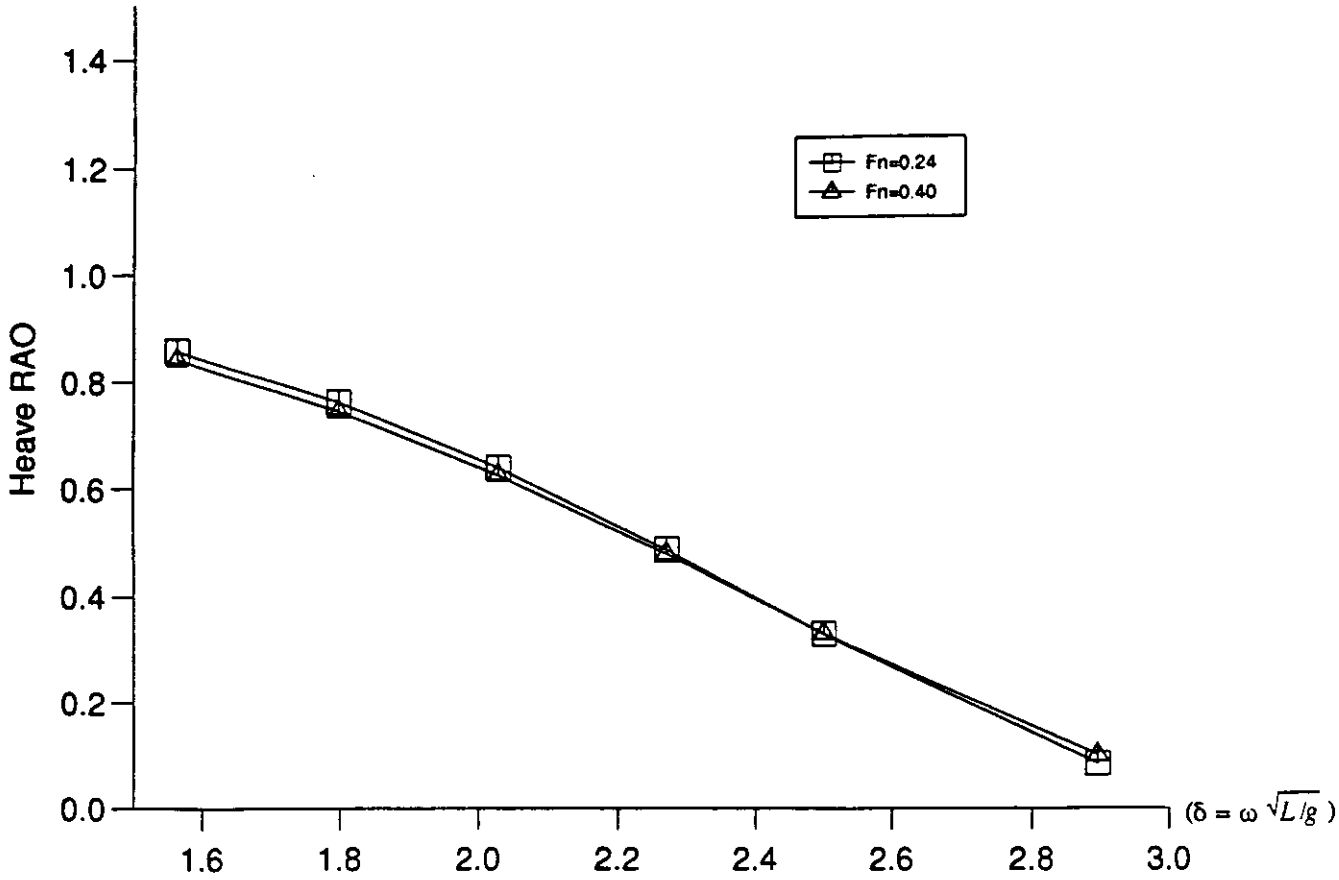

Fig.B1(b) Heave RAOs for Trimaran model F ; Fn=0.24 and 0.40, heading 30 deg.

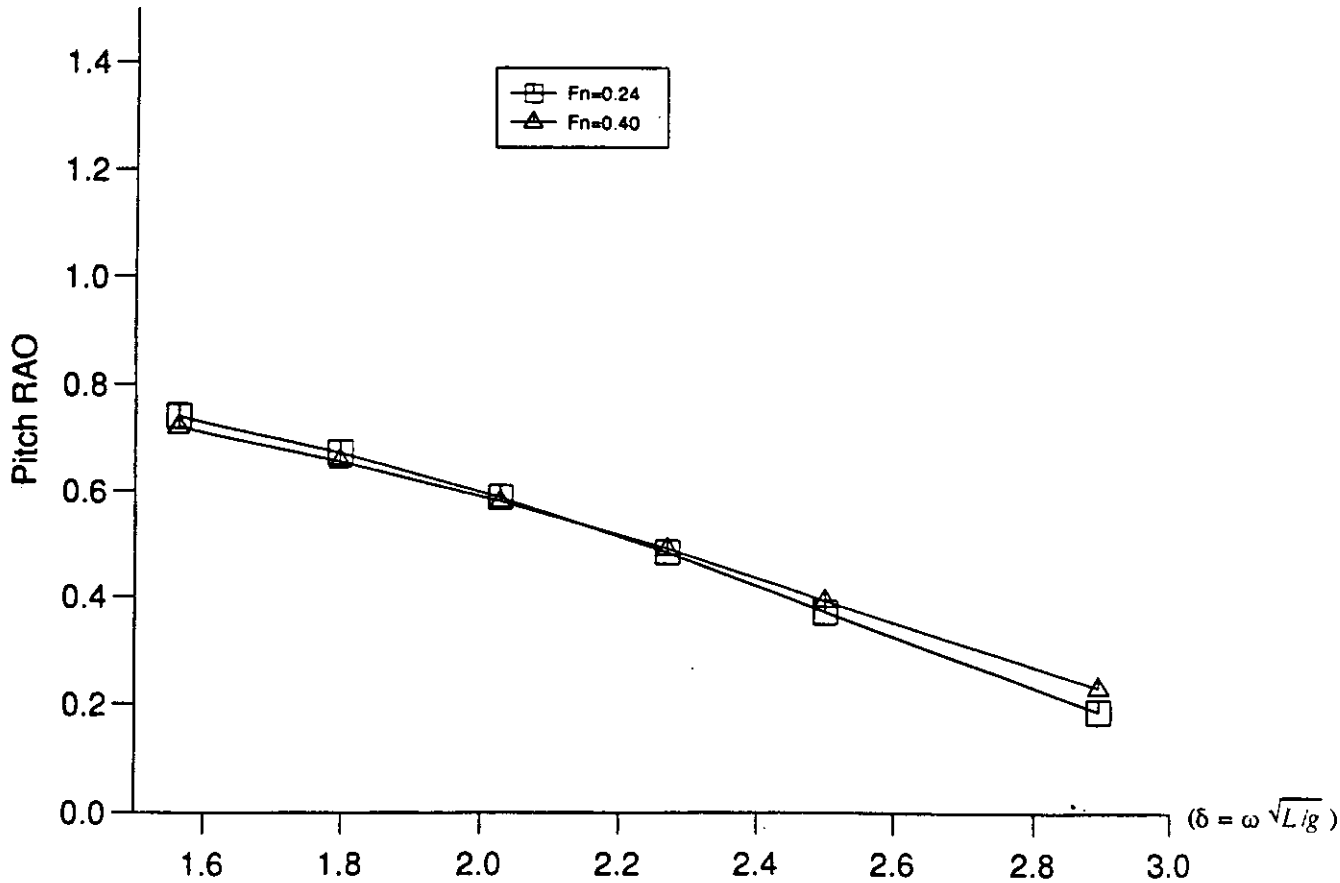

Fig.B2(b) Pitch RAOs for Trimaran model F ; Fn=0.24 and 0.40, heading 30 deg.

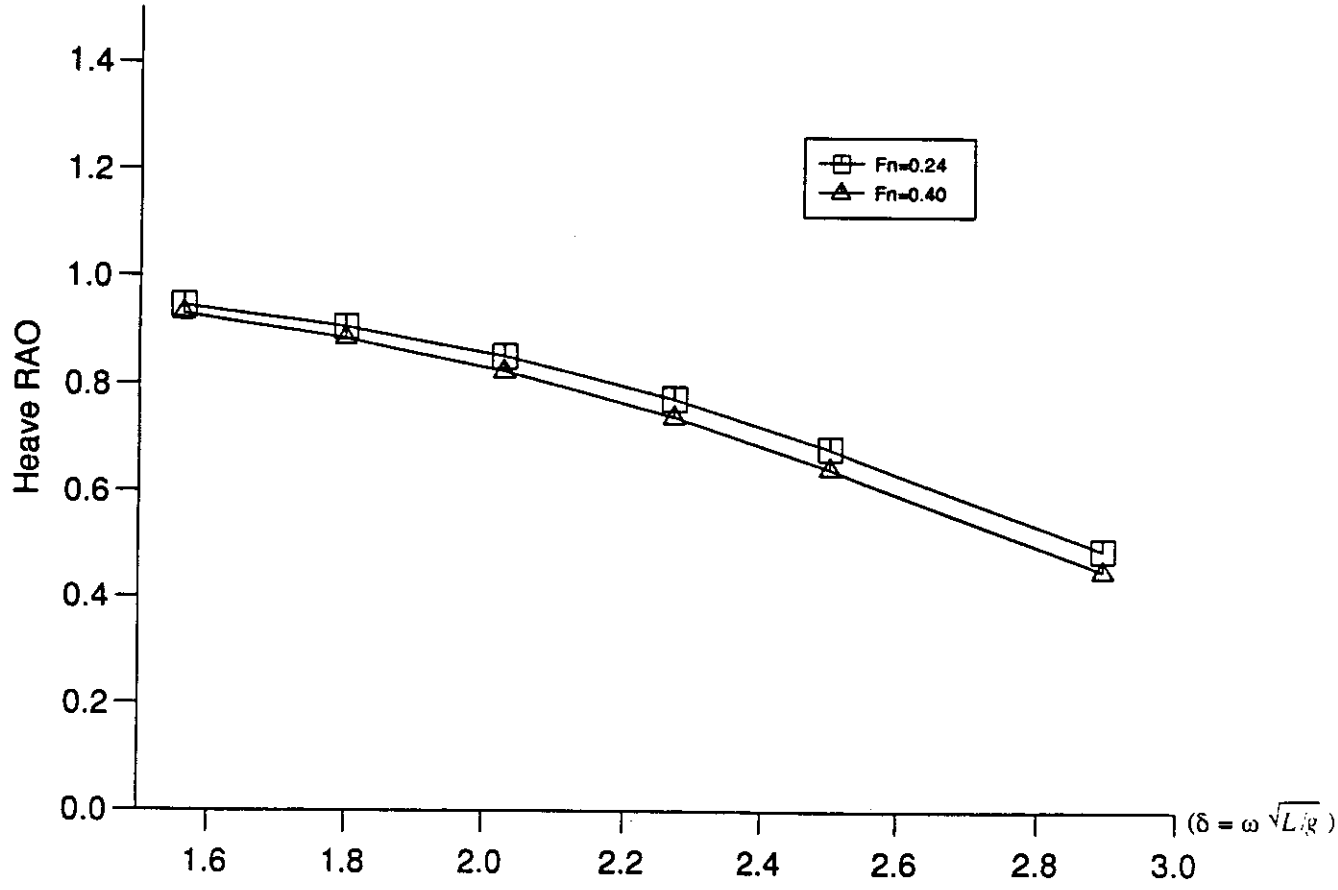

Fig.B1(c) Heave RAOs for Trimaran model F ; Fn=0.24 and 0.40, heading 60 deg.

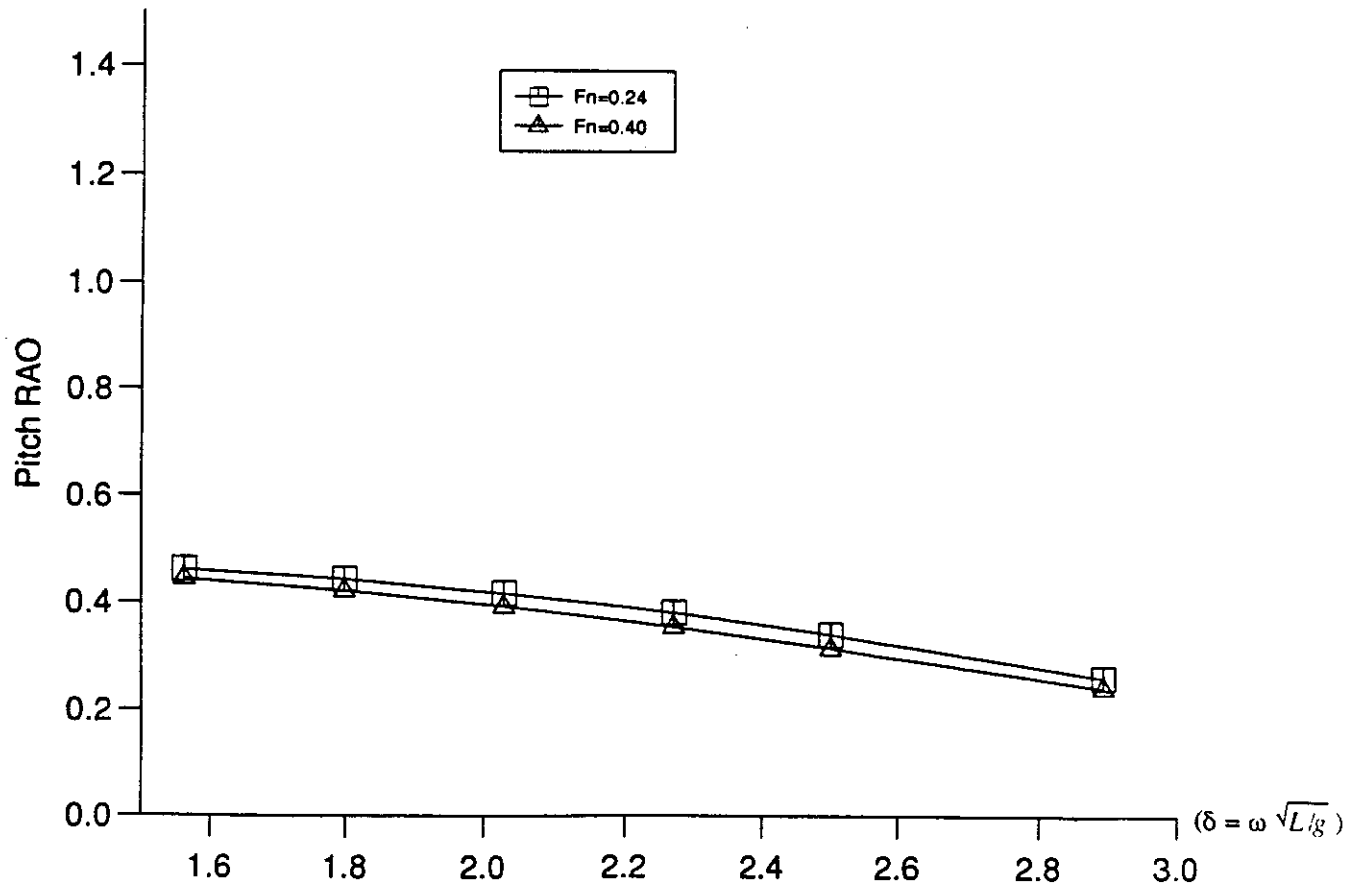

Fig.B2(c) Pitch RAOs for Trimaran model F ; Fn=0.24 and 0.40, heading 60 deg.

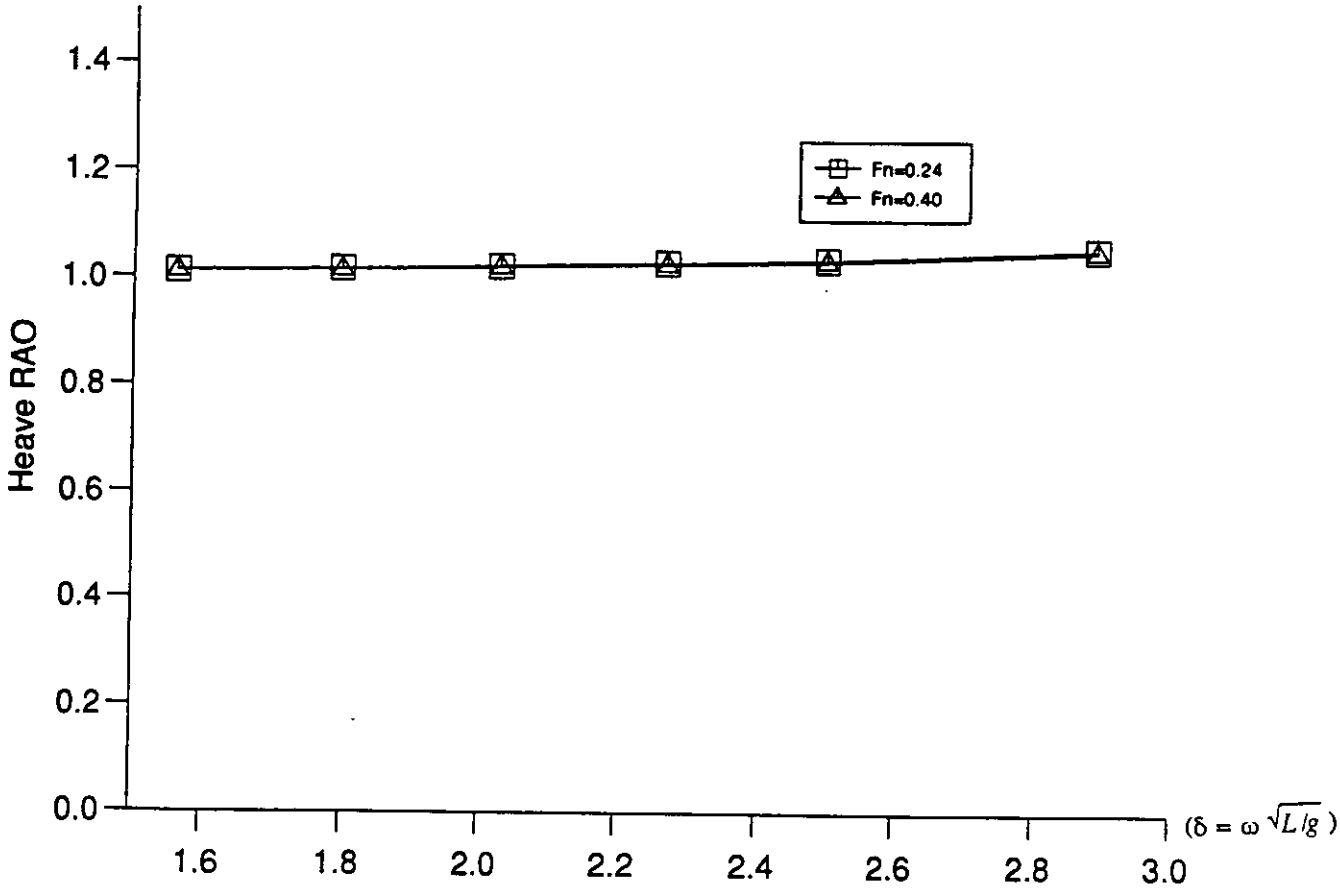

Fig.B1(d) Heave RAOs for Trimaran model F ; Fn=0.24 and 0.40, heading 90 deg.

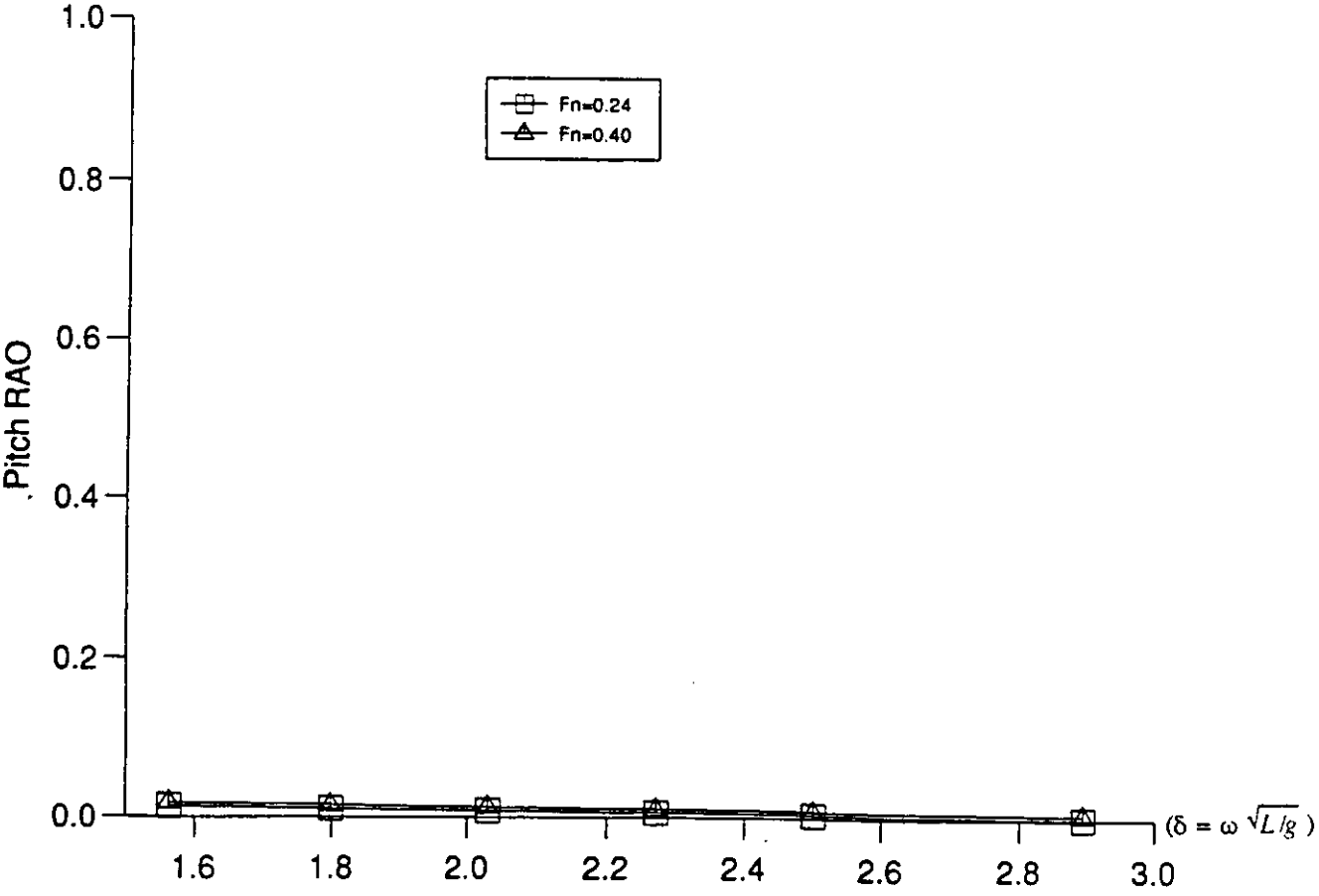

Fig.B2(d) Pitch RAOs for Trimaran model F ; Fn=0.24 and 0.40, heading 90 deg.

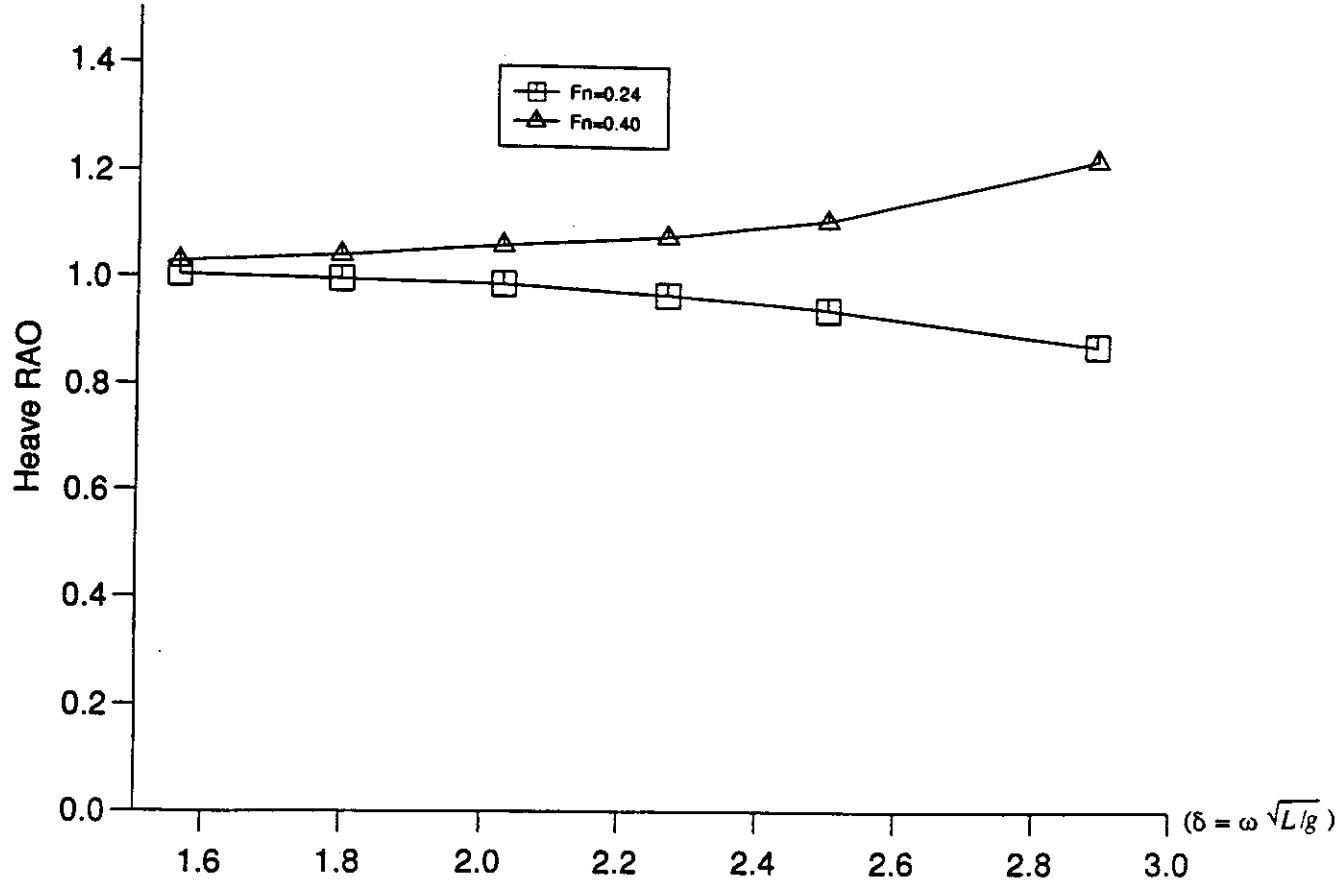

Fig.B1(e) Heave RAOs for Trimaran model F ; Fn=0.24 and 0.40, heading 120 deg.

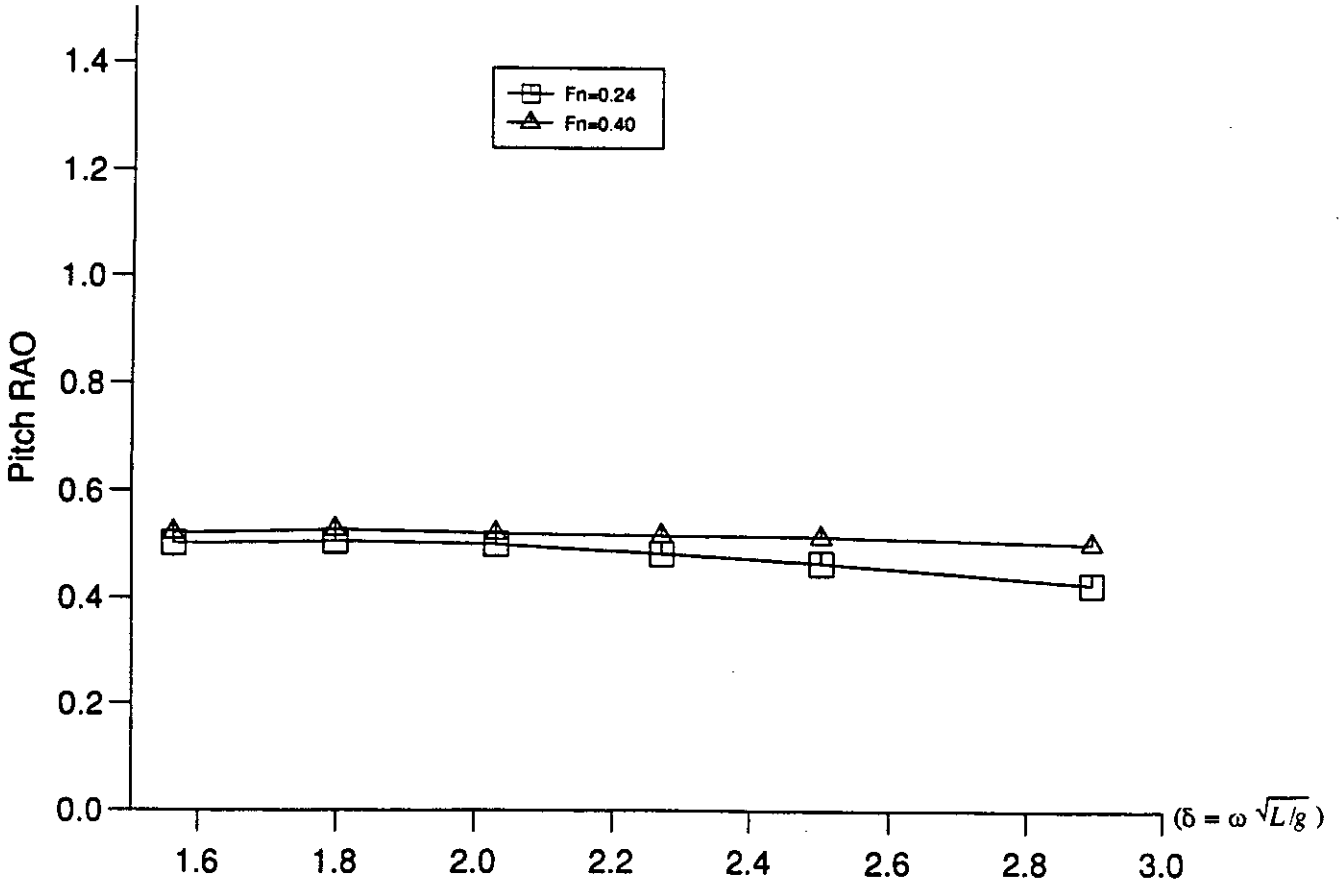

Fig.B2(e) Pitch RAOs for Trimaran model F ; Fn=0.24 and 0.40, heading 120 deg.

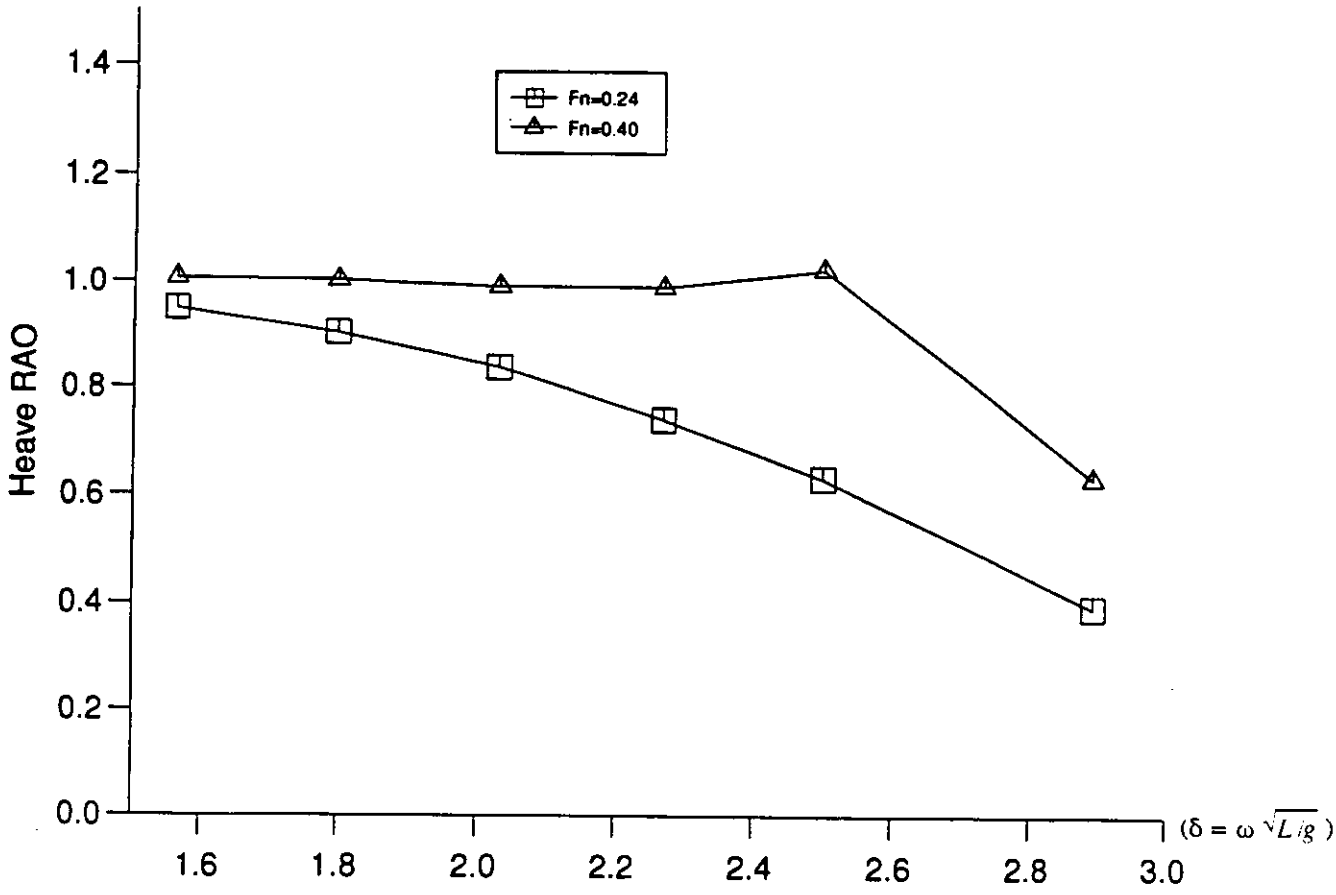

Fig.B1(f) Heave RAOs for Trimaran model F ; Fn=0.24 and 0.40, heading 150 deg.

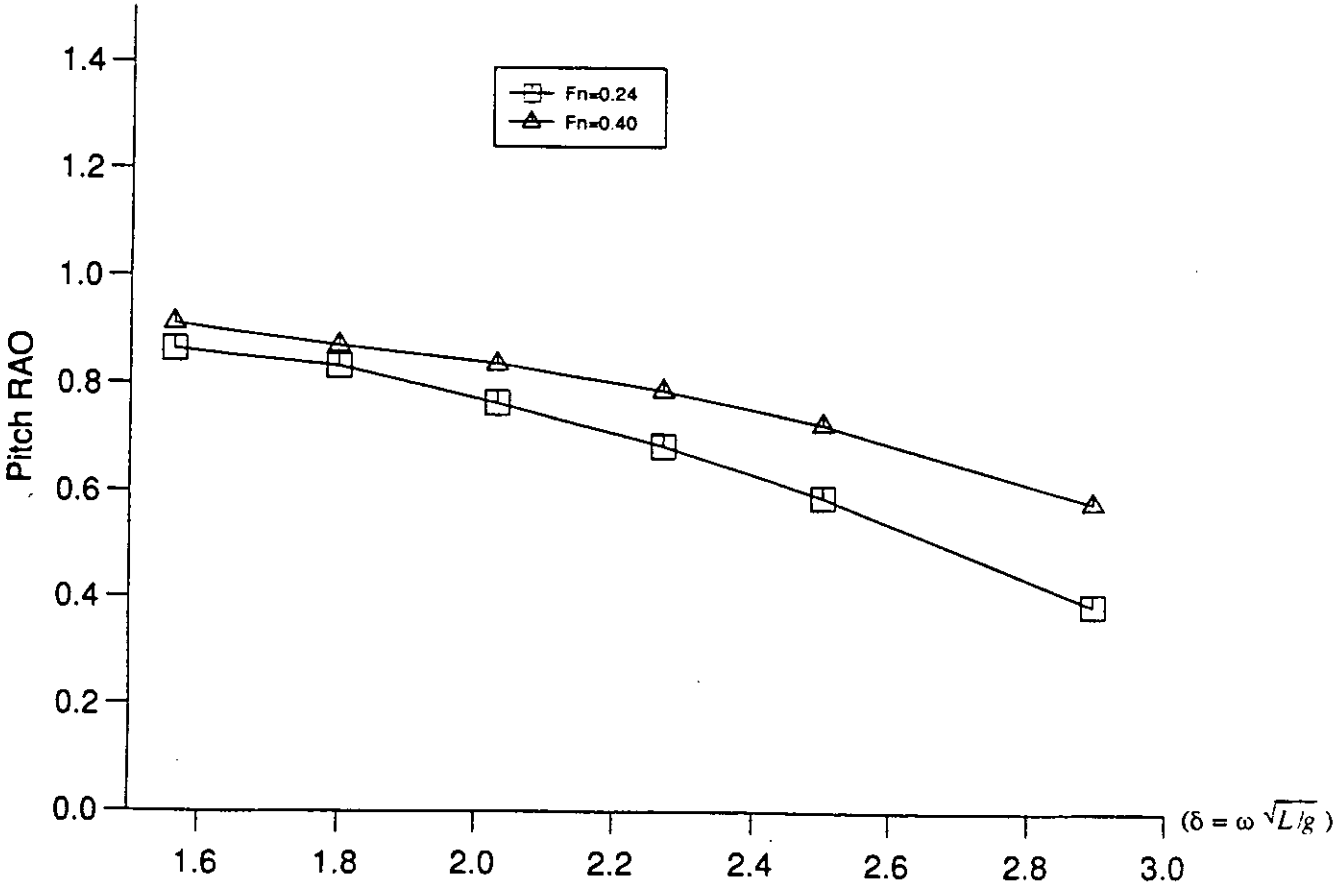

Fig.B2(f) Pitch RAOs for Trimaran model F ; Fn=0.24 and 0.40, heading 150 deg.

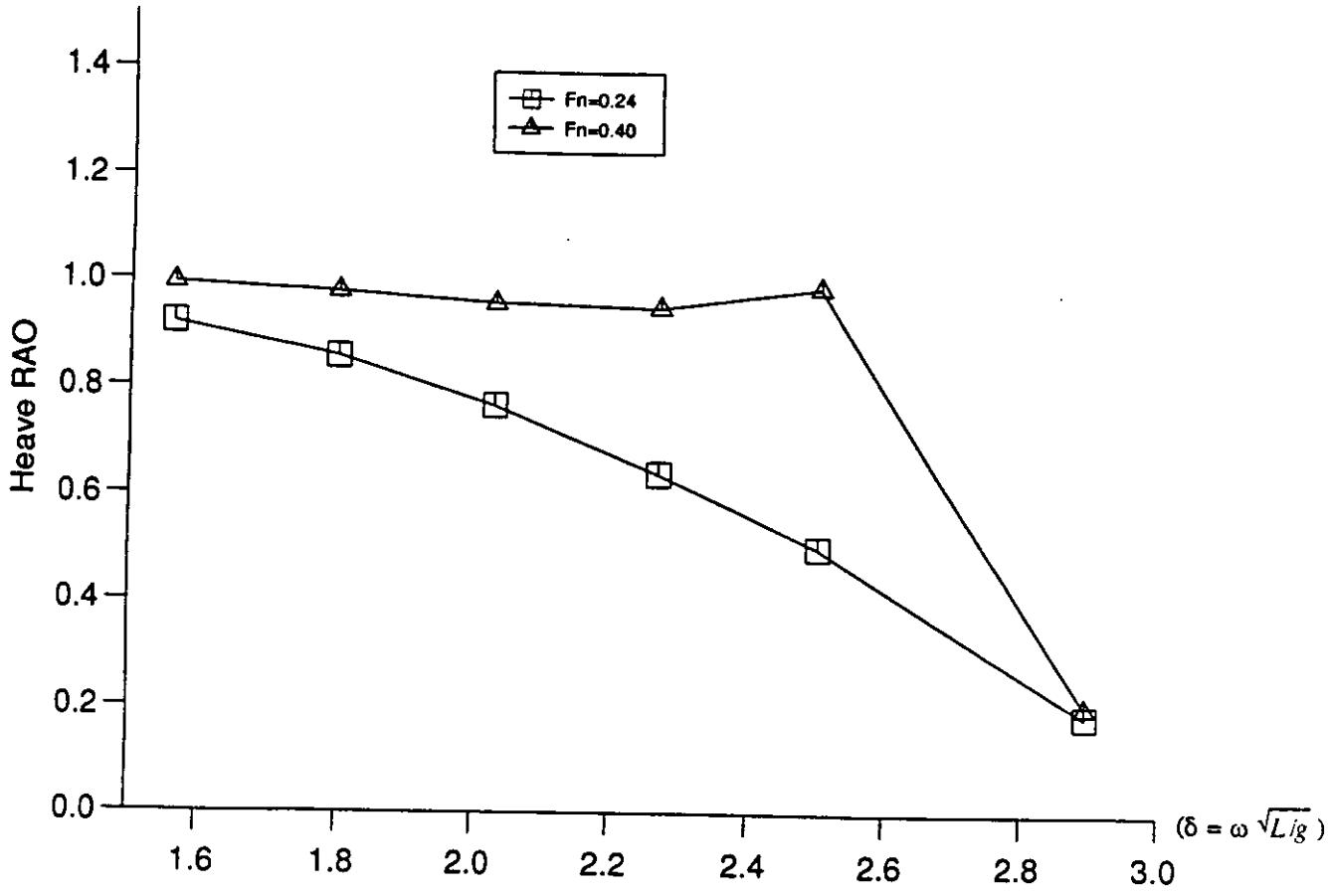

Fig.B1(g) Heave RAOs for Trimaran model F ; Fn=0.24 and 0.40, heading 180 deg.

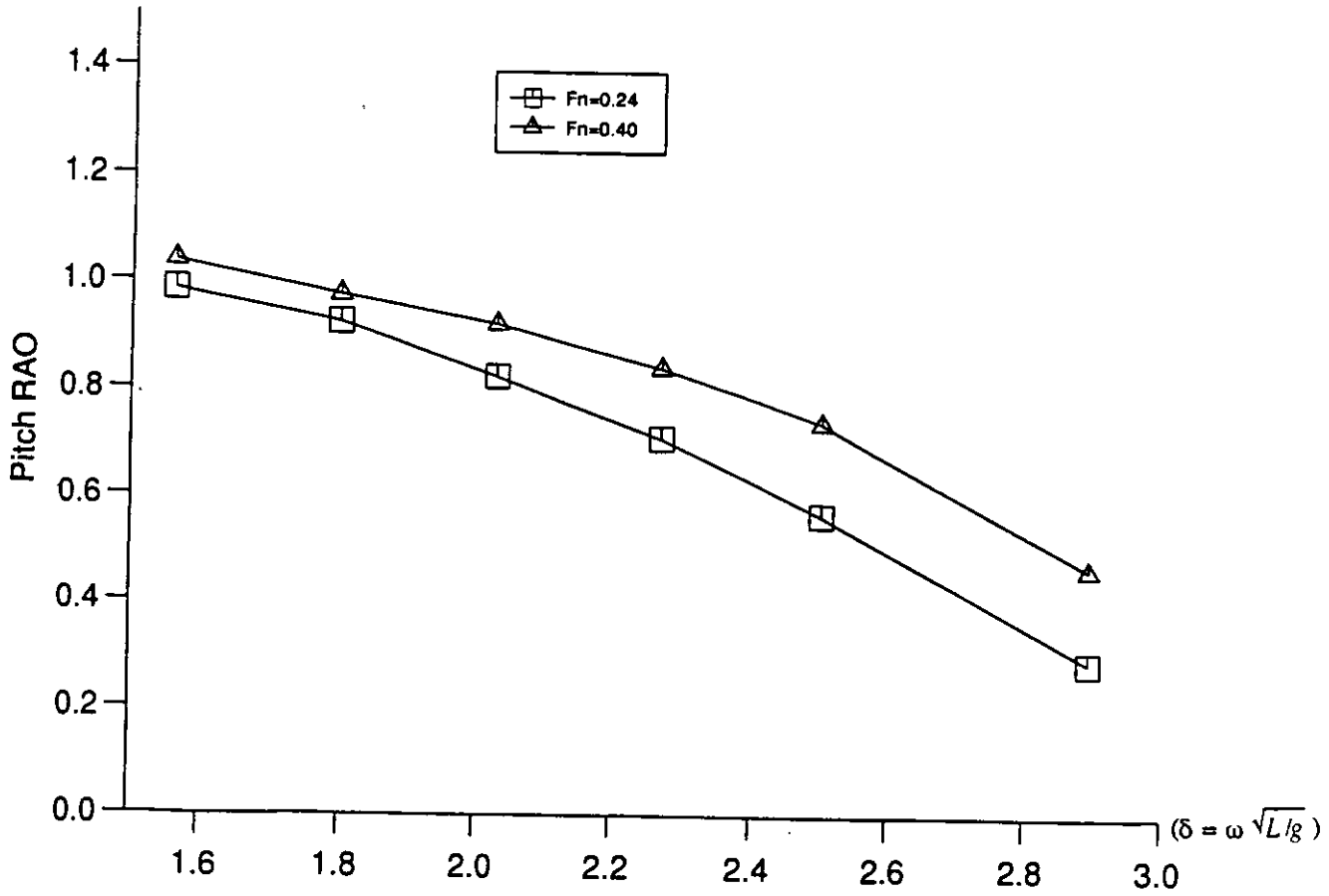

Fig.B2(g) Pitch RAOs for Trimaran model F ; Fn=0.24 and 0.40, heading 180 deg.

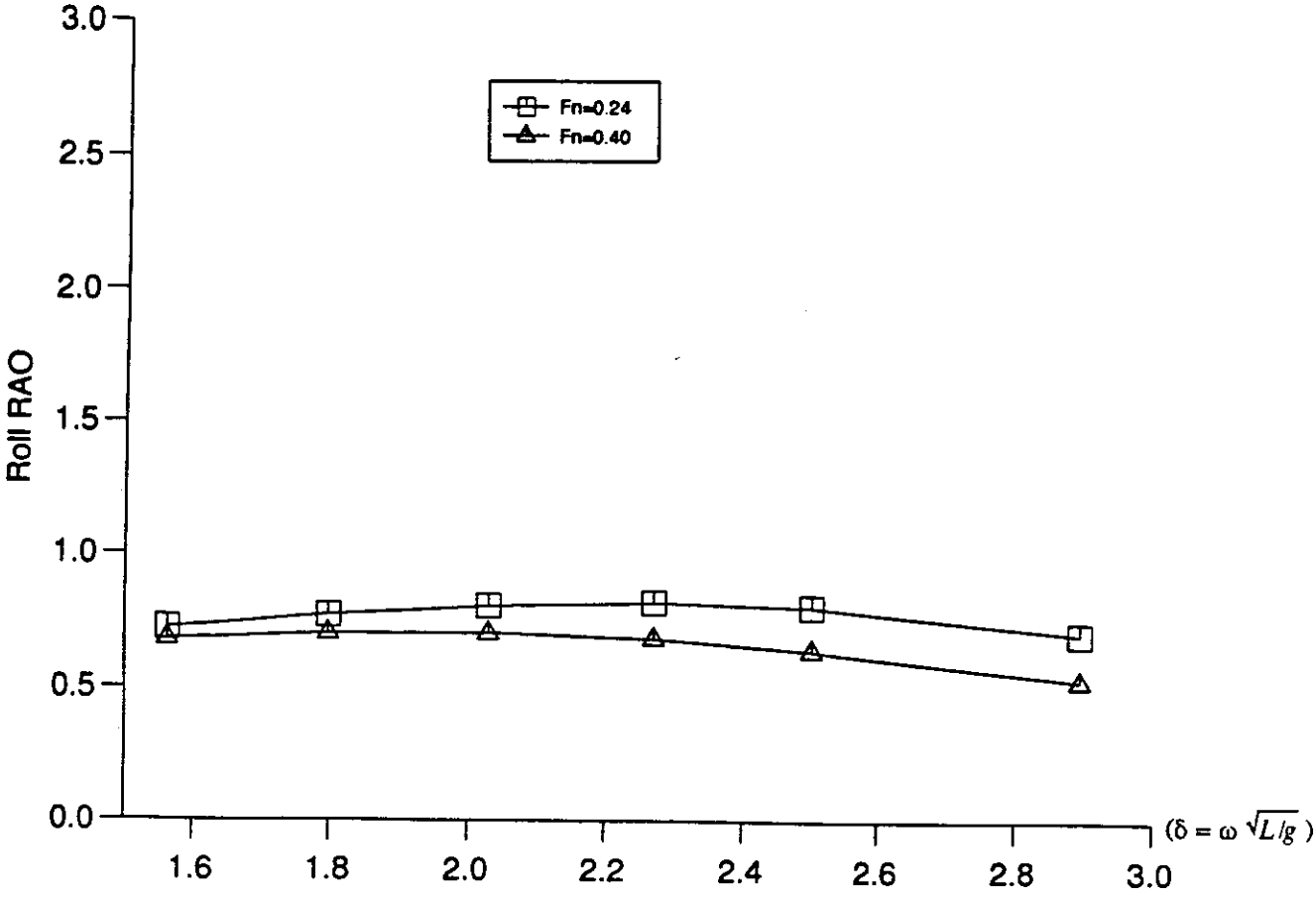

Fig.B3(a) Roll RAOs for Trimaran model F ; Fn=0.24 and 0.40, heading 30 deg.

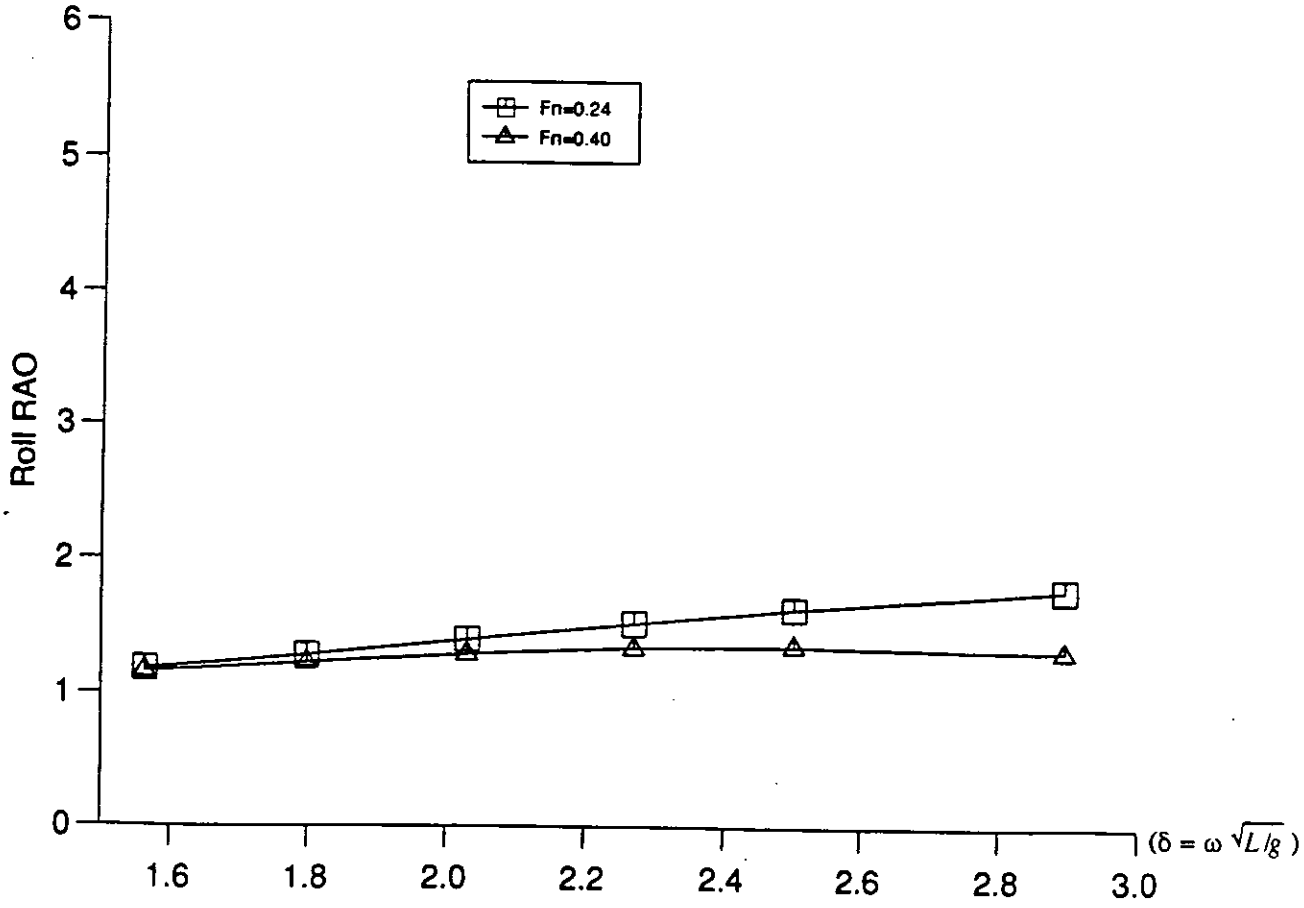

Fig.B3(b) Roll RAOs for Trimaran model F ; Fn=0.24 and 0.40, heading 60 deg.

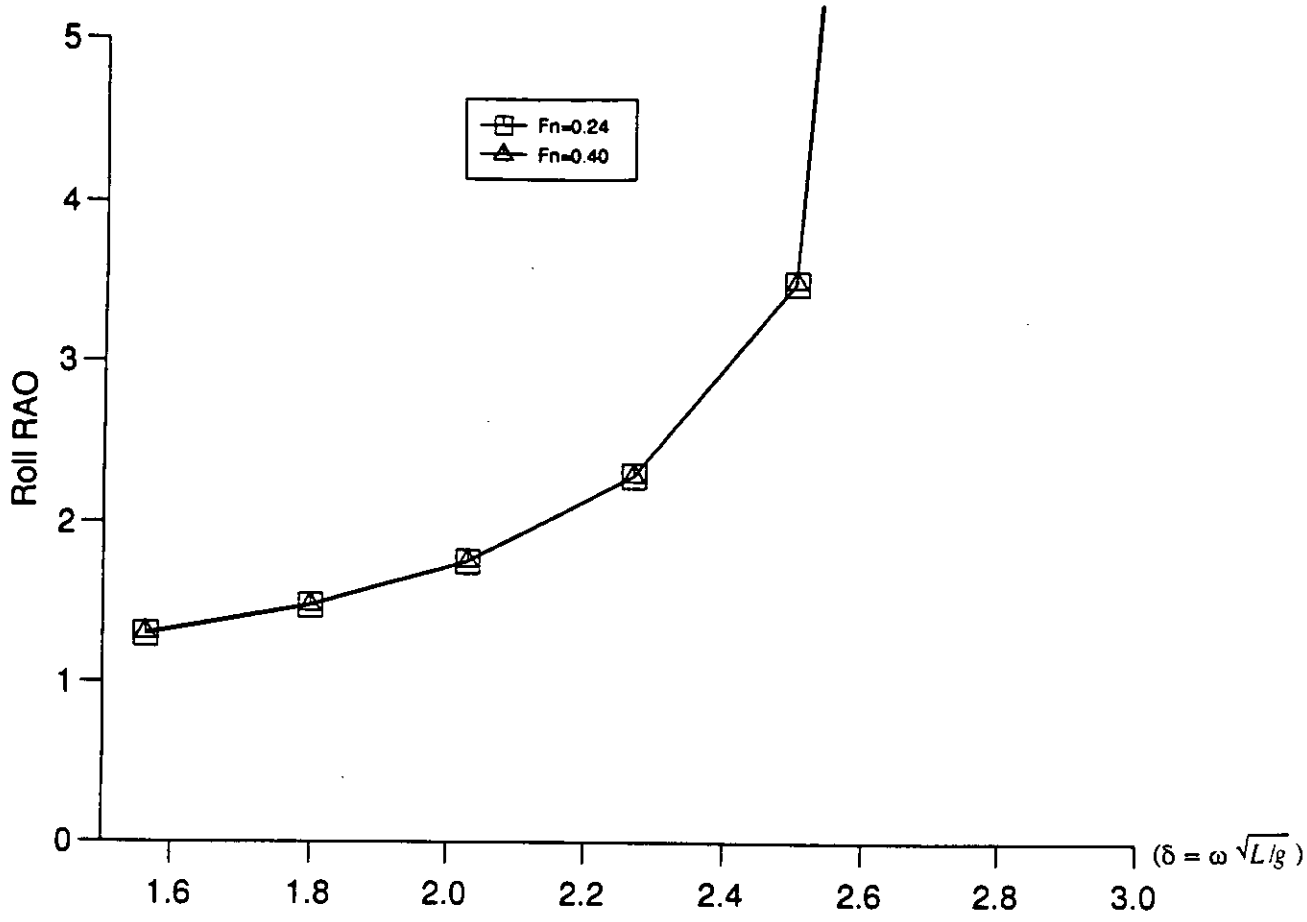

Fig.B3(c) Roll RAOs for Trimaran model F ; Fn=0.24 and 0.40, heading 90 deg.

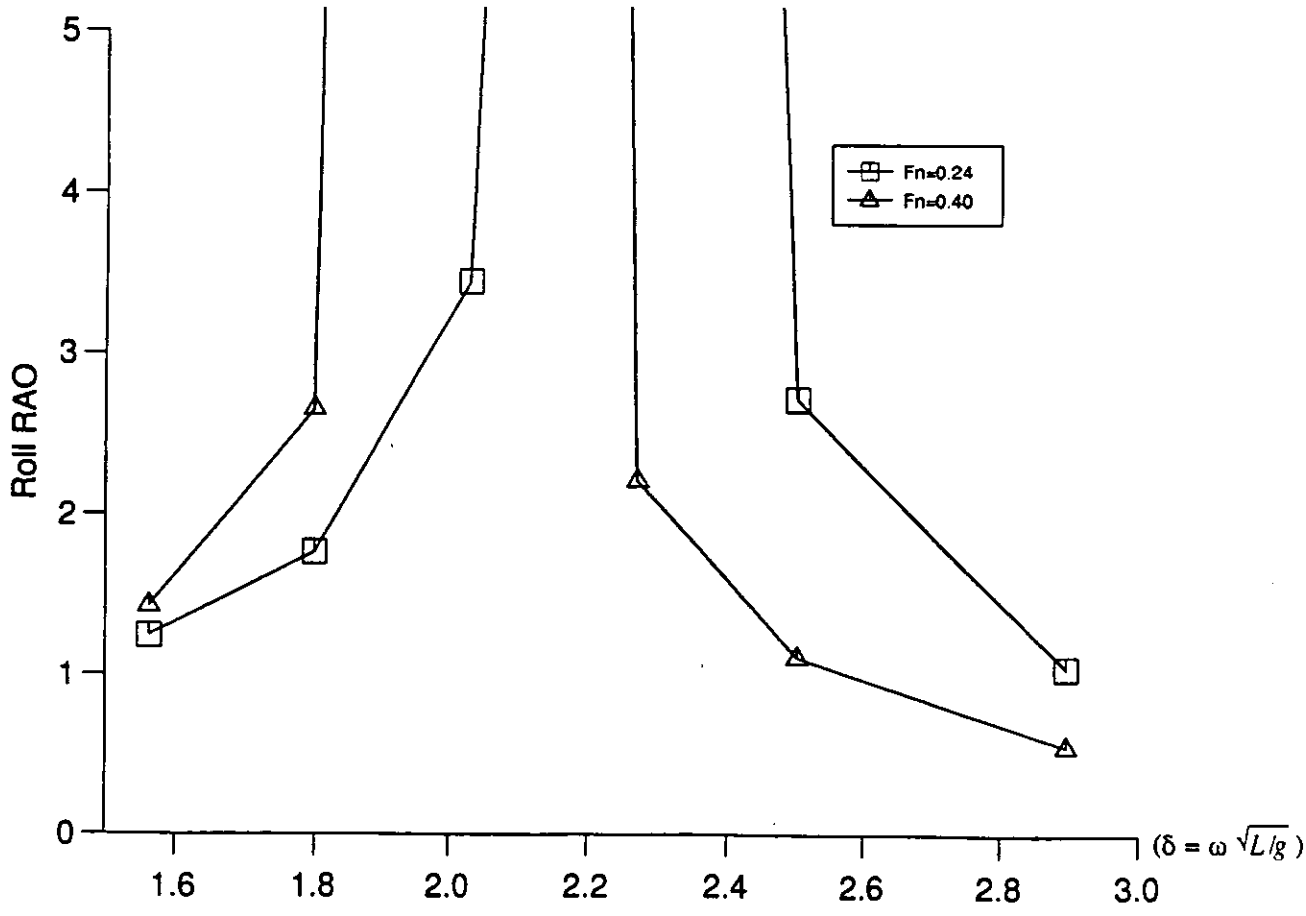

Fig.B3(d) Roll RAOs for Trimaran model F ; Fn=0.24 and 0.40, heading 120 deg.

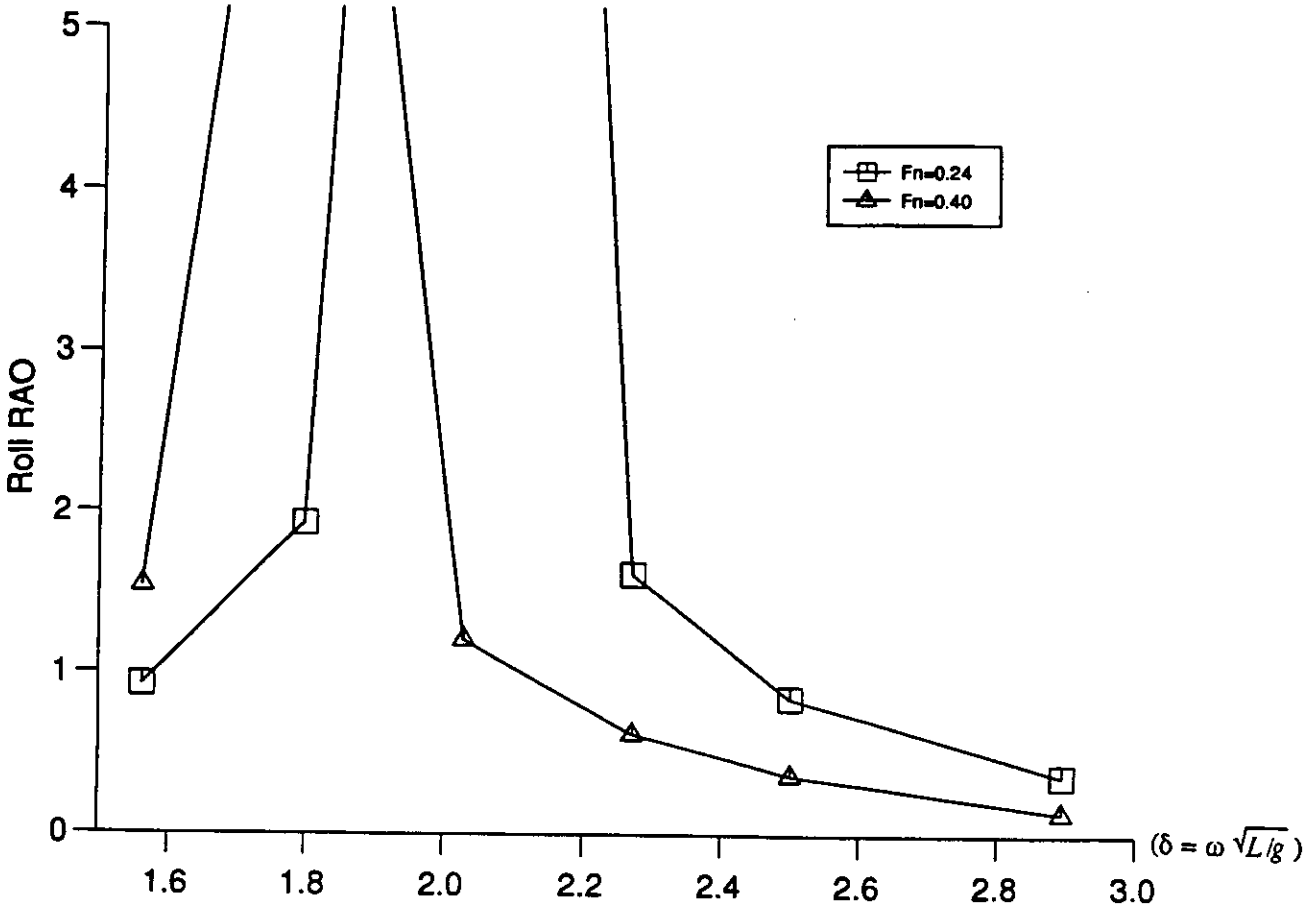

Fig.B3(e) Roll RAOs for Trimaran model F ; Fn=0.24 and 0.40, heading 150 deg.